

Potential Use of Abandoned Underground Coal Mine AS-029 as a Reservoir for Ground  
Source Heat Pumps, Athens, OH

A thesis presented to  
the faculty of  
the Voinovich School of Leadership and Public Affairs of Ohio University

In partial fulfillment  
of the requirements for the degree  
Master of Science

Andreana Madera-Martorell

August 2020

© 2020 Andreana Madera-Martorell. All Rights Reserved.

This thesis titled  
Potential Use of Abandoned Underground Coal Mine AS-029 as a Reservoir for Ground  
Source Heat Pumps, Athens, OH

by  
ANDREANA MADERA-MARTORELL

has been approved for  
the Program of Environmental Studies  
and the Voinovich School of Leadership and Public Affairs by

Dina L. López  
Professor of Geological Sciences

Mark Weinberg  
Dean, Voinovich School of Leadership and Public Affairs

### **Abstract**

MADERA-MARTORELL, ANDREANA, M.S., August 2020, Environmental Studies  
Potential Use of Abandoned Underground Coal Mine AS-029 as a Reservoir for Ground  
Source Heat Pumps, Athens, OH

Director of Thesis: Dina L. López

Ground source heat pumps (GSHPs) have been used for heating and cooling applications in areas where the thermal gradients are normal. Unlike conventional heating and cooling systems, ground source heat pumps rely on ground or underground water temperature which is more constant than air temperature. Abandoned underground coal mines (AUMs) have been used as heat exchangers for ground source heat pumps in countries such as Nova Scotia, the Netherlands and states like Pennsylvania. Ohio has around 147 abandoned underground mines located close to towns and with sufficient water and heat available in the groundwater for heat exchange using ground source heat pumps.

This project characterizes the potential of the AUM AS-029 located in Athens, Ohio, as a reservoir for GSHP technology in Ohio University or The Plains. Monitoring of the hydraulic and thermal response of groundwater wells around the mine was performed and a hydrogeological model was constructed in Visual MODFLOW to better understand the flow of water through the mine. Additionally, a thermal model of the mine was created considering the overburden thickness of the mine.

Three monitoring wells were studied, one to the north of the mine and 2 to the South in The City of Athens well field in the Hocking River valley. Groundwater in the

wells respond to precipitation and changes in ambient temperature with a higher response in the wells with lower depth. One of the City of Athens wells, A10, has an unusual response with a high conductivity due to a nearby underground salt deposit. Ground water modeling and modeling of the heat absorbed by the mine shows that mine AS-029 can be used to receive heat, it cannot be used to give heat due to the low temperature of the groundwater in this area. The volume of water that circulates through the mine is not easily exchanged since only 0.03% is exchanged every day and it takes 2,900 days to substitute 100% of the water within the mine. For a change in temperature in the mine water of 10 C, 0.23 MW of heat could be absorbed. The mine could theoretically provide 2.43% of Ohio University's heating/cooling system with this increase in temperature. In conclusion, mine AS-029 may serve as a geothermal reservoir for buildings for a small number of buildings at Ohio University or for Athens High School in The Plains.

## **Dedication**

*This thesis is dedicated to my mother's heart.*

### **Acknowledgments**

Foremost, I would like to express my sincere gratitude to my advisor Dr. Dina L. López for the continuous support of my Master's study and thesis, for her patience, enthusiasm, knowledge and advice. She is a true pillar in the geoscience field and an inspiration to all Latina women geoscientists. Besides my advisor, I would also like to thank my committee members Dr. Natalie Kruse for her unconditional support and time, and to Dr. Daniel Che for his guidance and insightful comments. A special thanks to the American Power Electric Foundation for funding this project.

My sincere thanks to Jennifer Bowman, Nora Sullivan and The City of Athens for their assistance and help in installing the sensors in the water wells. I would also like to thank Dr. Greg Nadon for his assistance and advice with the geology and stratigraphy of the study site. I thank my fellow colleagues in the Environmental Studies program for accompanying me in the field and for providing feedback on my work.

I would like to thank my parents Eugenio Madera and Nydiabel Martorell who always encouraged me to pursue a Master's degree and helped me move to Ohio. My father is part of this thesis since he helped me install the sensors in the wells. Without the love and support from both of them I would not be writing this thesis. In addition, I would like to thank my partner Mohamadjavad Haghghat Manesh for his loving support through my ups and downs.

Last but not least, I would like to thank God for all his blessings.

## Table of Contents

	Page
Abstract.....	3
Dedication.....	5
Acknowledgments.....	6
List of Tables .....	9
List of Figures.....	10
Chapter 1: Introduction.....	12
Background.....	12
Study Area .....	13
Project Goals and Significance .....	14
Chapter 2: Literature Review.....	17
Ground Source Heat Pumps.....	17
Geology.....	19
Abandoned Underground Coal Mines in Ohio .....	21
Acid Mine Drainage in Ohio.....	23
Underground Mine Water as a Heat Source .....	24
Hydrogeology .....	25
Legal and Licensing .....	28
Current Heating/Cooling Systems at Ohio University.....	29
Previous Work and Case Studies .....	29
Chapter 3: Methodology .....	34
Monitoring of Water Level and Temperature in Wells .....	35
Temperature, Pressure and Hydraulic Head Sensor Installation and Data Collection.....	37
Water Well Properties.....	37
Geographical Data of the AUMs .....	38
Stratigraphy of the Mine Area .....	38
Average Precipitation, Ambient Air Temperature and Barometric Pressure .....	39
Storage, Porosity and Conductivity Properties of Rocks.....	39
Data Analysis and Modeling.....	40
Transient Data Analysis.....	40

Visual MODFLOW Groundwater Model.....	40
Thermal Modeling .....	44
Total Heat Extractable/Exchangeable within the mine.....	45
Chapter 4: Results and Discussion.....	47
Potentiometric Maps .....	47
Physical Model.....	48
Monitoring Wells .....	52
Transient Data Analysis.....	53
Precipitation vs Hydraulic Head. ....	53
Precipitation vs Conductivity.....	56
Precipitation vs Well Temperature. ....	59
Well Temperature vs Ambient Temperature.. ....	60
Hydraulic Head vs Conductivity.....	64
Hydraulic Head vs Well Temperature. ....	66
Groundwater Flow Modeling.....	66
Steady State Model .....	66
Calibration of Steady State Model.....	76
Sensitivity Analysis .....	79
Zone budget .....	80
Thermal Modeling .....	85
Total Heat Exchange Within the Mine .....	88
Conclusions.....	92
Implications.....	94
Future Work .....	94
References.....	95
Appendix A: Transient Data Analysis Graphs.....	101
Appendix B: Cross correlation graphs .....	111
Appendix C: Tables .....	119

## List of Tables

	Page
Table 1 Average values for the different parameters recorded by the monitoring wells for 6 months.....	53
Table 2 Initial conductivity and porosity values assigned to geologic units prior to calibration. Time is irrelevant in this case because simulations are steady state.....	72
Table 3 Values assigned to the head observation wells.....	73
Table 4 Values assigned to the pumping wells.....	73
Table 5 Initial values used for River Package in Visual MODFLOW prior to calibration. ....	75
Table 6 Calibrated conductivity values of all the geologic units and the resulting mean error after calibration. ....	77
Table 7 Calibrated conductance values of all the river and the resulting mean error after calibration. ....	78
Table 8 Values used to calculate the amount of heat.....	89
Table 9 Values used to calculate the percentage. ....	90
Table 10 Variables used to calculate the volume of the mine that exchanges water every day and how many days it takes to substitute all of the water within the mine. The area of the mine, water in the mine and volume were extracted from the results of Riley et al. (2018). The fraction of the volume of the mine water was obtained from the results of Richardson et al (2016).....	91

## List of Figures

	Page
Figure 1 Study site and its proximity to Ohio University and The Plains. ....	14
Figure 2 Potential mines for GSHP installation sites.....	15
Figure 3 Different types of ground source heat pump installations.....	18
Figure 4 Geology surrounding the study site AS-029 .....	21
Figure 5 Abandoned coal mines in Ohio and its saturation rate .....	23
Figure 6 Estimated groundwater flow direction of AS-029.....	26
Figure 7 Watershed surrounding the study site.....	27
Figure 8 Previous calculationa of overburden thickness mine water temperatures.....	32
Figure 9 Location of water wells surrounding AS-029 .....	35
Figure 10 Location of monitoring wells .....	36
Figure 11 Relationship between overburden thickness and mine temperature.....	45
Figure 12 Flow regime of water table of the study site .....	48
Figure 13 Area selected for modeling purposes .....	49
Figure 14 Geologic map of Athens used to construct the cross section .....	51
Figure 15 Stratigraphic cross section of the study site .....	52
Figure 16 Daily precipitation and hydraulic head in monitoring wells .....	55
Figure 17 Cross correlation of the hydraulic head and daily precipitation of The Plains well.....	56
Figure 18 Daily precipitation and conductivity in well A10 .....	58
Figure 19 Cross correlation of the conductivity and precipitation of well A10 .....	59
Figure 20 Cross correlation of the temperature of well A10 and the ambient temperature .....	62
Figure 21 Cross correlation of the temperature from The Plains well and the ambient temperature .....	63
Figure 22 Depth of the monitoring wells plotted against the well temperature.....	64
Figure 23 Hydraulic head and conductivity values from The Plains well.....	65
Figure 24 Area extracted from ArcGIS and imported into Visual MODFLOW .....	67
Figure 25 Inactivated and activated cells in the model.....	68
Figure 26 Map view of the geologic units assigned to the model .....	69
Figure 27 Cross sectional view of the geologic units assigned to the model .....	70
Figure 28 Mine AS-029 and its respective cells in the model .....	71

Figure 29 Water wells assigned to the model .....	74
Figure 30 River boundaries assigned to the model.....	76
Figure 31 Resulting values of the calibrated model.....	78
Figure 32 Sensitivity analysis for hydraulic conductivity and river conductance .....	80
Figure 33 Zone budget of AS-029 .....	82
Figure 34 Direction of the flow of water in the model .....	83
Figure 35 East-West transect of the direction of the flow of water in the model .....	84
Figure 36 North-West transect of the direction of the flow of water in the model.....	85
Figure 37 Graph produced with the calculations of the overburden thickness of the mine and the temperature of the mine water.....	87
Figure 38 Representation of the temperature of the mine.....	88

## Chapter 1: Introduction

### Background

Geothermal energy is the heat that comes from the Earth's core due to the slow decay of radioactive particles or the heat left from when the planet formed and accreted (Glassley, 2010). This heat can be transported to shallower regions due to groundwater circulation that raises heat and steam through the fractures and reaches shallow areas as well as conductive transport of heat in materials of the crust. This clean renewable resource can be used to generate electricity through geothermal power plants when the enthalpy is high as in volcanic regions, or it can be used to and heat or cool buildings through ground source heat pumps (GSHPs) when the thermal gradients are normal. Abandoned underground coal mines in southeastern Ohio have been previously studied to pose as possible heat exchangers in GSHP systems (Richardson et al., 2016).

In general, there are two types of geothermal energy; high temperature and low temperature. The high temperature are areas where volcanism and/or tectonics processes are present, in these areas geothermal power plants can be installed. Low temperature are areas where groundwater circulation along fracture zones bring heat to shallow areas, in these areas ground source heat pumps (GSHPs) can be installed (Barbier, 2002). According to the United States Department of Energy's webpage, geothermal power plants are restricted to areas with volcanism or tectonism present, unlike these, GSHPs can be installed anywhere where the ground temperature ranges from 7 °C to 24 °C.

Ground source heat pumps can work all year long by transferring heat from the ground or water to heat buildings or transferring the heat from inside the building to the

ground and work as a cooling system. Most GSHPs exchange heat from groundwater or soils, the efficiency of these devices depends on the ability to extract or inject heat or to from these reservoirs and the amount of heat in them (Gass and Lehr, 1977).

Conventional heat pumps depend on air temperature which varies constantly, GSHP's depends on the more constant ground temperature, especially in temperate climates where the ground temperature is relatively stable throughout the year. These devices reduce fossil fuel consumption and the cost of space heating and cooling (Sanner et al., 2003).

An example of a successful heat exchanger reservoir is abandoned underground mines (AUMs). Locations around the world such as Nova Scotia and the Netherlands have been successfully using mines as heat exchangers in GSHP systems (Verhoeven et al., 2014). Universities in United States such as Marywood University in Pennsylvania have GSHP systems heating and cooling their buildings, cities such as Park Hills, Missouri have also employed these systems (Watzlaf and Ackman 2006). In this thesis, the use of abandoned underground coal mine AS-029 as a potential heat exchanger is investigated. This mine is close to Ohio University and the community of The Plains in Athens County, Ohio (Figure 1).

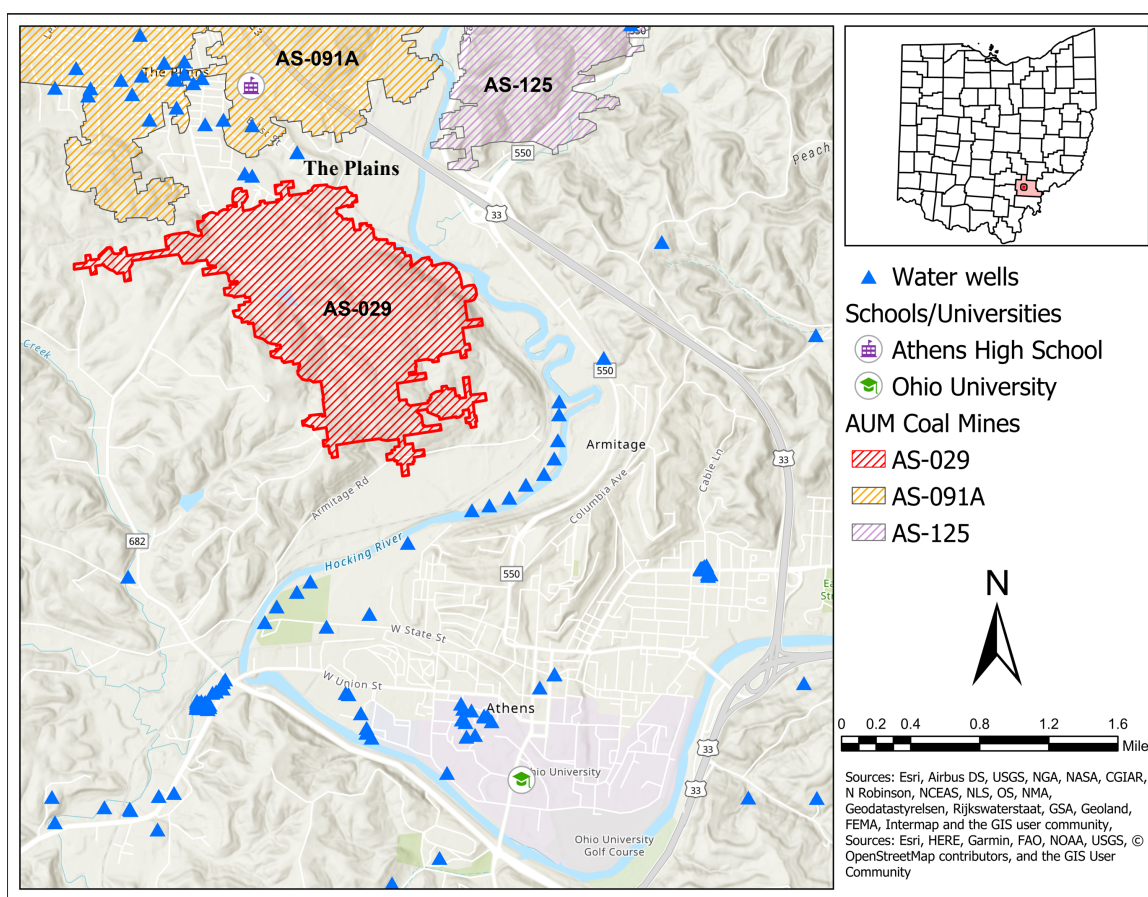
### **Study Area**

The AUM AS-029 is located in Northwestern Athens County, Ohio, and was chosen for thermal characterization and analysis to verify its potential to serve as a heat exchanger for GSHPs in Ohio University (Figure 1). The mine is approximately 2 miles from Ohio University and could serve as an opportunity to enhance the university's heating and cooling system. AS-029 is located in The Plains near the Athens High

School which could also serve as an opportunity to enhance the school's heating and cooling system.

**Figure 1**

*Study site highlighted in red bold and its proximity to Ohio University and The Plains. The blue triangles represent the water wells surrounding the mine.*



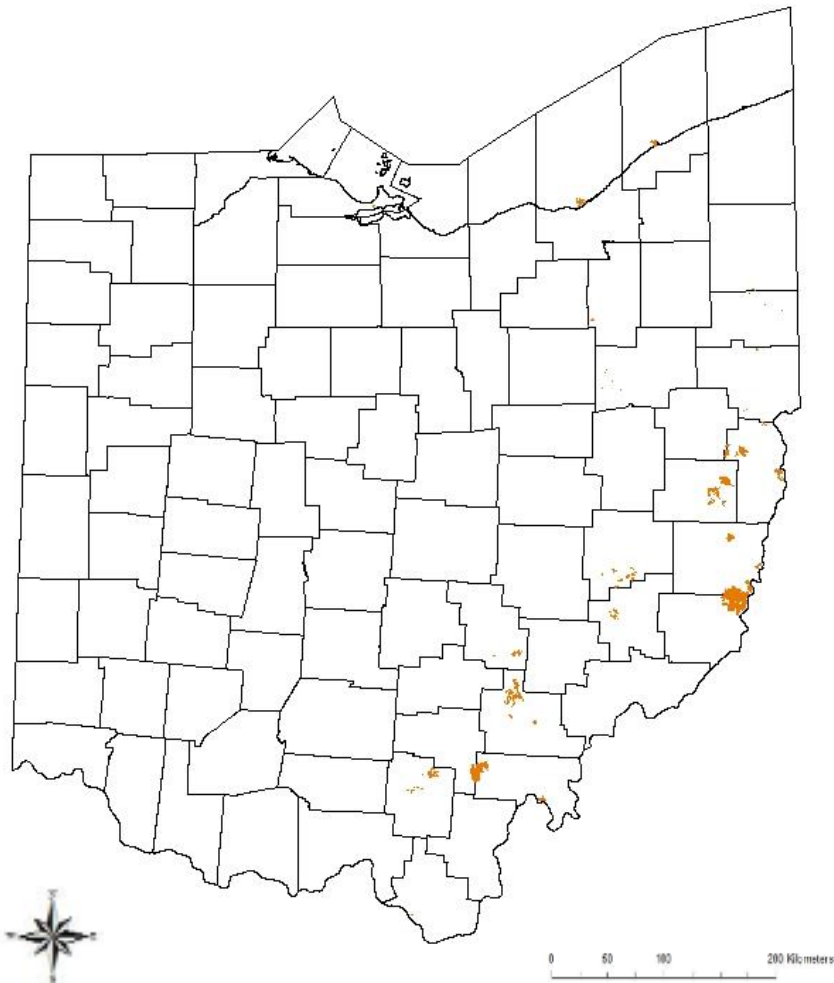
## Project Goals and Significance

Ohio has a large amount of AUMs of which Richardson (2014) estimated 147 possible mine sites that can be used for GSHP installations in Ohio (Figure 2). These

mines have an average  $10^{10}$  kJ/C° of heat energy available to extract and serve as heat exchangers in a GSHP system (Richardson et al., 2016). Mine AS-029 has not been previously characterized hydrologically for GSHP implementation, the goal of this research focused on the hydrogeological properties and the thermal response of the mine.

## Figure 2

*Potential mines for GSHP installation sites identified by Richardson (2014).*



This information may be utilized as an assessment approach for other mines located within Athens, Ohio. However, it was first necessary to determine the heat capacity of the mine, the topography and stratigraphy of the area for drilling and installation. In this thesis, hydrogeological studies were performed in order to confirm the adequate performance of GSHPs. The results of this study can be used as a pilot study for the implementation of AUMs as heat exchangers in southeastern Ohio and to benefit conventional heating/cooling systems.

The objective was to determine if AS-029 has the amount of volume and flow of water and heat necessary for the application of a GSHP that can benefit Ohio University's heating/cooling system by reducing cost and greenhouse gas emissions, or it can be used for that purpose by The Plains. The purpose of this research was to determine the potential of AS-029 as a geothermal resource by defining its thermal and hydrogeological properties. For that purpose, monitoring of the hydraulic and thermal response of groundwater wells around the mine was done and a hydrogeological model was constructed in Visual Modflow to better understand the water and heat that flows through the mine. The goal was to determine if AS-029 has the amount of volume and flow of water and heat necessary for the application of a GSHP that can supplement Ohio University's heating/cooling system by reducing cost and greenhouse gas emissions, or if it can be used for that purpose by The Plains.

## Chapter 2: Literature Review

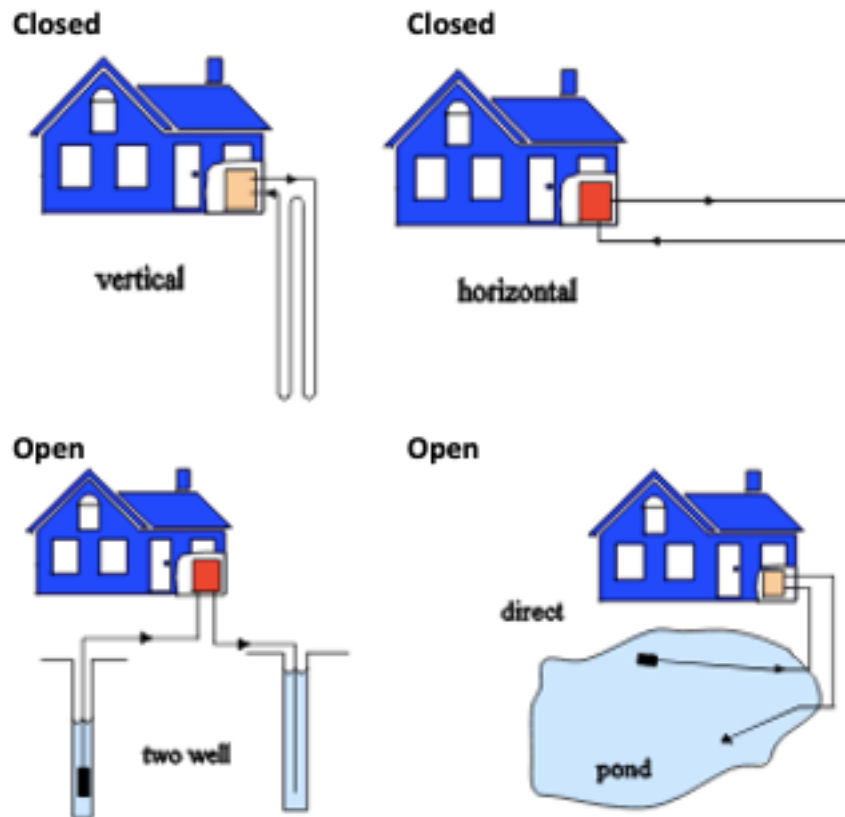
### Ground Source Heat Pumps

The first heat pump was developed in 1852 by Lord Kelvin. In the 1940s this concept was modified using the ground as a heat source (Curtis et al., 2005). Unlike the constant variation of air temperature for air pumps, ground source heat pumps (GSHPs) can successfully absorb or release heat from/to soils or groundwater with a more constant temperature in the ground from the Earth's internal heat. During the heating cycle the GSHPs circulate a fluid through a closed loop system which absorbs the heat from the ground and delivers the heat into the building, this process is reversed for cooling by injecting the heat in the building to the ground (Stylianou et al., 2017).

There are four types of GSHPs (Figure 3); horizontal closed loop, vertical closed loop, well/lake closed loop and well/lake open loop. The closed loop systems circulate an antifreeze solution through the loops which absorbs the heat and transfers it to the building. The open loop system directly pumps the water from surface body water or water underground and circulates through the system and turns back to the ground once it has exchanged the heat (Mustafa Omer, 2008; Lund et al., 2004). These devices are a clean renewable energy source which can heat and cool building. Heat pumps can be used in a system of coproduction with fossil fuels by delivering electricity and heat.

**Figure 3**

*Different types of ground source heat pump installations. The top two are closed loop systems and the bottom two are open loop systems (Modified from Lund et al, 2004).*



Air-source heat pumps work by using the outside air as a heat source, they extract the heat from the building and is discharged to the outside air, for heating purposes it absorbs the heat from the outside air and diffuses it inside the buildings (Watzlaf and Ackman, 2006). In air source heat pumps the air temperature is constantly changing, during the winter these devices require supplemental heating such as electrical heating when the temperature outside is below 0 °C (Lund et al., 2004). In the winter, the ground

is typically warmer than the outside air, and in the summer the ground is cooler than the outside air, therefore, GSHPs are more efficient than air-source heat pumps (Healy and Urgus, 1997; Gass and Lehr, 1997).

Conventional heating and cooling systems are powered by fossil fuels which accounts for greenhouse gas emissions; however, ground source heat pumps reduce fossil fuel consumption by using the ground as a heat exchanger (Ohmer, 2008; Healy and Urgus, 1997). The installation of these devices in Ohio will reduce the greenhouse gas emissions. Ground source heat pumps can achieve energy savings up to 70% compared to other traditional heating and cooling systems (Stylianou et al., 2017). Before installing GSHPs, the geology and the hydrogeology must be studied to confirm the adequate performance of these devices.

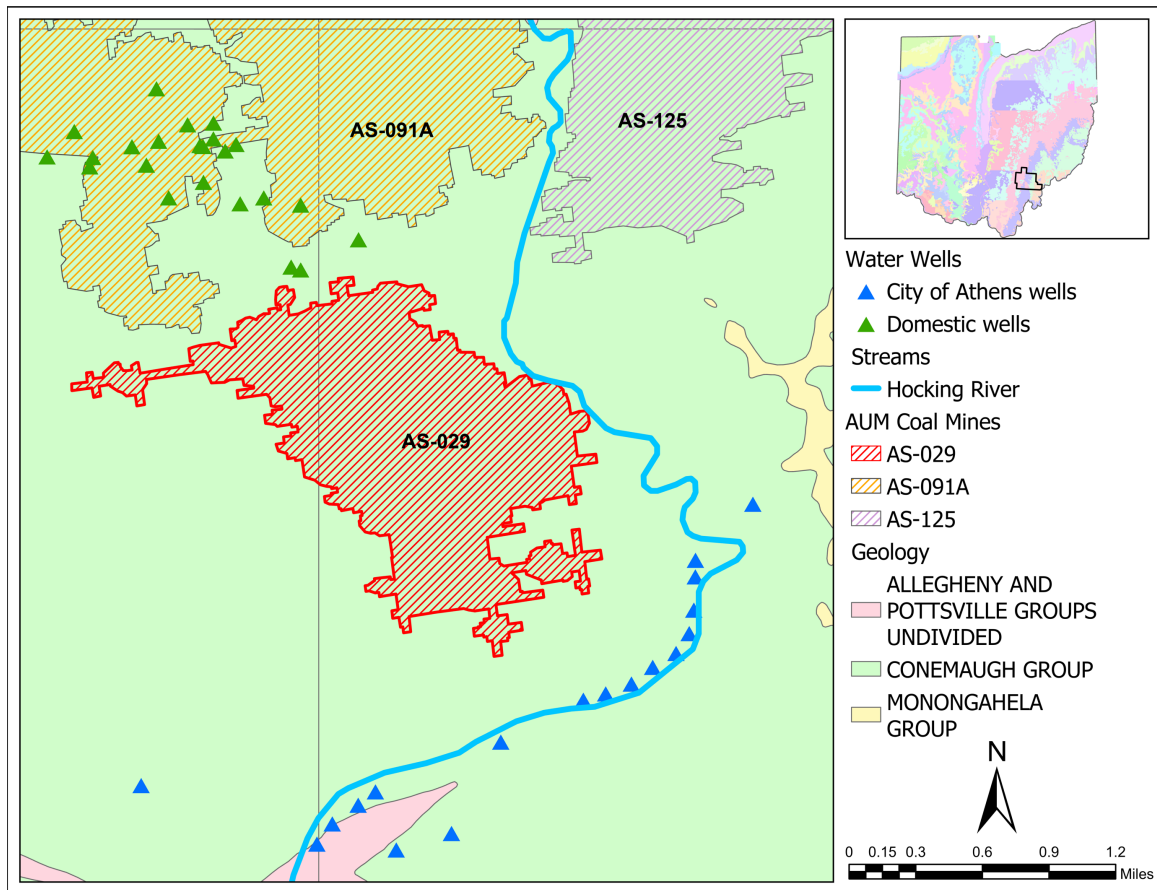
### **Geology**

It is important to consider the geological conditions of the area when installing a GSHP. Parameters such as surface temperature, sub-surface temperatures, thermal conductivities and diffusivities of the soil and rock layers, rock strength are also important for the excavation and drilling required (Busby et al., 2009). In addition, if the system is going to exchange heat with groundwater as it is the case in the mine application, the flow and temperature of the water are also important. The geology surrounding the study area was mapped by Sturgeon (1958); the descriptions below come from the map of the Athens, Ohio quadrangle. The different lithologies observed in the area are presented in Figure 4. The Dunkard Group is dominated by mudstone, shale, siltstone, sandstone and thin beds of limestone and coal of the Permian (Slucher 2006;

Sturgeon 1958). The rest of the lithology surrounding the area is Alluvium sediments (Quaternary) and Illinoian Terrace (Pleistocene). Rocks in eastern Ohio generally dip to the southeast about 30 feet per mile (Crowell, 2008). According to the Ohio Department of Natural Resources, the overall geology of the wells around the area contain shale, sand, clay, coal and gravel. Water bodies surrounding the mine include the Hocking River and its tributaries (Crowell et al, 2011). In this area the Middle Kittanning coal seam is found. This coal bed is the most important of Ohio known for its workable thickness of around 3-5 feet thick, and the Athens area is one of its very important mining centers. The Middle Kittanning coal typically consists of three benches separated by layers of shale or clay (Bownocker and Dean, 1929). A cyclothem is when coal and marine units with other lithologic types occur in a stratigraphic succession (Weller, 1931). There are only two cyclothem in Ohio and one of them is related to the Middle Kittanning coal and the other is related to the Anderson coal (Sturgeon and Merrill, 1949; Stout, 1947).

**Figure 4**

*Geology surrounding the study site AS-029.*



### **Abandoned Underground Coal Mines in Ohio**

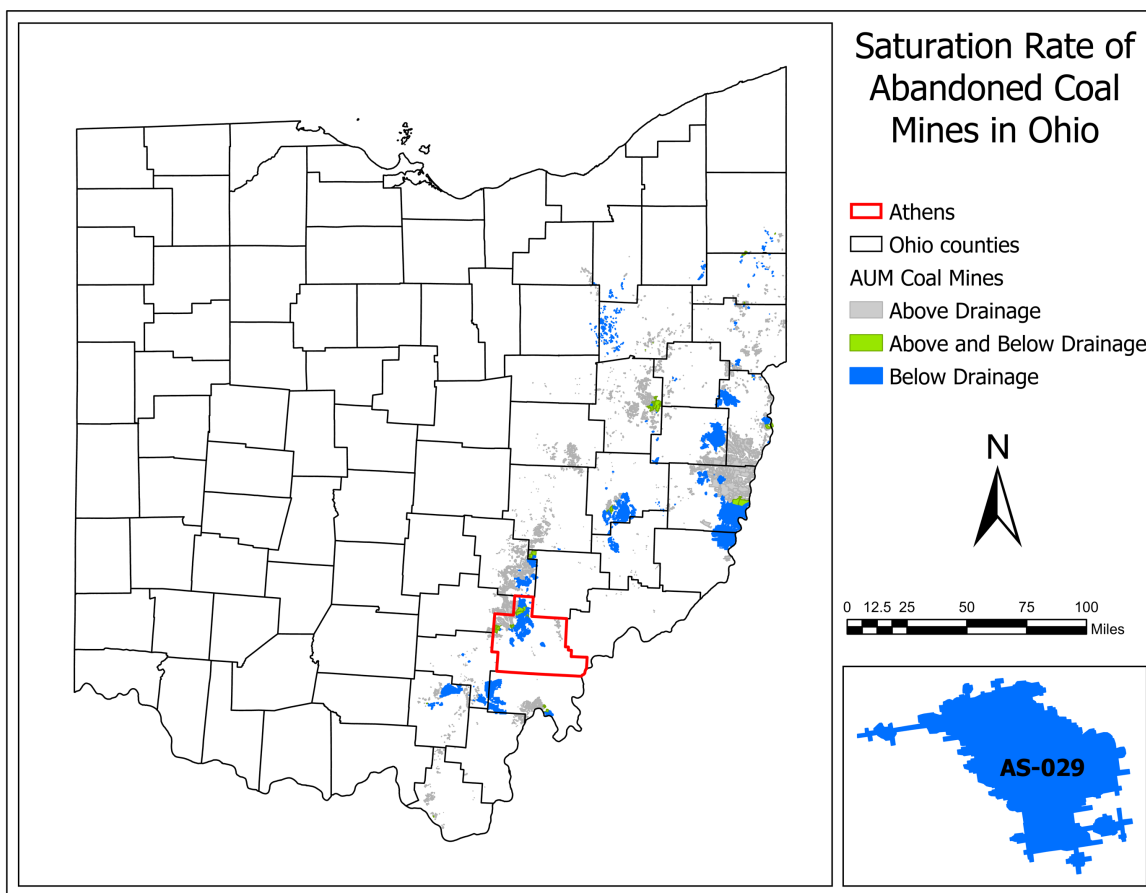
Mines that have ceased operation before the current mining and reclamation laws were effectuated are referred to as abandoned underground mines (AUM). During exploitation, water has to be pumped out of the mine to create an accessible space. If the pumps are switched off after a mine is abandoned, the mine will gradually fill with groundwater if it is below drainage. If the pumps are not switched off the pumping will

continue and will prevent water filling (Banks et al., 2017). Many abandoned underground coal mines are flooded and are located under populated areas of the United States, therefore some of them can be utilized as geothermal heat exchangers. Mines can transfer heat toward or away from GSHPs due to groundwater recharge and flow, this allows more heat to be extracted or injected. Additionally, mines, bedrocks and soils are all thermally stable, but, water in mines have a better thermal conductivity (Watzlaf and Ackman 2007). Ohio is known for its valuable coal mining and mineral extraction and for being the third largest coal-consuming state in the USA. Ohio also has approximately 4,000 AUMs including some underwater (Crowell, 2008).

Most of the AUMs in southeastern Ohio are completely flooded, while the rest are partially flooded (Figure 5). Potential heat exchanger sites for GSHP geothermal systems are mines that are flooded with groundwater below drainage and near population areas (Richardson et al., 2016). Therefore, southeastern Ohio is an excellent potential site for GSHP implementation. A study conducted by Richardson et al., 2016 identified 147 possible mine sites for GSHP installations in Ohio.

**Figure 5**

*Abandoned coal mines in Ohio and its saturation rate, Athens county highlighted in red and mine AS-029 highlighted in blue which confirms that the mine is completely flooded.*



### Acid Mine Drainage in Ohio

Eastern Ohio is located in the Appalachian basin which contains the Appalachian coal field, this coal is known for having a high sulfur content (Crowell, 2005). This area has been mined since the early 1800's because many coal deposits are present in the area. Due to the high sulfur content, these mining areas are mostly affected by acid mine drainage (AMD) which is produced when sulfides (e.g. pyrite) are oxidized to sulfate

and metals (e.g. Fe and Mn) (Singer and Stumm, 1970). Surface and underground coal mines may produce acid mine drainage (AMD) when it is exposed to oxygen if there is not enough carbonates in the nearby rocks, which is a problem in the Appalachian coal region (Helsel, 1983). However, in underground coal mines AMD production depends on the degree of flooding in a mine, if a mine is completely flooded, or also referred to as below drainage, there is no oxygen entering and AMD will be less likely to be produced (Lambert et al., 2004). Mines that are above drainage or above/below drainage of the water table have a higher risk of producing AMD. If AMD is produced in an underground coal mine, there are technologies that can control acid mine drainage production.

Inundation is a technology that consists of flooding the underground coal mine with water to deprive the pyrite of oxygen (Skousen et al., 1998). Nowadays, there are materials in the market that can resist acidity and could be used to construct the piping in a mine that has some water acidity. A closed loop system should be used in a mine like this. Therefore, even if a mine is not completely flooded, there is a chance it can be used for GSHP.

### **Underground Mine Water as a Heat Source**

Typically coal mines have a good accessibility making them an excellent source for the use of mine water for geothermal energy applications (Watzlaf and Ackman, 2006). Thermal storage in mines is substantial and yields several tens or hundreds of  $L s^{-1}$  of water due to large volumes of mine pool waters and void space (Banks et al., 2017), as well as relatively fast moving water. The chemistry of the mine water should be considered as well when studying its potential to serve as a heat exchanger. It is better if

the AUM is completely flooded without the presence of oxygen flowing through, due to the presence of sulfide minerals in coal that can oxidize when exposed to water and oxygen to produce Acid Mine Drainage (AMD) (Banks et al., 2017).

### **Hydrogeology**

According to the mine maps from the Ohio Department of Natural Resources (ODNR), the mine AS-029 is an abandoned underground coal mine that is below drainage with a coal elevation of 150.3 m. The coal seam thickness around AS-029 is approximately 2 m thick and an effective volume (volume minus pillars) and total volume of  $2.6E+06 \text{ m}^3$  and  $4.3E+06 \text{ m}^3$  respectively (Richardson et al., 2016). The groundwater flows to the East as seen in Figure 6, and the maximum and minimum estimated recharge area are  $4.7 \text{ km}^2$  and  $2.2 \text{ km}^2$  respectively (Richardson et al., 2016). The estimated amount of water in AS-029 is over 443 millions of gallons, with temperatures between  $11.9 \text{ }^\circ\text{C}$  and  $13.8 \text{ }^\circ\text{C}$  (Riley et al. 2018; Richardson et al., 2016). The drainage basin surrounding AS-029 at a HUC 12 is Coates Run-Hocking (Figure 7).

**Figure 6**

*Estimated groundwater flow direction of AS-029 (Richardson, 2014).*

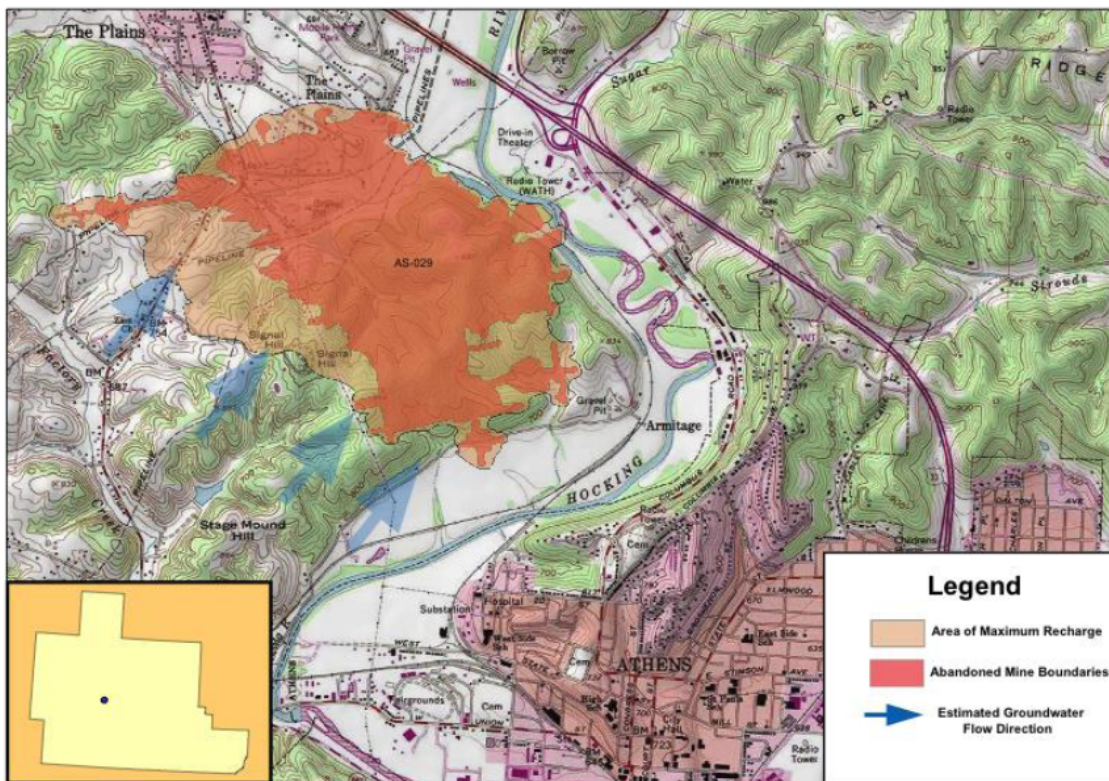
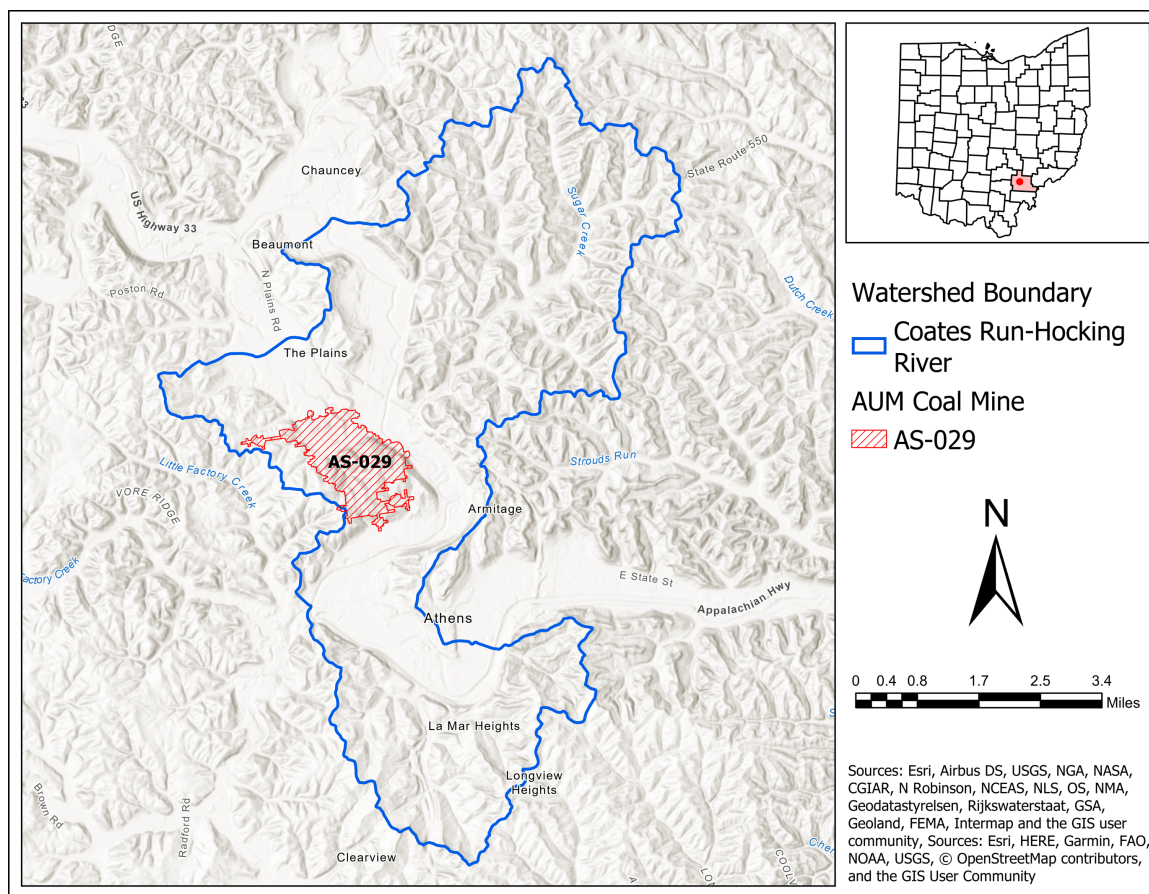


**Figure 7**

*Coates Run-Hocking river basin surrounds the AUM AS-029 at a HUC 12.*



The New Pittsburgh Coal Co. was the mining company that exploited AS-29. The exploited seam was the Middle Kittanning No. 6. Currently, AS-029 does not have any wells drilled or open shafts, they were closed long ago. Therefore, mine AS-091A located to the North of AS-029 was used as reference for the geology by extracting the data from the wells intercepting this mine, both mines are not interconnected. AS-0191A is an abandoned underground coal mine that is below drainage with a coal elevation of 160 m.

Its operator was the Hocking Valley Mining Co. and the exploited seam was Middle Kittanning No. 6. Wells surrounding AS-029 within approximately less than 1.5 miles from the mine were used for correlation and the production of geologic cross sections. Active mines near AS-029 include mine IM-2083, which is a surface mine that was exploited by Cochran Wrecking and Salvage.

### **Legal and Licensing**

Banks et al. (2017) stated that one of the main problems of utilizing mine water as a heat exchanger was the uncertainty over legal and licensing issues. This will not be a problem for the application of GSHPs in Ohio. According to the 4 Restatement of the Law 2d (1979), Torts, Section 858:

“A proprietor of land or his grantee who withdraws ground water from the land and uses it for a beneficial purpose is not subject to liability for interference with the use of water by another unless:

- The withdrawal of ground water unreasonably causes harm to a proprietor of neighboring land through lowering the water table or reducing artesian pressure,
- The withdrawal of ground water exceeds the proprietor’s reasonable share of the annual supply or total store of ground water, or
- The withdrawal of the ground water has a direct and substantial effect upon a watercourse or lake and unreasonably causes harm to a person entitled to the use of its water.”

The installation of a closed loop GSHP system in AUM AS-029 will not pose as a risk and would be allowed in Ohio under these terms that do not affect any other person

entitled to the reasonable use of this water (Riley et al., 2008). In a closed loop system, water will not be withdrawn from the system.

### **Current Heating/Cooling Systems at Ohio University**

Ohio University's heating and cooling system are powered by the central steam plant Lausche, which is fueled by natural gas, and the West Green Chilled Water Plant central chillers. According to the Facilities and Management office webpage, the university has not been using coal in the steam boilers since November 2015. The steam generated serves its purpose to heat buildings, generate domestic hot water, laboratory research, cooking and team dryers. The Lausche plant also produces steam to run two electric chillers and a condensing steam turbine chiller which weigh 2,500 tons each. For conversion purposes a cooling ton is considered to be equal to the amount of heat that is needed to melt one ton of ice in one day. The West Green Chilled Water Plant cools much of the campus, the remaining part of the campus is chilled by their own chillers or less modern chillers such as window air conditioners. It is anticipated that the campus steam load will increase from 180,000 pounds per hour (pph) to 224,000 pph if the university does not invest in reducing energy use. According to the Utility Master Plan 2017 of the Facilities and Management office, they university has been evaluating different heating systems that can reduce the carbon footprint.

### **Previous Work and Case Studies**

The possibility of implementing low temperature geothermal energy in Ohio University has been studied previously. The mine AS-029 has also been previously studied for its potential use as a geothermal reservoir. The Facilities and Management

office evaluated in their Utility Master Plan 2017 the possibility of replacing the current steam system with a different heating system that would be more efficient, reduce steam load and reduce energy use. One of the options that would best balance carbon reduction and cost efficiency was implementing a hot water district systems and small geothermal wells system to support a portion of Ohio University. This transition would involve the construction of a chiller and hot water plant which would incorporate two 25,000 mbh hot water generators and a 2,500 ton heat recovery chiller. An additional geothermal plant would be constructed to house an additional 2,500 ton heat recovery chiller and a steam to water heat exchanger. According to the Facilities and Management office, it is best for the geothermal system to support a portion of the campus instead of a large geothermal system for the following reasons:

- Large scale geothermal well systems are not a proven technology, there is no large scale system operating for more than 10 years.
- The campus does not have enough space for a wide geothermal system.
- Ohio University's geographic location has periods throughout the year where the outside air temperature would require natural gas based heating system or carbon free electric resistance heat.

Richardson et. al (2016) researched 147 possible mine sites to serve as heat exchangers in GSHPs systems in Ohio. One mine in particular was studied for GSHP application at the Corning Mine Complex in Perry County, Ohio where the results indicated a stable temperature in the mine throughout the year and  $3.45 \times 10^{10}$  kJ/C° heat energy available (Richardson et al., 2016). The results of this study discovered that the

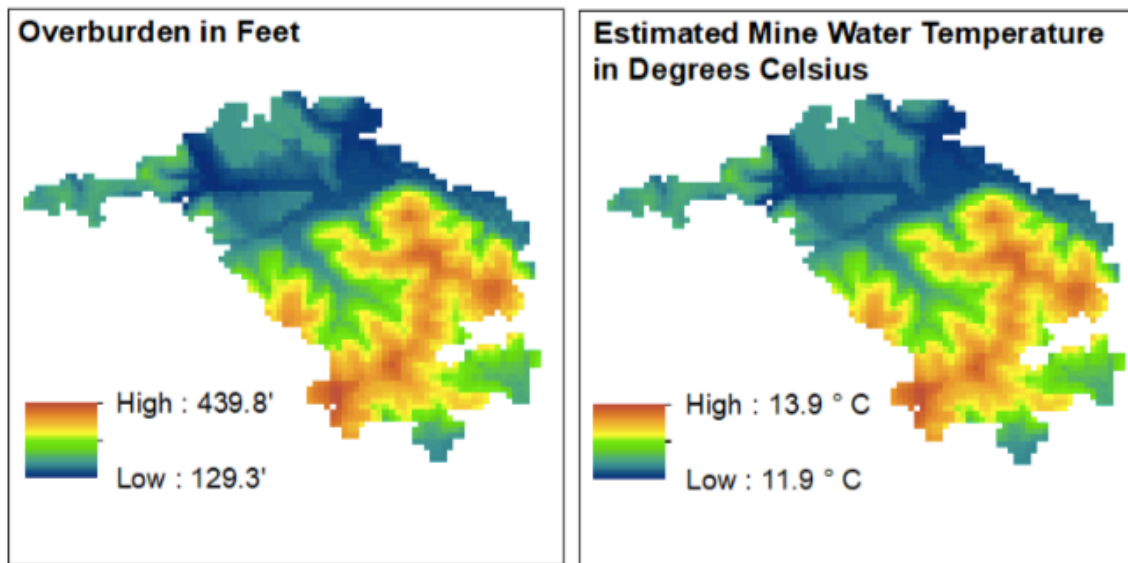
mine water temperature is positively correlated to the overburden thickness of the mines. The AUM AS-029 was also considered in this project. Certain hydrological parameters were estimated by using the physical parameters of the mine and inputting them into different equations. The results of these calculations resulted in a volume of  $4.3E+06 \text{ m}^3$ , an effective volume of  $2.6E+06 \text{ m}^3$ , a minimum recharge area of  $4.7 \text{ km}^2$  and a maximum recharge area of  $2.2 \text{ km}^2$ . Richardson et al. (2016) also calculated the thermal properties and heat extractable from AS-029. According to his results the total heat extractable from the mine was  $1.09E+10 \text{ kJ/y}$  and the average estimated temperature of the mine was  $13.2 \text{ }^\circ\text{C}$ . Other hydrologic calculations were also performed in this study resulting in a mean recharge to groundwater of  $51 \text{ mm/y}$  and a mine water velocity of  $2.3E-06 - 1.0E-06 \text{ m/s}$ .

The Facilities Management & Safety from Ohio University conducted a follow up study from Richardson's work by re-characterizing his assessment of AS-029 as a heat exchanger. The study used GIS-based estimation techniques and more conservative data estimates including cost estimations for a pipeline between the mine and Ohio University's district plant (Riley et al., 2018). The study estimated the effective mine volume by developing and assessment of the void area and volume of AS-029 resulting in a volumetric estimation of approximately 443,800,267 gallons of water in the mine. The area of the mine was calculated by using GIS resulting in  $9,245,837 \text{ ft}^2$ . Additional parameters were calculated such as the theoretical heat extractable from the mine which was  $7.04 \text{ E}+09 \text{ kJ}$  per 1 degree Celsius of  $\Delta T$ . This study also performed an overburden analysis, continuing Richardson's (2014) research discovery of the correlation between the thickness of overburden and temperature of the mine water. Georeferenced images

AS-029 and a Digital Elevation Model (DEM) of the surface of the Earth were compiled to calculate the difference in values between the two surfaces to represent the overburden thickness of the mine. The mine water temperature was also calculated by considering the geothermal gradient, the formation depth of the mine and the average ambient temperature. The results of the overburden and mine water temperature calculations are presented in Figure 8. The study concluded a possibility of running supply and return pipelines between AS-029 and Ohio University's Lausche Heat Plant. Riley et al. (2018) mentioned that for this to be effective, the water of the mine must be sampled and its chemical composition and temperature should be analyzed.

### Figure 8

*Results from the calculations of overburden and mine water temperatures. The areas with higher overburden are the areas with higher temperatures (Riley et al. 2018).*



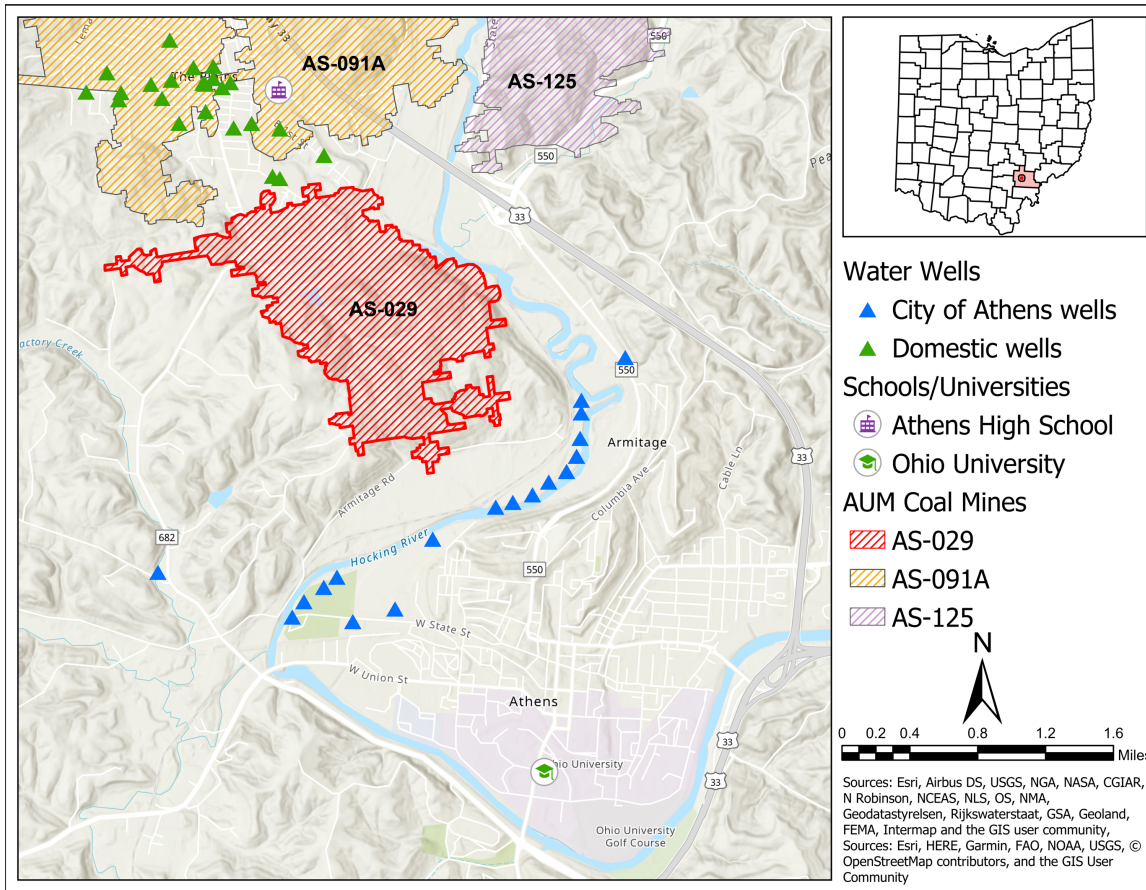
Successful implementations of GSHPs in other AUMs includes Marywood University in Pennsylvania. The AUM Marvine Mine is below the university and provides cooling for the Center for Architectural Studies since 2010, the successful \$530,000 project has paid for itself in less than three years (Legere, 2014). Communities such as Heerlen, Netherlands have been also benefited by this clean renewable resource since 2008. In 2014 Herleen announced an upgrade from its pilot system to a full-scale larger structure which has reduced carbon dioxide emissions by 65% (Verhoeven et al., 2014).

### **Chapter 3: Methodology**

This investigation includes field work activities as well as analysis of data, construction of a physical model of the mine area, modeling of the hydrological conditions of the mine, and calculation of the possible heat absorbed by the mine. The software used in the following research include Arc Map, Microsoft Excel, Surfer 12.0, Past and Visual MODFLOW. There is no access to the mine water because the shafts were closed and there is no wells intercepting the mine. However, there are wells around the mine that include domestic wells in The Plains to the North and water supply and monitoring wells for the City of Athens to the South, in the river valley of the Hocking River (Figure 9). These wells were used to understand the underlying geology of the mine and to install sensors in three monitoring wells to evaluate the response of the water level and temperature to precipitation events and changes in air temperature. In addition, there are several oil and gas wells that intercept the mine, these were not considered due to the lack of stratigraphic information in each of them at the level of the mine and water wells. Fieldwork was performed to install sensors in the wells and conduct the hydrogeological study of the mine.

**Figure 9**

*Location water wells surrounding AUM AS-029.*



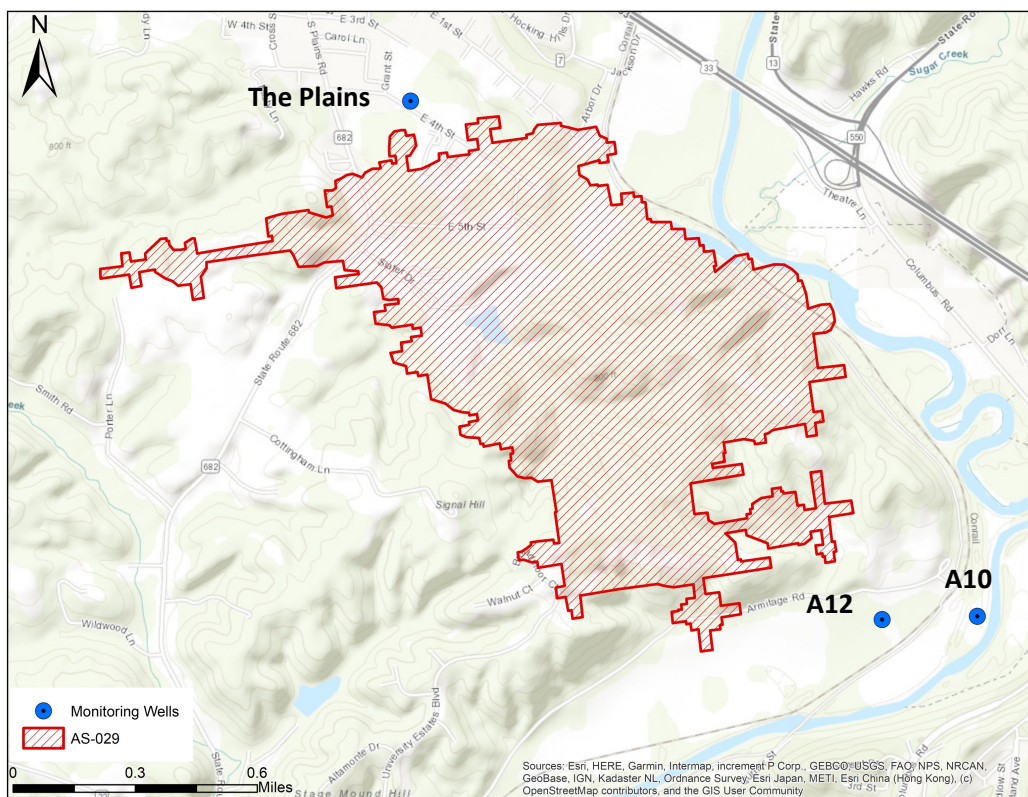
**Monitoring of Water Level and Temperature in Wells**

AS-029 does not have any wells. Therefore, domestic and water supply wells surrounding AS-029 inside a range of 1.5 miles, were considered for well monitoring. Right of Entrance (ROE) documents were sent to all of the well owners of The Plains and the City of Athens Water office. We were able to gain ROE from one of the property owners of The Plains and the City of Athens Water granted us access to two of their

monitoring wells. Therefore, the total of wells used for monitoring were three monitoring wells, 1 well North and 2 wells South (Figure 10). The well to the north is a domestic well labeled as The Plains, the two wells to the South are water monitoring wells from The City of Athens wells are labeled A10 and A12 as seen in Figure 10. Sensors to measure barometric pressure, head, conductivity and temperature were installed in the wells from July 4, 2019 until January 28, 2020. These recorded barometric pressure, hydraulic head, conductivity and temperature.

### Figure 10

*Location of the wells where sensors were installed for monitoring hydrological parameters.*



### ***Temperature, Pressure and Hydraulic Head Sensor Installation and Data Collection***

Data collection of hydrological parameters were performed by installing sensors into each monitoring well. The hydraulic head, conductivity and temperature were measured using a Van Essen CTD Diver and the barometric pressure was measured with a Van Essen Baro. These measurements were taken every 5 minutes and the data was collected from the sensors bi-weekly or monthly and downloaded into the Diver program and exported as Excel files. Upon installation, an industrial water level indicator was used to record the depth to the water level and depth of the bottom of the well. The sensors were left installed at the same depth for each data collection event, to ensure data accuracy.

### ***Water Well Properties***

There are two groups of water wells: The City of Athens water wells and the domestic wells. The properties of the domestic wells were extracted from the well reports displayed in the Ohio Department of Natural Resources Water Well Locator Web map, these are displayed in Appendix C. The City of Athens provided the “2017 Groundwater Monitoring Report Drinking Water Source Protection Program” document where the water well details were displayed. These two sources provided water well properties such as coordinates, water elevation, well depth, geology, pumping rate and elevation. These properties were extracted and used for the construction of the physical model and groundwater model. For the physical model the stratigraphy found in the well log reports of the domestic water wells was considered to understand the underlying geology of the area. The water level found in the reports were plotted to construct potentiometric maps

to establish flow regimes. The pumping rate, and well depth were used to input them in the pumping well parameters in the groundwater model.

### ***Geographical Data of the AUMs***

Physical characteristics of the mine were studied. Geographic data such as mine code, mine name, API number, operator name, abandonment date, flooded or partially flooded, mine volume, coal seam and the mine's elevation were extracted from the Ohio Department of Natural Resources mine web map. An estimation of the coal seam thickness, coal elevation, average depth of the mine and surface elevation were extracted from digital elevation models of the Middle Kittaning coal and surface through ArcMap and the Ohio Department of Natural Resources mine web map.

### ***Stratigraphy of the Mine Area***

For the purposes of the physical model, the underlying geology was important for constructing stratigraphic layers in the model. The water well log reports from the Ohio Water Wells ODNR map viewer were used to produce stratigraphic cross sections of the area. However, the well log reports had a lack of continuity in the strata making it harder to correlate the stratigraphic layers. The geology of this area is characterized by cyclothems produced by the rising and lowering of sea level during the deposition time. However, because this area was a coastal area and the stratigraphy was interrupted by rivers and other features, often the layers lack continuity and it is difficult to follow a continuous layer in the geological cross section. Therefore, the Geologic map of Athens County was considered to identify the geology of the area (Sturgeon, 1958). The area of The Plains is mostly Pleistocene Illinoian Terrace dominated by sand and gravel of the

Quaternary. This geologic unit was considered as the uppermost sandstone layer.

According to Sturgeon (1958) the area surrounding the Hocking River is composed of Recent Alluvium mainly composed of river valley sediments. This geologic unit was added as the river valley sediments layer. Due to the discontinuous layers of the cyclothem a mix layer was added in underlying layers where the geological layers are not continuous. Digital elevation model (DEM) of the coal layer were examined to know the depth of the coal layer and add it to the model. The coordinates and coal elevation of the mine AS-029 were obtained from the Mines of Ohio Map Viewer from the Ohio Department of Natural Resources webpage and were used to add the mine layer with a top and lower surface for the mine. The lowest geologic unit is the shale layer below the coal since in most cases there is a layer of shale surrounding the coal layer.

#### ***Average Precipitation, Ambient Air Temperature and Barometric Pressure***

The following data was provided by the Scalia Laboratories weather station in Athens, Ohio located about 4.6 miles to the south of AUM AS-029. Hourly measurements were taken of the ambient air temperature and precipitation data from the dates July 4, 2019 until January 28, 2020.

#### ***Storage, Porosity and Conductivity Properties of Rocks***

The storage, porosity and conductivity properties of the rocks present in the overlying strata were collected from literature to include in the hydrogeological model (Twumasi, 2018; Fetter, 2001; Freeze and Cherry, 1979; Domenico and Schwartz, 1990). These values were included in the respective strata layers of the hydrological model and then calibrated and modified to get a minimum percent of error.

## **Data Analysis and Modeling**

### ***Transient Data Analysis***

A transient data analysis of the head, well temperature, air temperature and precipitation were performed. The hydraulic head, well temperature and conductivity data were extracted from the sensors installed in the three wells surrounding the mine. These values were originally taken every 5 minutes and later averaged to hourly and daily measurements. The precipitation and air temperature data were collected from the Scalia Laboratory in Athens, these values were originally hourly and later averaged to daily measurements. Autocorrelation and cross-correlation data analysis were performed with the program PAST (Hammer et al., 2001) to determine lag times between hydraulic head and precipitation, temperature and precipitation, as well as lag times between heads and temperatures between different wells. This information was used to determine the travel time of the recharge and heat pulses produced by precipitation.

### ***Visual MODFLOW Groundwater Model***

MODFLOW is a finite-difference flow model software introduced by the United States Geological Survey (USGS) to simulate groundwater flow (Harbaugh, 2005; Hariharan and Shankar, 2017). For this project, Visual MODFLOW a graphical user interface for the USGS MODFLOW, was used to construct a groundwater flow model of AS-029. Visual MODFLOW is mainly used for groundwater flow and contaminant transport models, it is different from MODFLOW since it does not use only text files as input data it uses Excel files, Surfer grids, GIS and AutoCAD data as input files making it

faster (Hariharan and Shankar, 2017) . For this project, Surfer grids, Excel files and GIS files were used to input data into the model.

A groundwater flow model helps understand how the water flows through an area depending on the hydraulic parameters and geology of the area. Visual MODFLOW is divided by the input, the run module and the output module which allows you to visualize the results. Information gathered from the results of the output model can help calculate the rate and direction of movement of groundwater (Khadri and Pande, 2016). It can also help to calculate how much water flows through a system, the velocity at which the water flows and the zone budget of specific areas. In the input model Visual MODFLOW has the tools to specify which cell corresponds to specific parameters such as geology, hydraulic conductivity, storage, specific yield porosity, zone budget, constant head and other different hydrological boundaries which are chosen depending on what is the aim of the model. The run module is where the user specifies what MODFLOW parameters it wants to run and to specify if it will be a steady state model or transient model. The output system of a groundwater flow model presents all the results and the hydraulic heads and groundwater flow rates with the specific parameters which are then are calibrated and adjusted to reduce bias of the simulated hydraulic head (Khadri and Pande, 2016). Groundwater flow models of underground coal mines have been previously done. Twumasi (2018) created a groundwater flow model for the Meigs Mine Complex in Meigs County, Ohio to understand the hydraulic conditions for the formation of mine pools and use that information to predict the formation of mine pools in future mines.

The groundwater model of AS-029 was created by gathering information from geologic maps, Digital elevation models, hydrological parameters, well logs, monitoring wells and pumping wells. Digital elevation models (DEM) were used to extract elevation values from the coal and topographic surface from ArcGIS Pro and then import these values to Visual MODFLOW. The surface elevation was used as the top of the upper layer and the coal as the middle layer. The model has basically 5 layers: sandstone layer, river valley sediments layer, a mixed layer for the discontinuous layers of the cyclothem, coal layer representing the Middle Kittanning coal seam, and a shale layer underlying the coal. The layers were assigned by using the “Add Layer” tool and subdividing the layers to have more nodes. The final grid has a total of 48 nodes in the E-W direction and 56 nodes in the S-N direction. The geologic units for this model were assigned initial values of hydraulic conductivity, porosity, specific yield and storage values to its respective cells according to the results of previous works in the area (Twumasi, 2018). Those values were changed to calibrate the model. The monitoring wells were added to the model as head observation wells and some of the pumping wells surrounding the mine were added as pumping wells to the model. Four pumping wells were located in The Plains (domestic wells) and four were the City of Athens pumping wells located to the South in the Hocking River valley. The average hydraulic head recorded from the sensors installed in the monitoring wells was used to input them into the head observation parameters. The pumping rates found in the water well reports from ODNR and the City of Athens were inputted into the pumping well parameters. In order to simulate the average water level in the river, The Hocking River boundaries were assigned to the respective grid cells.

Before assigning the respective cells to the river the conductance of the river was calculated. MODFLOW river packages use the streambed conductance equation (CRIV) to calculate the ability of the riverbed to conduct flow from the river to the aquifer (McDonald & Harbaugh, 1998).

$$CRIV = \frac{K_r L W}{M}$$

C = Conductance

$K_r$  = vertical hydraulic conductivity of the riverbed

L = length of the of the river channel in the cell

W = width of the river channel

M = thickness of the riverbed

Values used to find CRIV in the river are illustrated in the Results and Discussion.

After entering all the hydrological parameters into the input model the next step was to run the model. It is important to verify the graph of the run model as a steady state model and to determine percentage of errors comparing with the 3 observation wells.

The percent of error was fairly high therefore, the model was calibrated by calibrating the hydraulic conductivity values of the geologic units, one by one, until it reached a minimum percent of error, and repeating the process to reduce the error even further.

After reaching the minimum percent of error a sensitivity analysis was performed by inputting parameters of porosity and hydraulic conductivity of the different lithologies and river conductance. The percentage change in the river conductance, hydraulic conductivity and porosity was calculated by multiplying the calibrated value by the percentage change multiplier (0.8,0.9,1.1,1.2). Each altered value was changed in the

model and ran again to see the change in the root mean squared in the output model. The percentage change were plotted on the x- axis with the associated root mean squared on the y-axis as a graph to determine how sensible the errors were to changes in the calibration variables.

The last step of the groundwater modeling was to perform a zone budget. The Zone Budget package in Visual MODFLOW calculates sub-regional water budgets with the results from the steady state simulations and with the sub-regional areas specified by the users. For this model, two sub-regions were used, Zone 1 are the cells surrounding the mine and Zone 2 are the cells inside the mine. With the zone budget, the volume of water per unit time circulating through the mine was calculated. The finished model was used to create a numerical model of the study site than can simulate the groundwater flow equations. Results from this modeling include the groundwater velocities and the amount of water flowing through the mine.

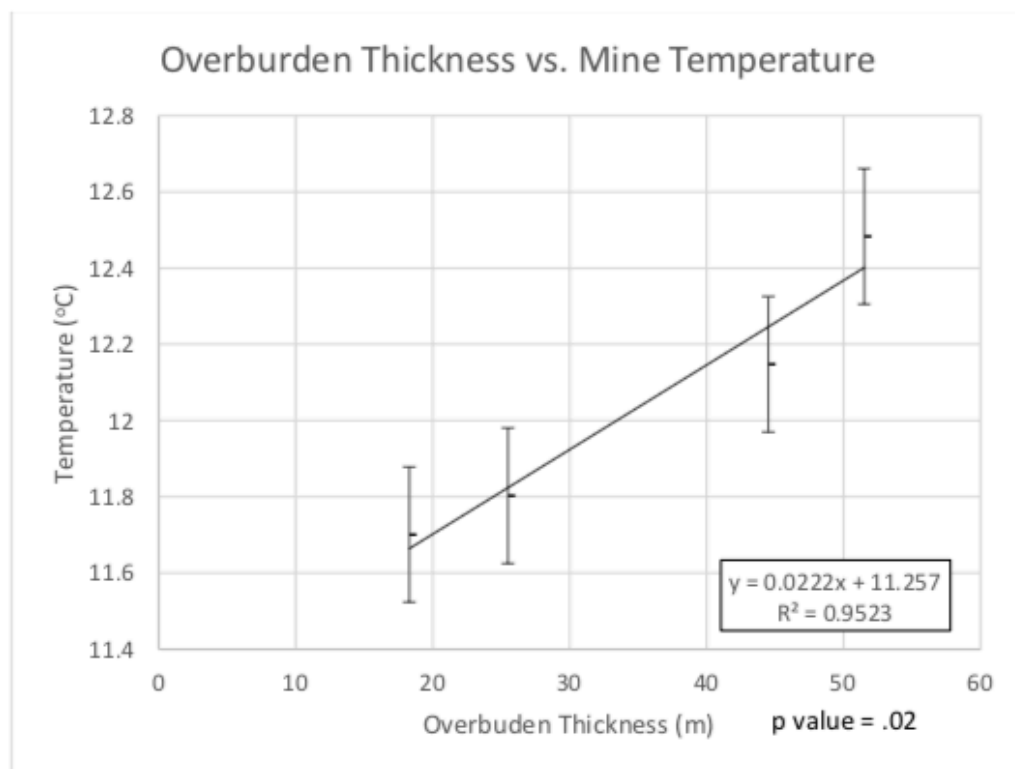
### ***Thermal Modeling***

Thermal modeling was performed by calculating the mine temperature using the overburden thickness temperature with the equation Richardson (2014) for the Corning Mine Complex in Perry County, Ohio, that has similar geology as AS-029. The calculated temperatures within the mine were used to create a temperature map with Surfer 12. The overburden thickness was calculated by subtracting the elevation of the surface from the top elevation of the coal. The thickness of the overburden value was then placed as the “x” value in the equation from Richardson (2014) to obtain

temperature values within the mine (Figure 11). The obtained values calculated from the equation were later imported into Surfer 12 to create a thermal map.

**Figure 11**

*Relationship between overburden thickness and mine temperature (Richardson, 2014).*



***Total Heat Extractable/Exchangeable within the mine***

To prove the mine's efficiency to exchange heat, the total heat that is available to extract or exchange from the mine was calculated with the following heat transfer equation extracted from Richardson et al., (2016):

Equation 1.1  $q=mC\Delta T$

Where:

$q$  – heat (kJ)

$m$  – mass of heat exchanger (kg)

$C$  – Heat Capacity of the Heat Exchanger (kJ/(kg\*°C))

$\Delta T$  – change of Temperature (°C)

A  $\Delta T=1^{\circ}\text{C}$  was used to obtain the heat exchanged per unit degree of temperature.

The water flowing through the mine was calculated in Visual MODFLOW with the Zone Budget package. This package uses the results from the steady-state model to calculate sub-regional water budgets (Harbaugh, 2005). As mentioned earlier, two water budget zones were specified for this model: Zone 1 and Zone 2. Once the zone budget grid cells selection was completed the next step was to run the steady-state simulation once again including the Zone Budget package. The resulting value of the water inflow or outflow Zone Budget 2, corresponding to the mine grid cells, was used to calculate how much heat could be absorbed by the mine per unit degree with the following formula:

$$\textit{Total heat exchange per unit time} = Fm * \Delta T * C$$

$Fm$  – Zone 2 water inflow or outflow (kg/s)

$C$  – specific heat capacity of water (4,186 J/kg°C)

$\Delta T$  – temperature change in the mine (°C)

## **Chapter 4: Results and Discussion**

### **Potentiometric Maps**

According to Majithia and Kohli (1997), potentiometric maps represent the pseudo-potentiometric surface of an aquifer and they are used to produce the direction of groundwater flow. The water well logs from ODNR were not used for stratigraphic purposes but they were considered for the physical model by using the well information such as: static water level, coordinates, surface elevation, aquifer identification, well ID and depth of well to construct potentiometric maps.

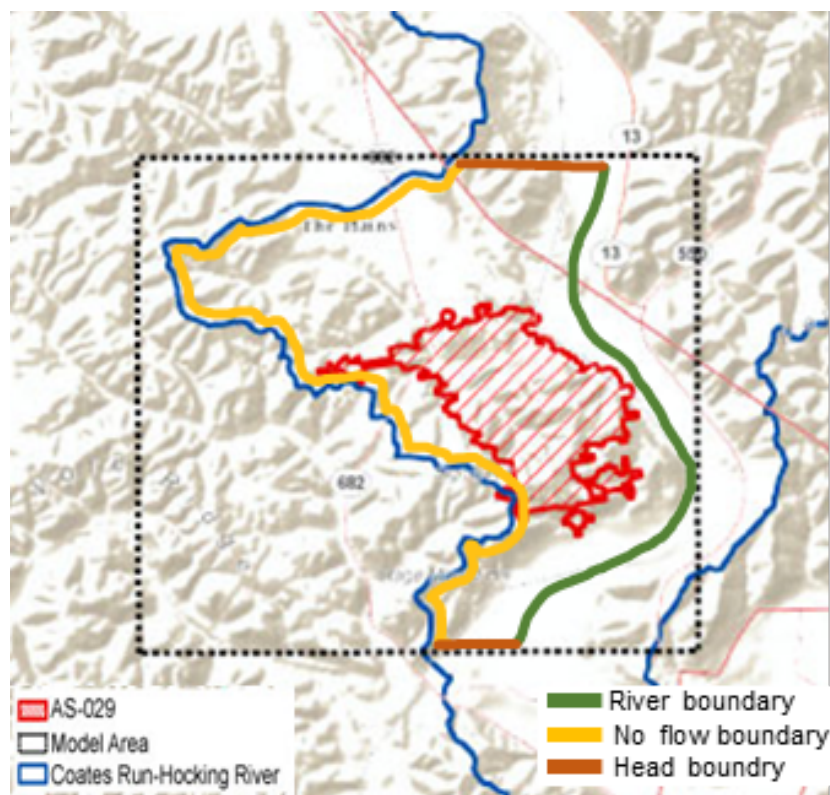
The potentiometric map for this study was constructed by importing the water level values and coordinates extracted from the wells from ODNR and the City of Athens into Surfer 12.0 using the kriging option (Figure 12). All the wells in this area were used for this map. The resulting Figure 12 shows that the water table is higher in the northern area where The Plains community is located and it is lower in the Eastern area. The effect of domestic pumping wells and pumping City of Athens wells can be observed in this map. They produce cones of depression in the water table map.



watershed boundary and the southern boundary which are both considered no flow boundaries. The green line represents the river boundary of the Hocking River. The orange line are the constant head boundaries that were obtained from the water table map mentioned in the previous section (Figure 13).

### Figure 13

*Area selected by using the watershed boundaries and Hocking River boundaries inside the study area. Yellow line represents the no flow boundaries, green line is the river boundary and the orange line is the constant head boundary selected for the purposes of modeling.*



Hydrogeological parameters, topography, stratigraphy and watershed boundaries were used to construct a physical model of the area surrounding AS-029. As it was discussed earlier, the well log reports from the ODNR webpage presented discontinuity making it difficult to correlate the strata. Therefore, the stratigraphy of the area was determined by creating cross-sections with the information gathered from the Geologic map of Athens County (Sturgeon, 1958), digital elevation model (DEM) of the Middle Kittanning Coal, DEM of the topography, and the mine shapefiles from ArcGIS (Figure 14, 15). The origin of each layer are explained below. The sandstone layer represents the area of The Plains is mostly dominated by sand and gravel. The river valley sediments layer represents the valley of the Hocking River which is mainly composed of alluvium sediments. The mix layer symbolizes the areas where there was discontinuity in the geology. The Middle Kittanning Coal and the AS-029 layer represent the area where the mine and coal are present. Lastly, the shale layer represents the typical layer of shale that is found surrounding a coal layer. The hydrological parameters (storage, conductivity, porosity) of these layers were extracted from literature and further on added to the groundwater model.

**Figure 14**

*Geologic map of Athens used to construct the stratigraphic cross section (Sturgeon, 1958). The red line represents the area used for the cross section.*

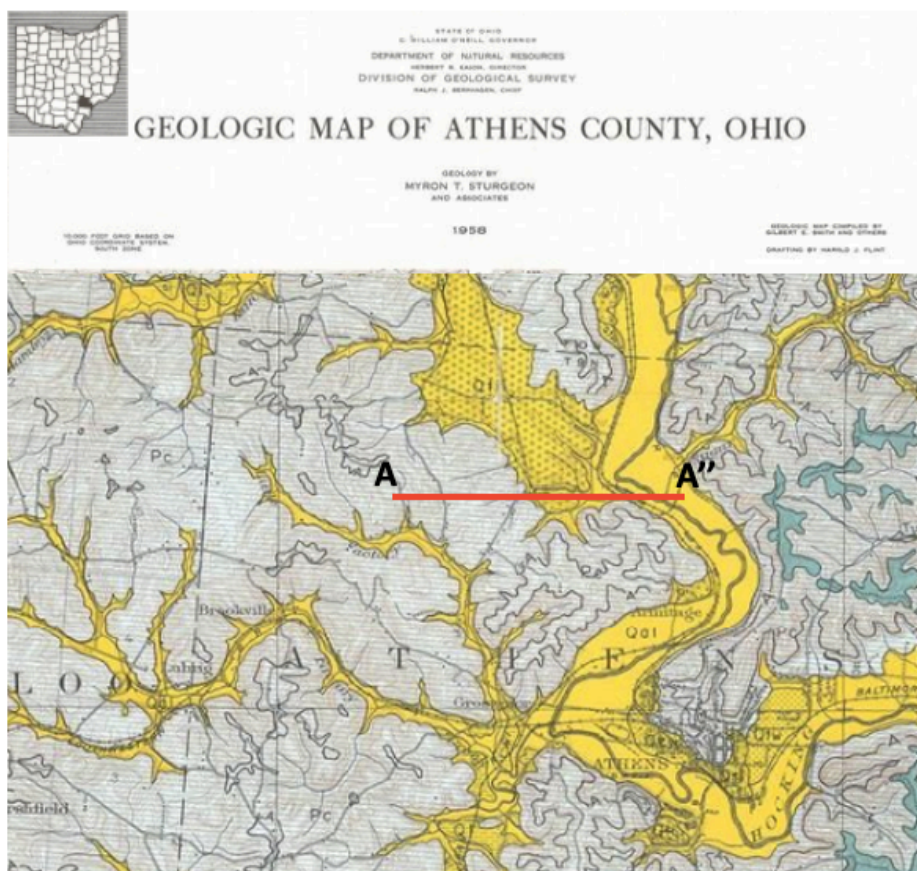
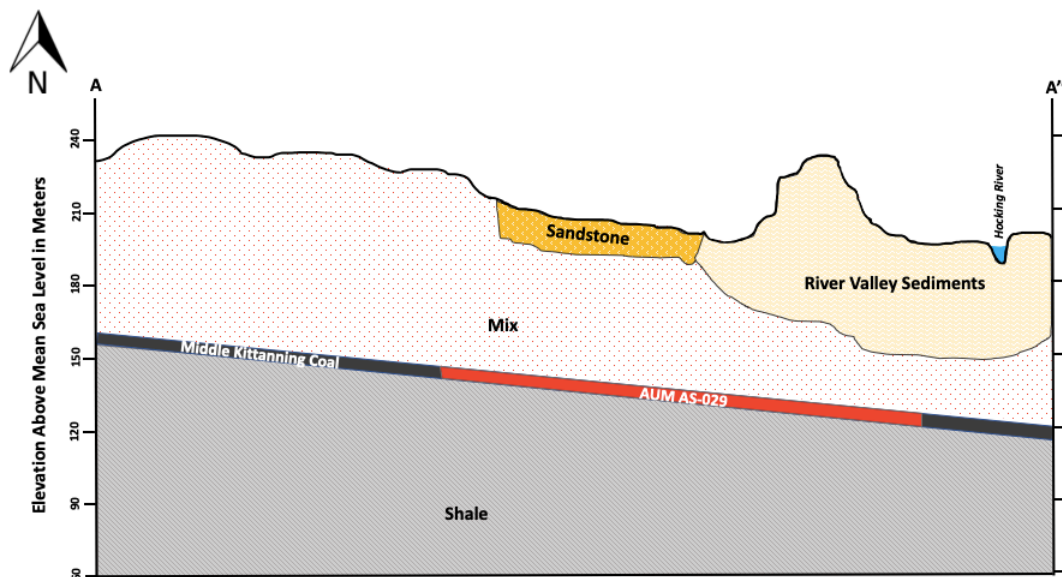


**Figure 15**

*Cross section constructed with the information gathered from the geologic map, well logs and digital elevation model of the coal and topography. Coal layer is represented as twice its original size for better representation.*



### Monitoring Wells

After collecting data for approximately 6 months, the data was organized in Microsoft Excel and certain calculations were performed. The average conductivity, barometric pressure, water level, and conductivity was calculated resulting in Table 1. A10 and A12 are the City of Athens wells and The Plains is the domestic well that was monitored. There was 1 Baro-Diver installed in The Plains domestic well where the for all the average barometric pressure was 1013.06 (cmH<sub>2</sub>O). The lowest average temperature recorded was of well A10, one of the City of Athens wells, this can be due to the fact that it is the shallowest well and it is nearer to the surface. Well A10 also

displayed the highest conductivity. Overall, the rest of the parameters did not differ much from each other.

**Table 1**

*Average values for the different parameters recorded by the monitoring wells for 6 months.*

<b>Monitoring Well</b>	<b>Depth of the well (m)</b>	<b>Pressure (cmH<sub>2</sub>O)</b>	<b>Temperature (°C)</b>	<b>Hydraulic Head (m)</b>	<b>Conductivity (mS/cm)</b>
<b>A10</b>	14.33	1347.84	12.16	188.05	4.41
<b>A12</b>	16.76	1423.30	12.38	187.29	0.46
<b>The Plains</b>	21.03	1251.07	13.74	202.94	0.38

### *Transient Data Analysis*

**Precipitation vs Hydraulic Head.** The data of the monitoring wells was plotted together with precipitation data from the Scalia Lab as a function of time for correlation and cross correlation purposes. The hydraulic head recorded from the sensors in the monitoring wells was plotted with the precipitation as seen in Figure 16. The decreasing head could be produced by the months with lower precipitation and lower recharge. In these graphs a noticeable pattern is observed, after heavy rain events the water head rises.

Cross-correlation analysis was done with the program PAST (Hammer et al., 2001) to identify the lag between the two variables that correspond to the highest correlation coefficient. The point of maximum and minimum correlation coefficient represents the lag time between two variables. It can be a positive or negative correlation. Wells A10 and A12 both have lag times of 88 days, correlation coefficient of 0.18 and p-values of 0.04 (Appendix B1, B2). The Plains well has a lag time of 49 days, a correlation

coefficient of 0.18 and a p-value of 0.03. Therefore, they all have a correlation between precipitation and hydraulic head. However, the lag time of The Plains well is the lowest (Figure 17). This may be due to its topographic location since The Plains well is farther away from the river valley and it is at a higher slope. Probably the infiltration water reaches first The Plains Well and water continues its circulation until it reaches the river area reaching the city wells later. The city wells receive vertical infiltration as well as water moving laterally towards the river.

**Figure 16**

*Precipitation (Scalia Lab) and the hydraulic head recorded from the monitoring wells.*

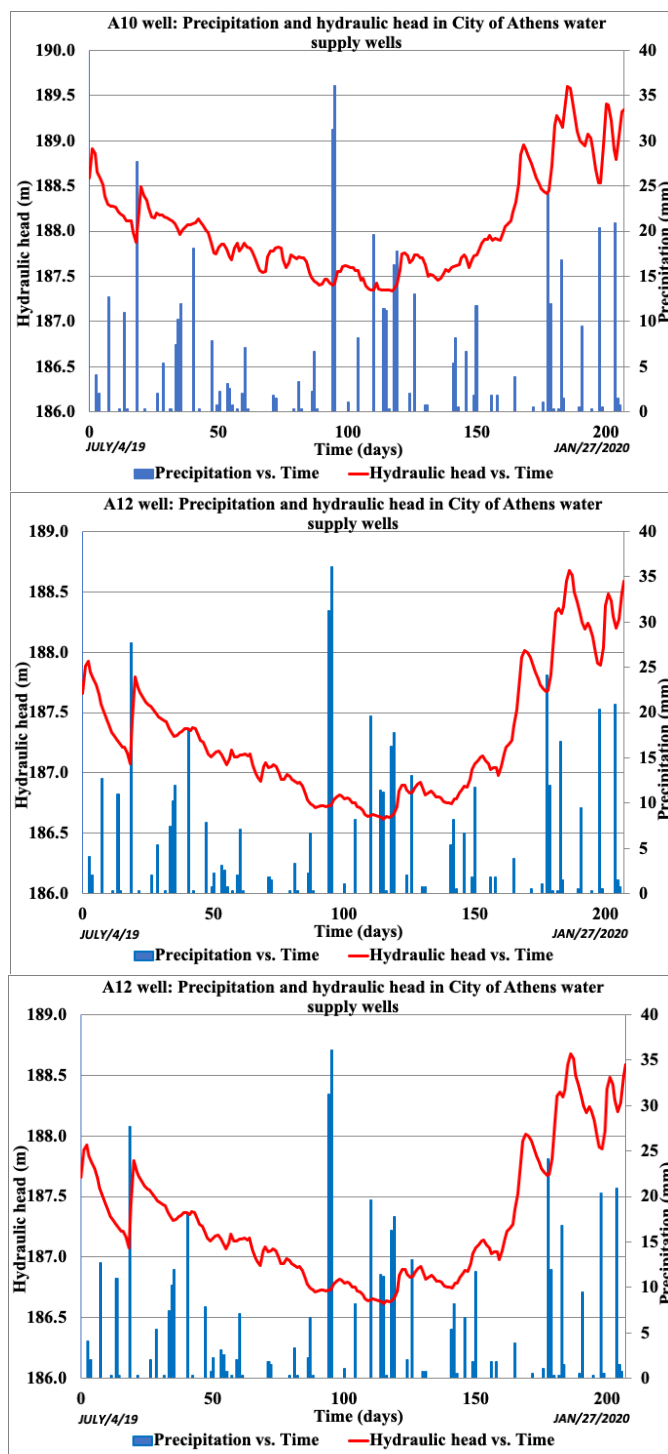
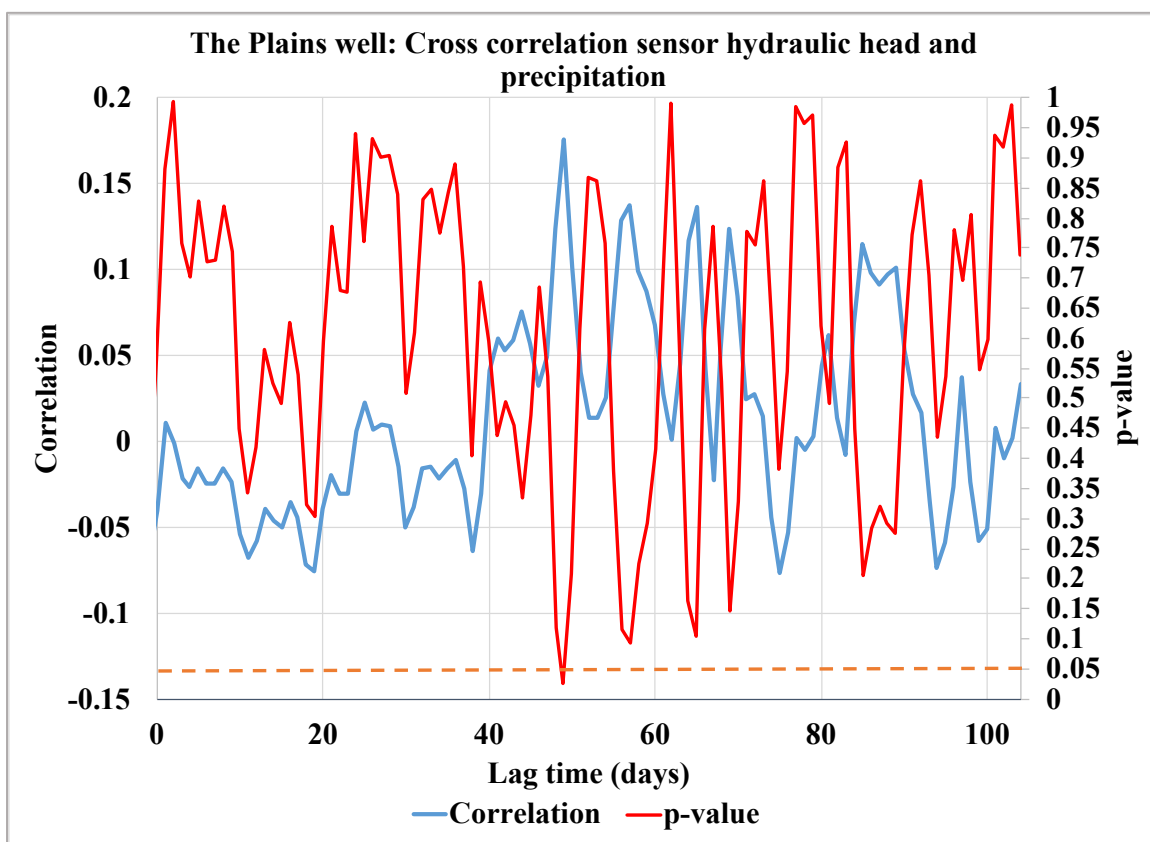


**Figure 17**

*Cross correlation of the daily hydraulic head recorded from The Plains monitoring well and the daily precipitation from the Scalia Lab. The orange dashed line represents the 0.05 value for the p-value.*



**Precipitation vs Conductivity.** As mentioned earlier well A10 was the well with different values from the rest of the wells and the highest conductivity. According to the City of Athens Water there used to be an old brine well 20 yards away from A10. Therefore, the high conductivity may be due to the proximity of the old brine well to A10, this brine well has been creating a chloride plume in the wellfield for many years. As seen in Figure 18 high precipitation events increased the conductivity some time after

precipitation. This is probably due to infiltrating water possibly mixing with the salt layer from the old brine well and groundwater flow transporting the brine to A10. This old brine well had been previously plugged and abandoned, however, the Ohio Department of Natural Resources funded a re-abandonment of the brine well in September 2019 to see if the chloride levels will start to decrease.

In order to determine the lag time of precipitation and conductivity, cross-correlograms of precipitation and conductivity were performed using the program PAST (Hammer et al., 2001). For conductivity and precipitation in well A10, the cross-correlogram of conductivity and precipitation is very complex, showing at least four points with correlation that have p-values lower than 0.05. However, the higher positive peak showed a lag of 103 days, a correlation of 0.29 and a p-value of  $p < 0.001$  (Figure 19). Even at zero lag the correlation was significant but with a lower value for the correlation coefficient. There is also a good negative correlation at 68 lags probably showing some dilution effects due to some rainfall events. Therefore, the p-value is lower than 0.05 confirming that there is a significant correlation between precipitation events and conductivity at well A10. The other wells were also plotted for precipitation and conductivity but there were no significant correlations between these variables for Well A12 and The Plains Well.

**Figure 18**

*High conductivity values recorded from the sensor installed in well A10. Red lines represent conductivity and blue line represents precipitation.*

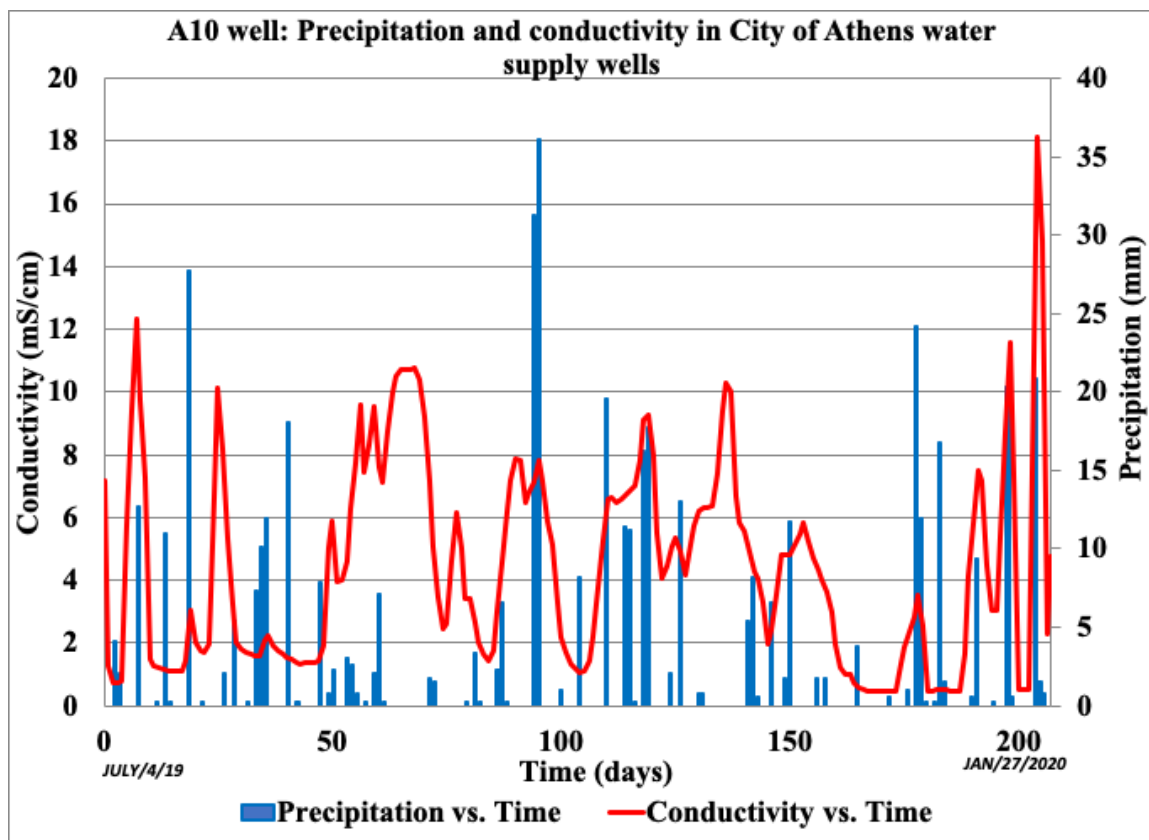
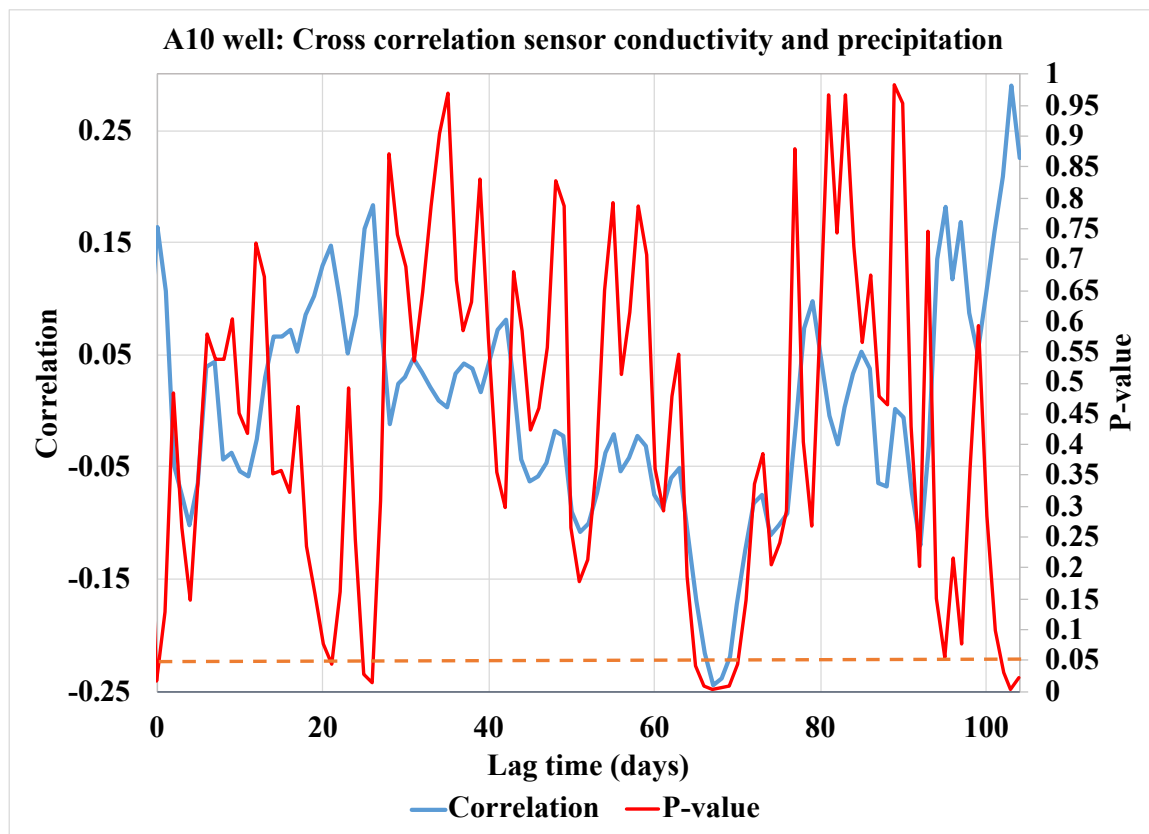


**Figure 19**

*Cross correlation of the daily hydraulic conductivity recorded from the A10 monitoring well and the daily precipitation from the Scalia Lab. The orange dashed line represents the p-value.*



**Precipitation vs Well Temperature.** The temperature recorded from the sensors installed in the well was plotted together with precipitation as a function of time to see if rain events or droughts affected the temperature of the well. As seen in Appendix A (Figures A4-A7), there are no specific patterns for the well temperature in the wells, the high periods of rain events do not show a consistent pattern of increasing or decreasing the temperature in the three wells. Most of the graphs display a relatively

constant temperature with a very small difference. Well A10 displays a difference of approximately  $\sim 0.2$  degrees Celsius in all the time period and well A12 a  $\sim 0.05$  degrees Celsius difference. However, The Plains well is the one with the lowest difference in temperature change of  $\sim 0.02$  degrees Celsius. The Plains well is the deepest well of all three wells, therefore, at deeper depths the temperature in water can remain more constant than if it is near to the surface.

Cross-correlograms were performed for sensor temperature and precipitation for all wells as seen in Appendix B (Figures B10-B12). The correlation coefficient and p-value for well A10 were 0.07 and 0.35 respectively and a lag time of 32 days, therefore there is no significant correlation between precipitation and sensor temperature in this well. The lag time is the lowest of all three wells since it is the shallowest well and it is near to the surface. The correlation coefficient and p-value for well A12 were 0.13 and 0.16 respectively and a lag time of 84 days, therefore, there are no significant correlation between precipitation and the sensor temperature in this well. However, The Plains well had a correlation coefficient of 0.27 and a p-value of  $p < 0.001$  with a lag time of 103 days. The correlogram of The Plains well has too much noise in the p-value making it harder to decide if there is a correlation or not between temperature and precipitation in this well. In general, we can say that if the infiltrating water affects temperature in these wells, the effect is very weak.

**Well Temperature vs Ambient Temperature.** Cross-correlation was performed for the well temperature values of each well against the ambient temperature. Well A10 has the lowest p-value of  $p < 0.001$  and highest correlation coefficient 0.91 value with the

lowest lag time of 33 days (Figure 20). This is because it is shallow and it is near the surface where the ambient temperature can affect the water temperature. The correlation in A12 is significant, the correlation coefficient is -0.67, a p-value of  $p < 0.001$  and the lag time is the highest with 104 days. Well A12 is the second shallowest, therefore it is still very near to the surface and the temperature in the water well can be affected by the outside temperature. The correlation coefficient and p-value for The Plains well were 0.17 and 0.06 respectively with a lag time of 87 days (Figure 21). Therefore, there is no significant correlation between temperature in The Plains well and the ambient temperature because it is the deepest well of all three monitoring wells and it is farther away from the surface where the ambient temperature cannot affect the water temperature. The temperature changes are damped at that depth. The average daily temperature values of each well were plotted against their depth (Figure 22). As seen in Figure 22, The Plains well is the deepest and shows the least variation in the temperature. This confirms the deeper the well the more constant the temperature in the water.

**Figure 20**

*Cross correlation of the daily temperature recorded from the A10 monitoring well and the ambient temperature from the Scalia Lab. The orange dashed line represents the 0.05 p-value.*

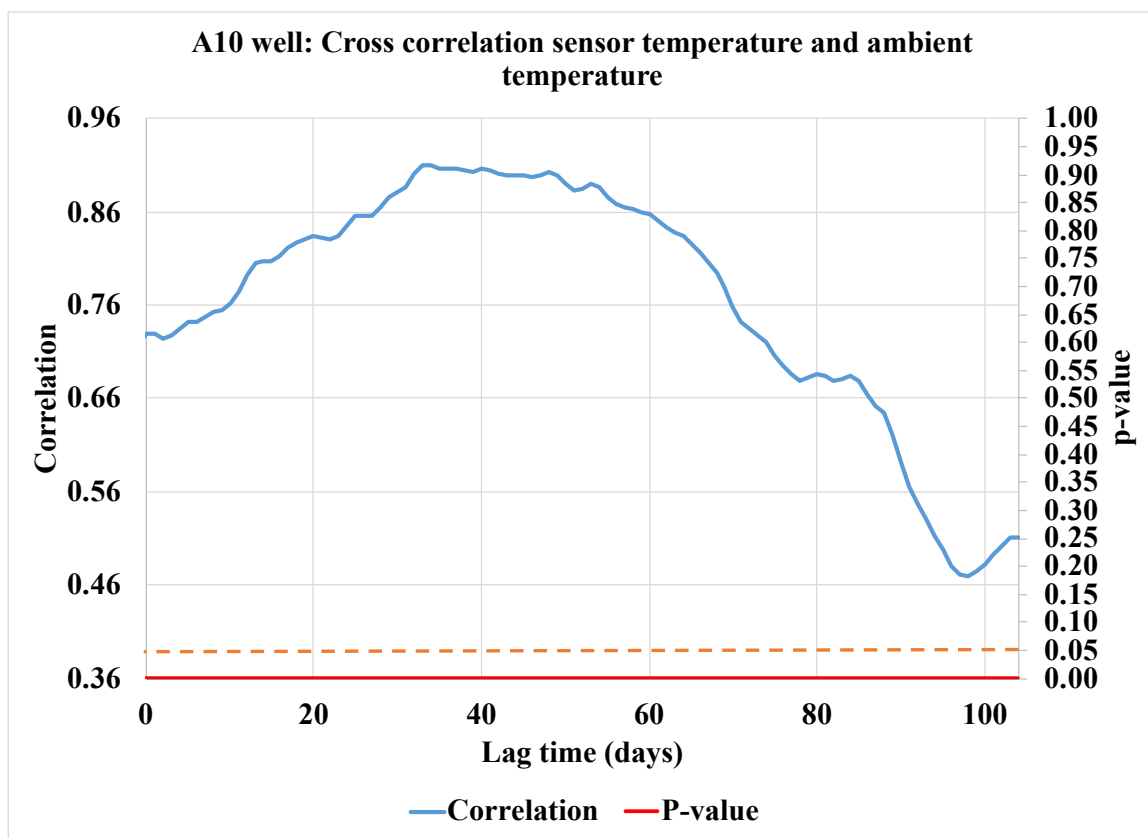


**Figure 21**

*Cross correlation of the daily temperature recorded from The Plains monitoring well and the ambient temperature from the Scalia Lab. The orange dashed line represents the 0.05 p-value.*

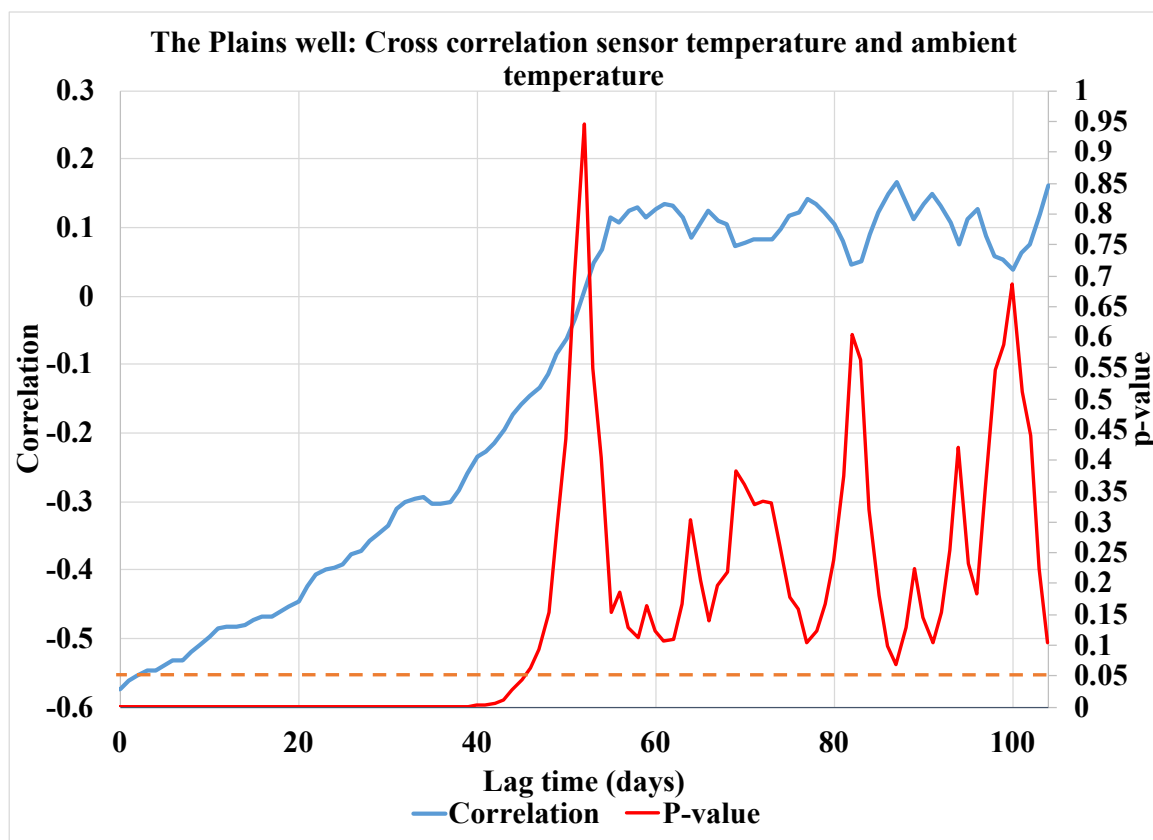
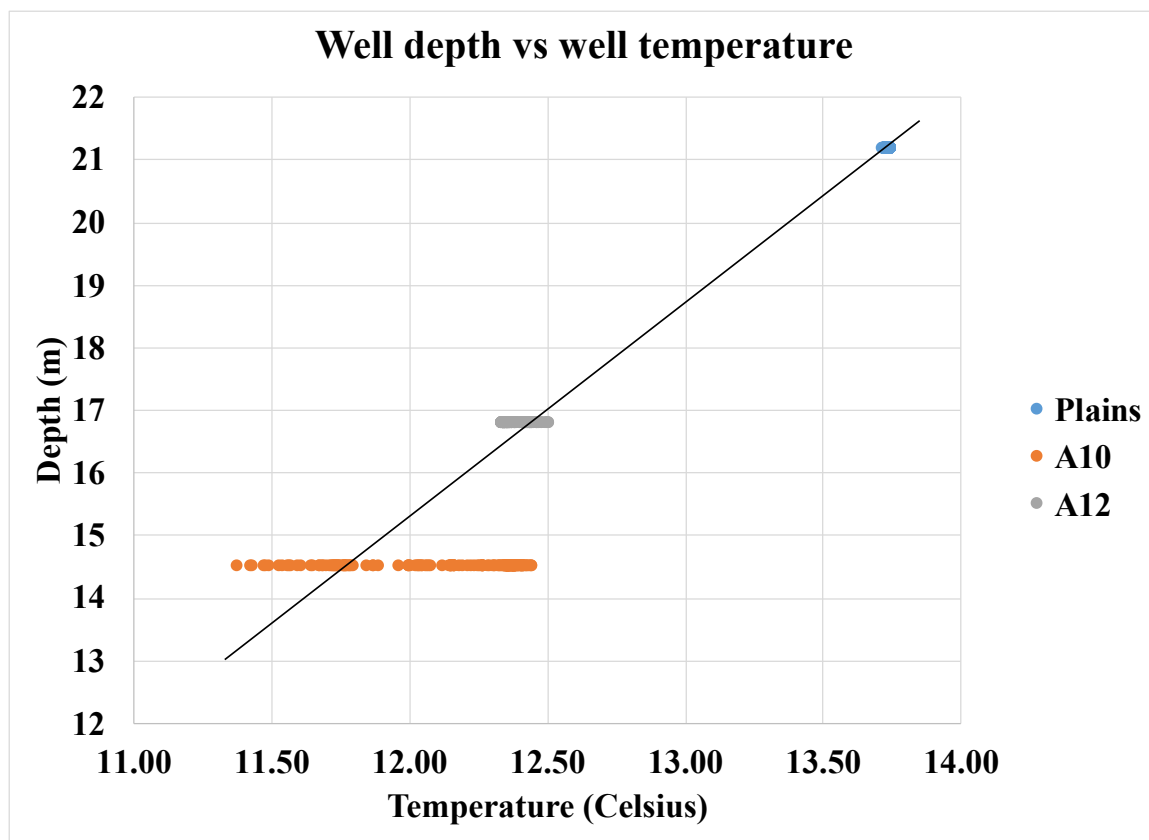


**Figure 22**

*Depth of the monitoring wells plotted against the average temperature recorded. The graph confirms that deeper wells have more stable temperatures.*

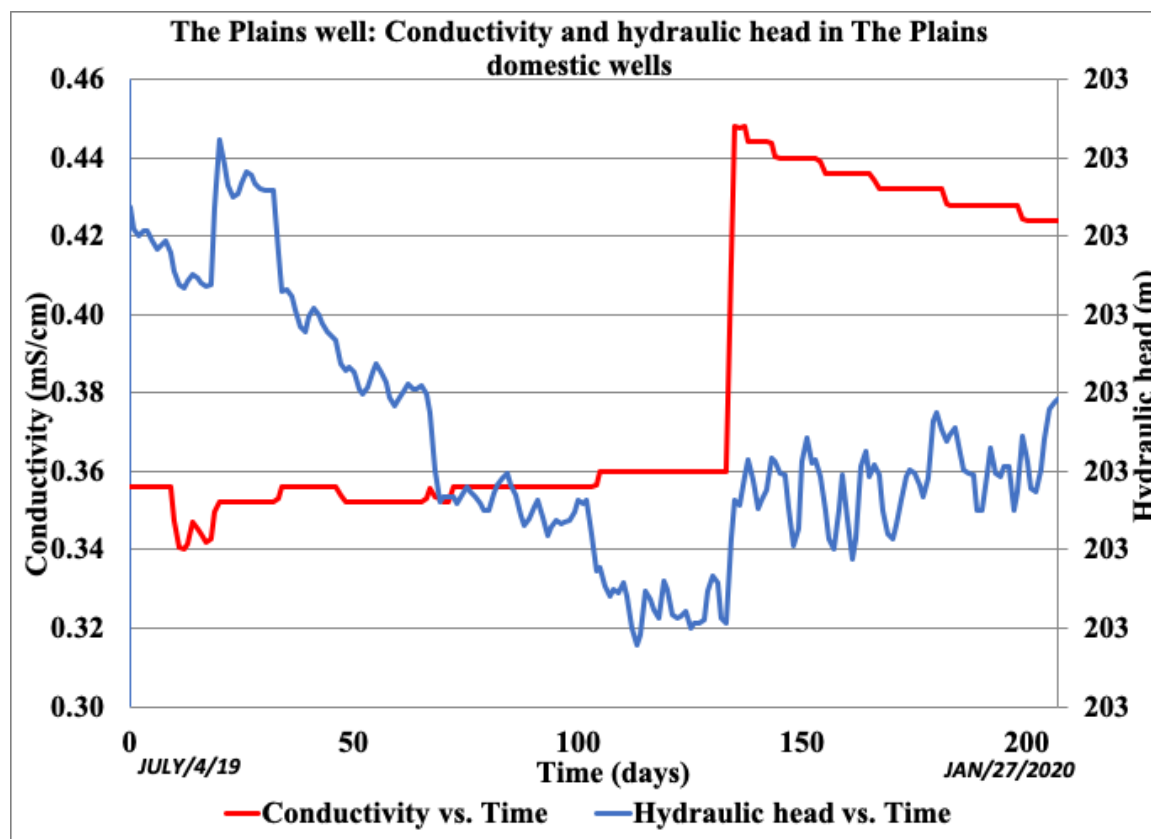


**Hydraulic Head vs Conductivity.** The conductivity recorded from the sensors installed in the well was plotted together with hydraulic head as a function of time to see if changes in water head had any effect on the hydraulic conductivity of the water in the well. As seen in Appendix A (Figures A6-A7), each well has a different pattern in the conductivity. For well A12 for most of the periods, when the hydraulic head increases the conductivity also increases. Well A10 has no specific pattern, lower or higher events of hydraulic head can decrease or increase the conductivity. This behavior for A10 and A12

is probably due to the proximity of the old brine well. The Plains well displays a very different pattern, as the hydraulic head decreases the conductivity increases and when the hydraulic head is high the conductivity is relatively stable (Figure 23). The stable conductivity in higher hydraulic heads may be due to more water diluting the water in the well and therefore stabilizing the conductivity.

**Figure 23**

*Hydraulic head and conductivity values recorded from the sensor installed in The Plains well. Red lines represent conductivity and blue line represents hydraulic head.*



**Hydraulic Head vs Well Temperature.** The temperature recorded from the sensors installed in the well was plotted together with hydraulic head versus time to see if changes in water head had any effect on the temperature of the water in the well. As seen in Appendix A (Figures A8-A10), there are no strong patterns for the well temperature in the wells. In the Plains well and A10 well as the hydraulic head decreased as the temperature increased. However, in the A12 well as the hydraulic head increased the temperature increased as well. Overall, the temperature changes are not drastic since the variations in the temperature are less than 1°C.

## **Groundwater Flow Modeling**

### ***Steady State Model***

Elevation values were extracted from digital elevations models in ArcGIS Pro of the coal and topographic surface (Figure 24). These elevation values were extracted with their coordinates and imported into Visual MODFLOW as grids. The initial grid of the model had a total of 56 columns and 46 rows with one layer representing the coal. The grid was modified by refining the columns and rows by two and by inactivating the cells outside of the watershed parameters. The final grid had 96 nodes in the E-W direction, 112 nodes in the S-N direction, and 32 nodes in the vertical direction. As mentioned previously, the boundary conditions for the modeled area were selected accordingly to the watershed boundaries and Hocking river streamline, therefore, the cells surrounding the outside of these boundaries were inactivated (Figure 25). Constant head boundary to the North of the model was obtained from the water table map from the previous Figure

12. A recharge value was assigned to the model with a start time of 0 days, a stop time of 1000 days and a recharge of 50 mm/yr.

**Figure 24**

*The square represents the area of the digital elevation models that was extracted from ArcGIS and imported into Visual MODFLOW.*

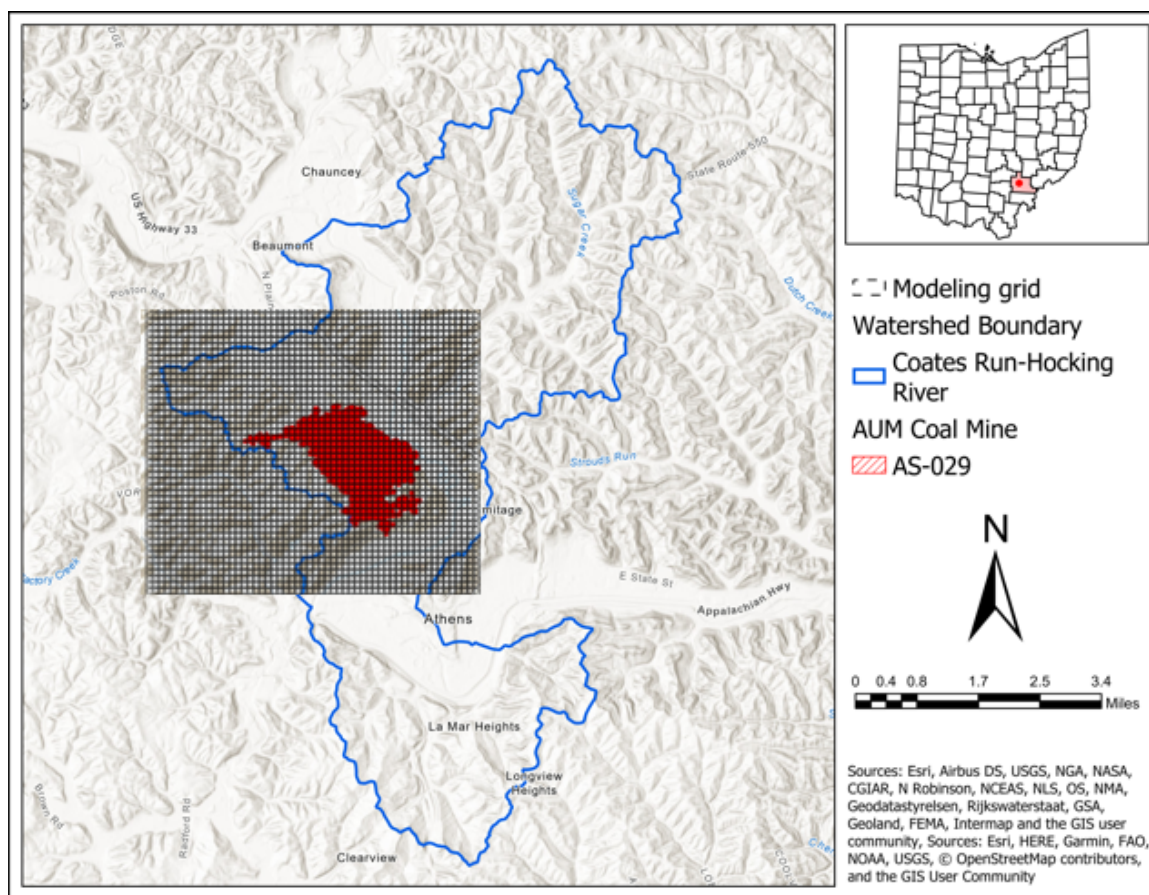
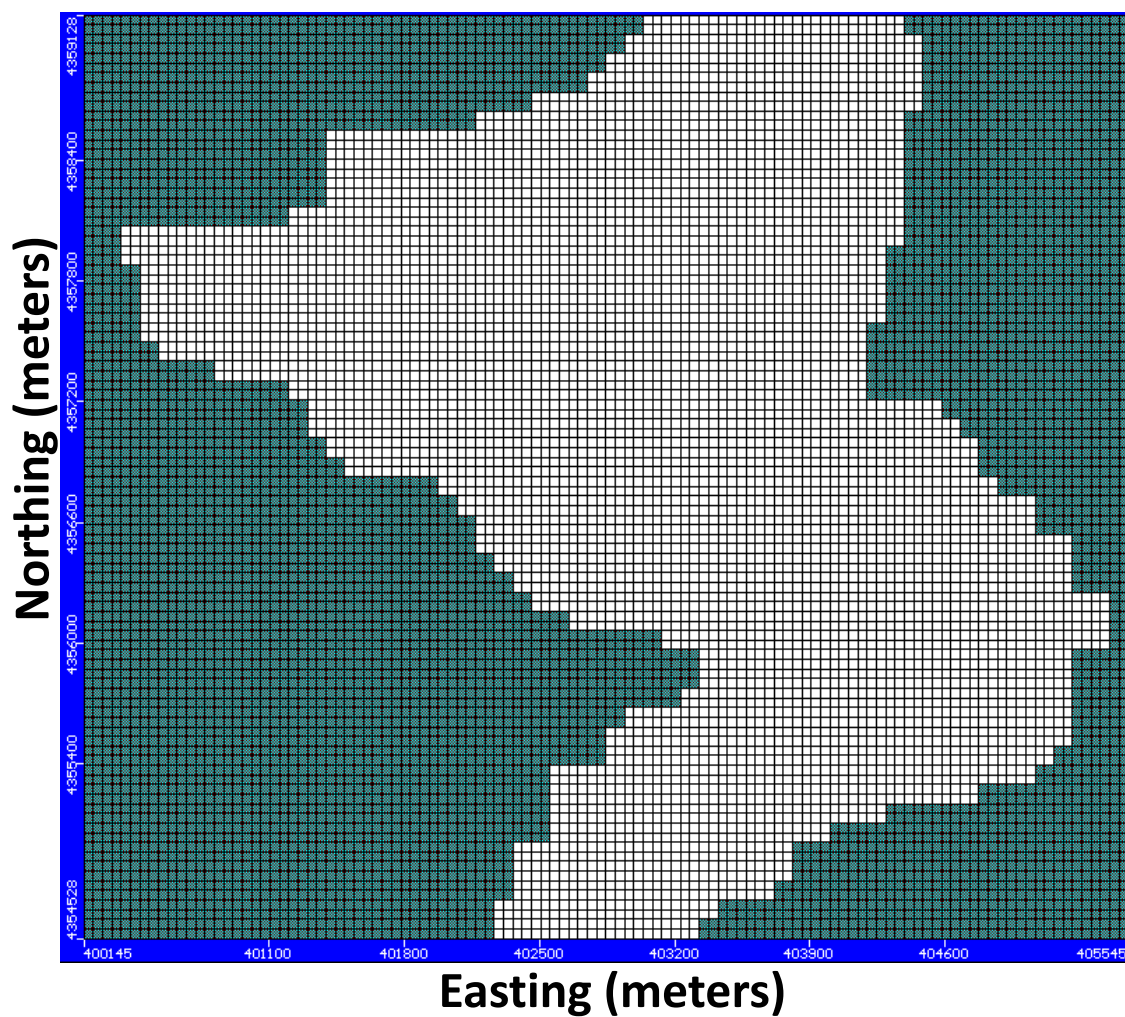


**Figure 25**

*Modeled area is represented by the white cells and the inactivated cells are the teal colored cells.*



The geology from the Geologic map of Athens County was considered to add more layers to the grid (Sturgeon, 1958). Layers were added to include the sandstone, river valley sediments, mine, shale, coal, mine top and a mix layer above the shale that

overlies the coal layer (Figure 26, 27). The corresponding cells for the mine area were assigned to the layers at which the mine is located (Figure 28).

**Figure 26**

*Map view of the geological units assigned to the model in their respective layers. The blue colored cells represent the Hocking River. The teal cells surrounding the modeled area represent inactivated cells. The red line represents the area covered in in the cross section in Figure 25.*

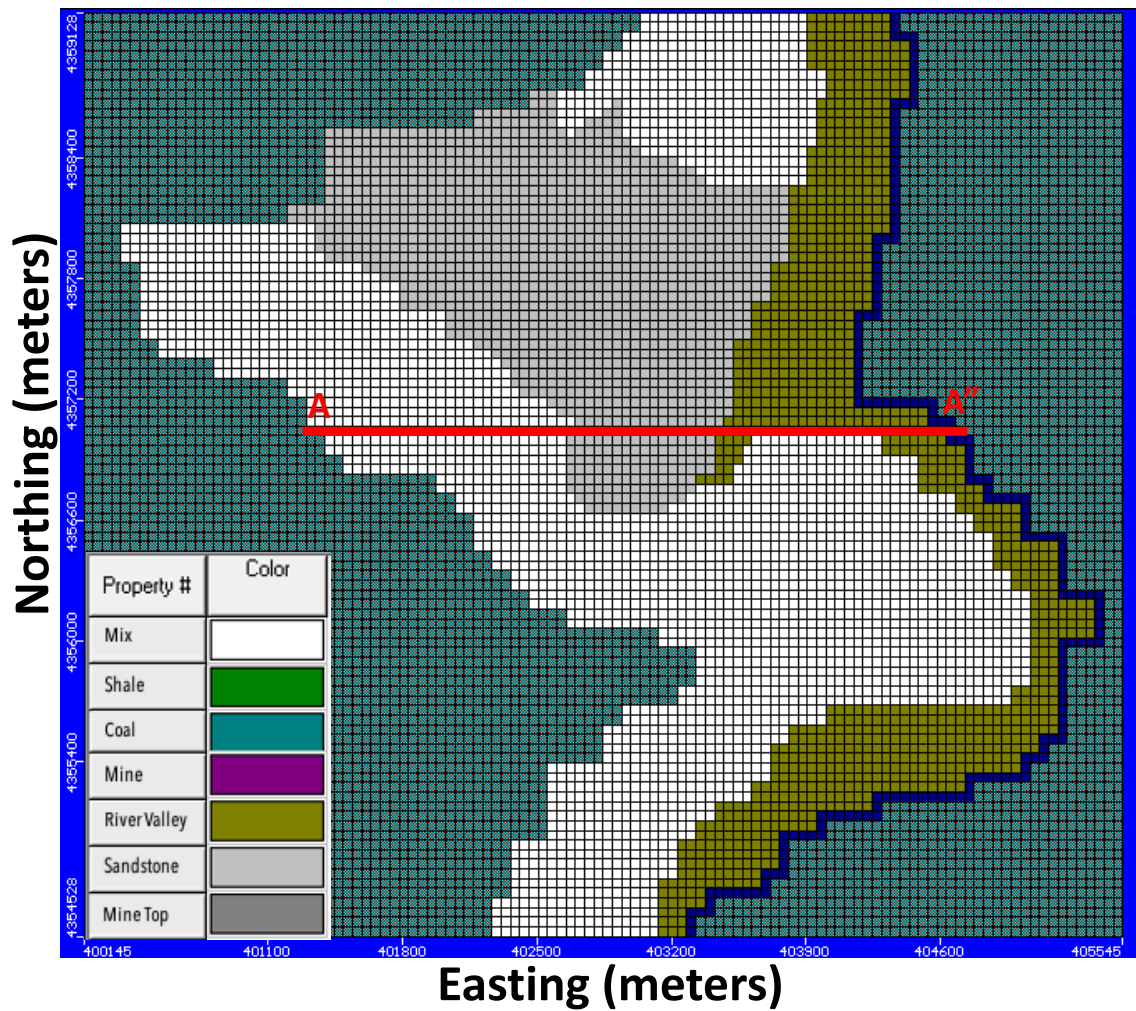


**Figure 27**

*Cross sectional view of the geological units assigned to the model in their respective layers. The blue colored cells represent the Hocking River. The teal cells surrounding the modeled area represent inactivated cells.*

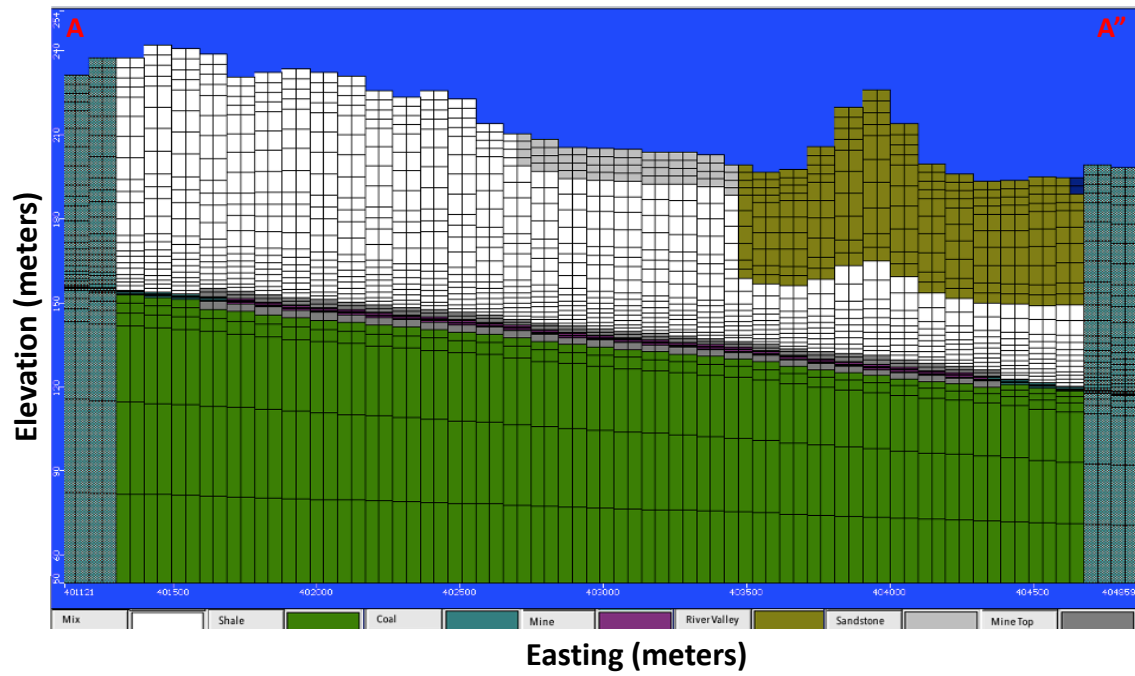
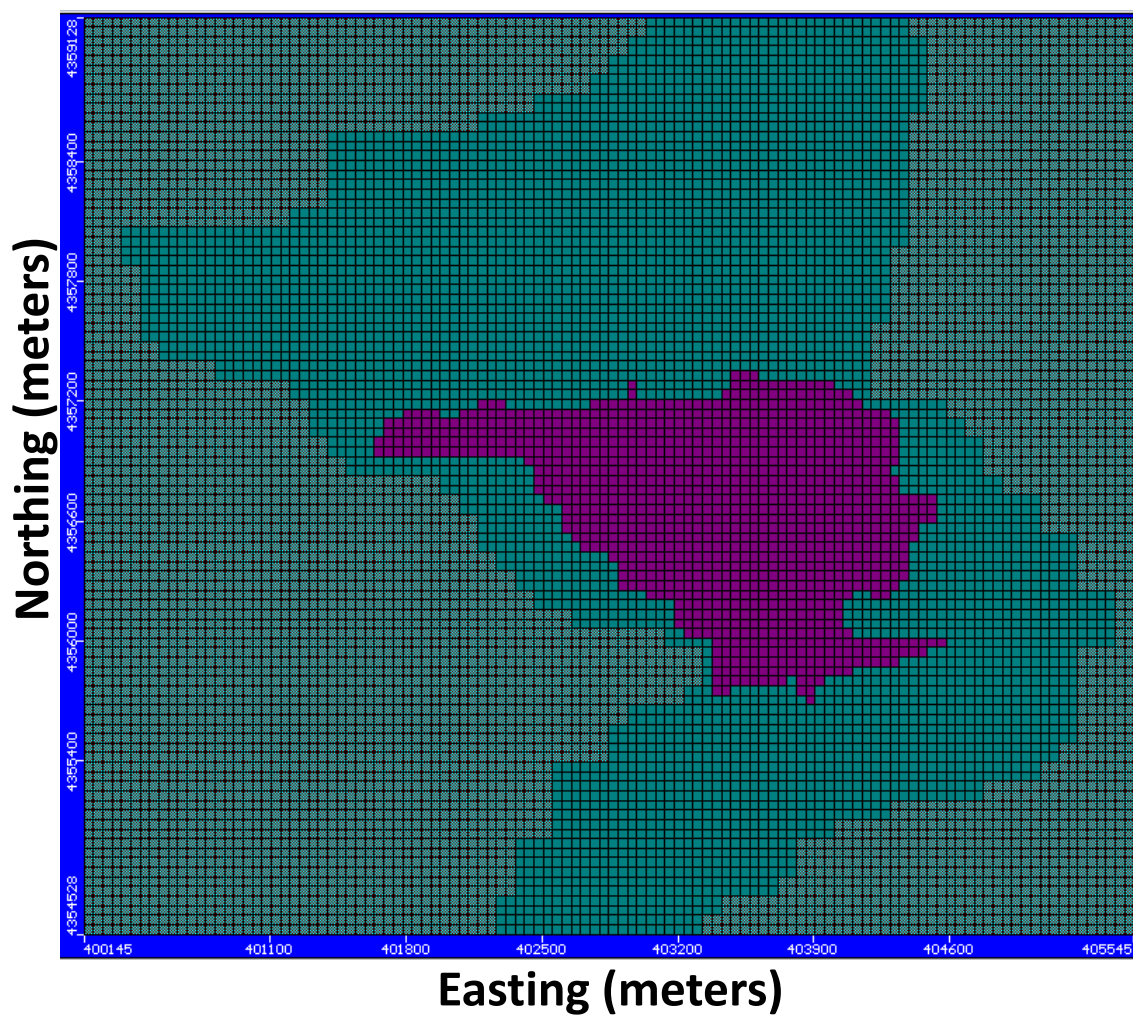


**Figure 28**

*Mine AS-029 assigned to its respective layers in the model. Fuchsia colors represent the mine, dark teal represents coal and light teal represents inactivated cells.*



The next step was to graphically assign the model input parameters for each of the geologic units. Initial hydraulic conductivity and porosity values for these geologic units were extracted from Domenico and Schwartz (1990), Freeze and Cherry (1979) and Twumasi (2018) and added to the respective layers in the grid (Table 2). The 3 monitoring wells were imported as head observation wells and the average static head was calculated for each well from the sensor data collection (Table 3). Other wells surrounding the head observation wells were imported as pumping wells and the average pumping rates in these were extracted from the Ohio Department of Natural Resources water well web map viewer and from the 2017 Groundwater Monitoring Report of the City of Athens (Table 4). After assigning the values to the head observation and pumping wells they were added to the model as represented in Figure 29.

**Table 2**

*Initial conductivity and porosity values assigned to geologic units prior to calibration. Time is irrelevant in this case because simulations are steady state.*

<b>Geologic Unit</b>	<b>Conductivity (m/day)</b>	<b>Porosity</b>
<b>Mix</b>	7.8E-5	0.15
<b>Shale</b>	9.90E-9	0.1
<b>Coal</b>	9.90E-8	0.1
<b>Mine</b>	5.00E-5	0.25
<b>River Valley Sediments</b>	8.62E-5	0.2
<b>Sandstone</b>	9.90E-6	0.2
<b>Mine Top</b>	6.00E-6	0.4

**Table 3**

*Values assigned to the head observation wells.*

<b>Head Observation Well</b>	<b>Head (m)</b>	<b>Elevation (m)</b>	<b>Time (days)</b>
<b>The Plains</b>	202.94	200.1	1000
<b>A10 City</b>	188.05	184	1000
<b>A12 City</b>	187.29	186	1000

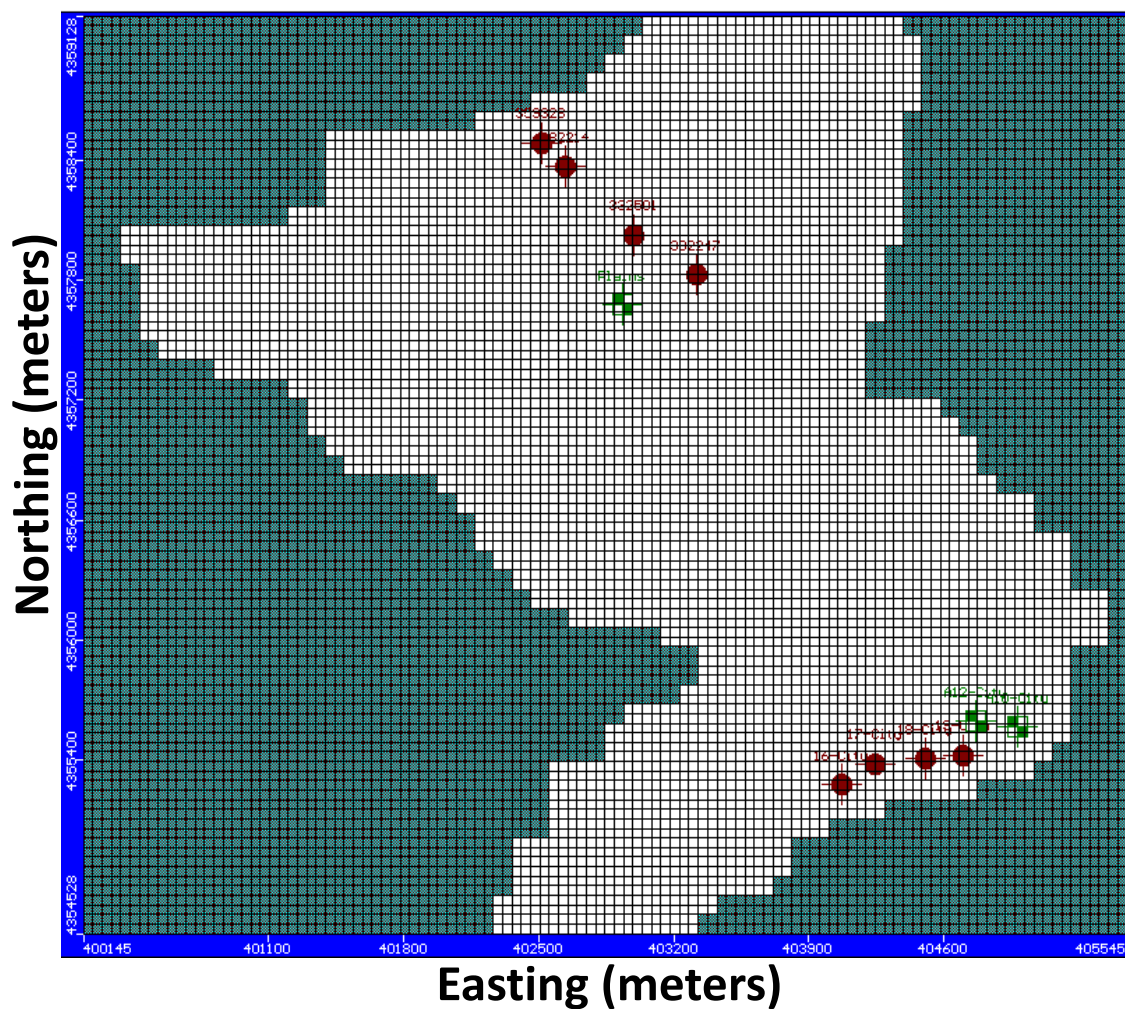
**Table 4**

*Values assigned to the pumping wells.*

<b>Pumping Well ID number</b>	<b>Screen Bottom (m)</b>	<b>Screen Top (m)</b>	<b>Time (days)</b>	<b>Pumping Rate (m<sup>3</sup>/days)</b>
359328	202	212	1000	-109
382214	202	213	1000	-196.2
332501	185	200	1000	-54
382247	202	208	1000	-163.5
19-City	175	186	1000	-1690
18-City	174	185	1000	-2044
17-City	174	185	1000	-2145
16-City	174	185	1000	-1936

**Figure 29**

*Water wells added to the model. The green circles represent the head observation wells and the red circles represent the pumping wells.*



The Hocking River boundaries were assigned to the respective grid cells to simulate the average water level in the river (Figure 30). Values for the river bottom elevation were extracted from [www.watersheddata.com](http://www.watersheddata.com) and values for the river stage were taken from the USGS gage station in Athens webpage. The ability of the riverbed to

conduct flow from the river to the aquifer was needed therefore the Conductance was calculated (Table 5). Constant head values were also added to the model. After inputting all the hydrological parameters, the run module was performed and the resulting graphs in the output presented a mean error of 5.32 m and a normalized RMS of 47.2%, which are consider as high values. Therefore, the initial values for the river conductance, hydraulic conductivity and porosity were later calibrated to reach a percent of error within acceptable criteria.

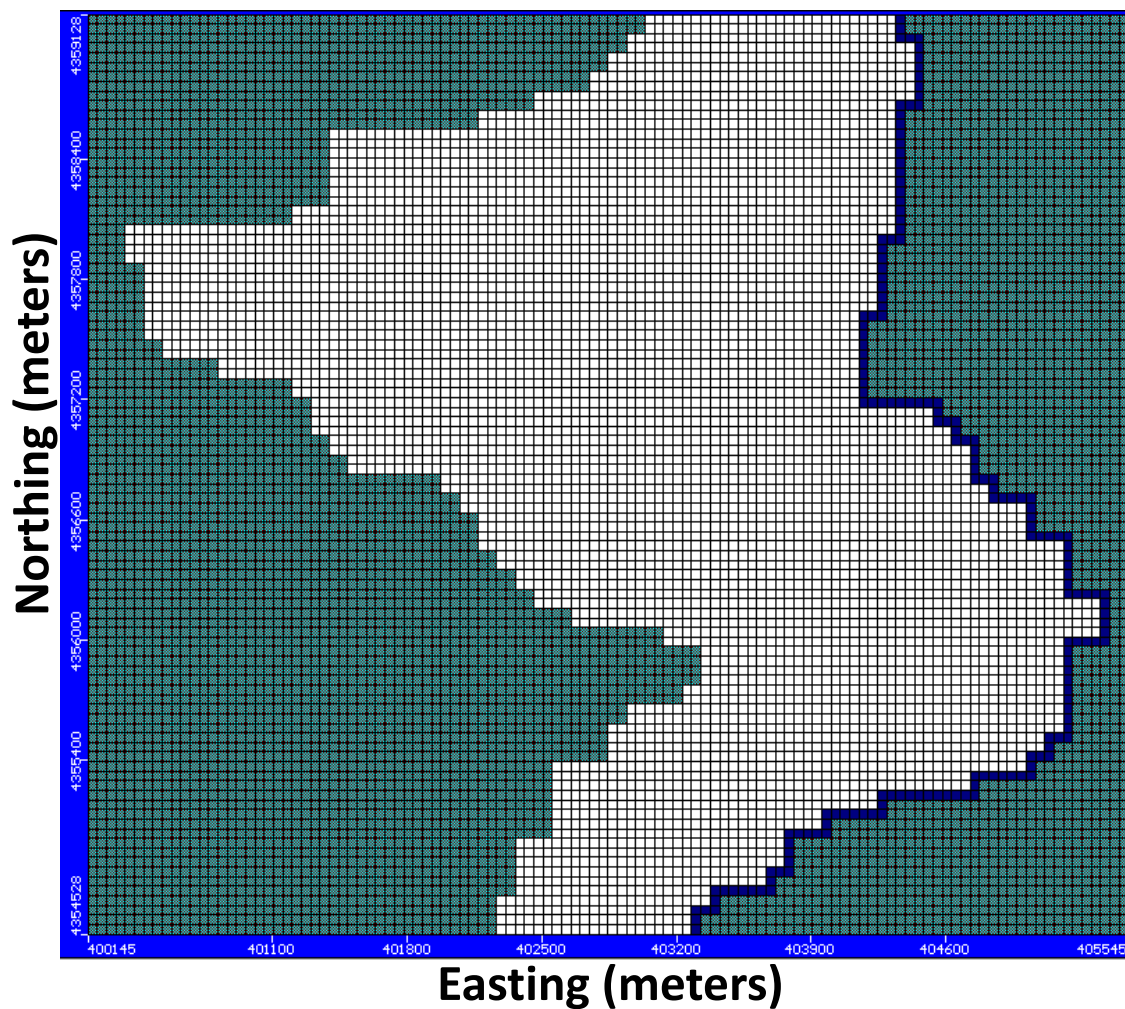
**Table 5**

*Initial values used for River Package in Visual MODFLOW prior to calibration.*

<b>Stream</b>	<b>Position of Stream</b>	<b>River Stage Elevation (m)</b>	<b>River Bottom Elevation (m)</b>	<b>Streambed Thickness (m)</b>	<b>Conductance (m/day)</b>
<b>Hocking River</b>	Beginning	196	194	1.22	4,645
	End	194.9	192.9	1.22	4,645

**Figure 30**

*River boundaries from the Hocking River assigned with its conductance values to the respective blue cells.*



### *Calibration of Steady State Model*

The original hydraulic conductivity values for the geologic units were calibrated and modified to get a minimum percent of error. Each input parameter was modified one per time. The resulting calibrated conductivity values are seen in Table 6. The original

river conductance was also calibrated to reach a minimum percent of error (Table 7). The original porosity values for the geologic units were also calibrated and modified to get a minimum percent of error, however, these did not display any change in the percent of error. The resulting graph and values can be seen in Figure 31 where all the wells fall inside the 95% confidence interval except for well A10. Typically, it is best to reach a lower mean error, however, after multiple calibrations this was the lowest value reached. The high mean error may be because there is not an exact representation of the stratigraphy of the area, consequently, the conductivity values of the layers cannot be calculated accurately.

**Table 6**

*Calibrated conductivity values of all the geologic units and the resulting mean error after calibration.*

<b>Geologic Unit</b>	<b>Conductivity (m/day)</b>	<b>Porosity</b>	<b>Mean error (m)</b>	<b>Normalized RMS (%)</b>
<b>Mix</b>	2.70E-06	0.15	3.10	24.7
<b>Shale</b>	5.40E-09	0.1	3.10	24.7
<b>Coal</b>	3.75E-05	0.1	3.10	24.7
<b>Mine</b>	2.61E-04	0.25	3.10	24.7
<b>River Valley Sediments</b>	2.90E-05	0.2	3.10	24.7
<b>Sandstone</b>	5.80E-05	0.2	3.10	24.7
<b>Mine Top</b>	6.10E-06	0.4	3.10	24.7

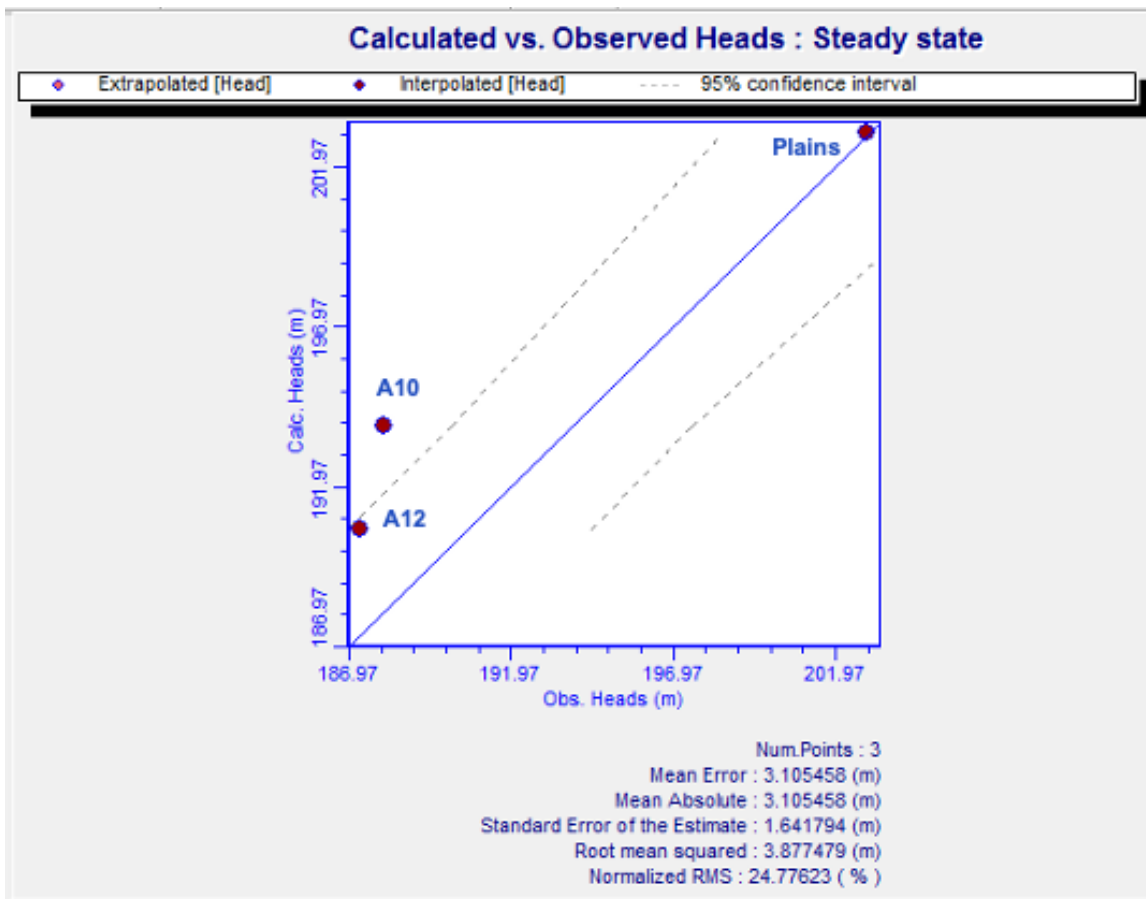
**Table 7**

*Calibrated conductance values of all the river and the resulting mean error after calibration.*

River	Conductance (m/day)	Mean error (m)	Normalized RMS (%)
Hocking River	100	3.10	24.7

**Figure 31**

*Resulting values for the calibrated model.*



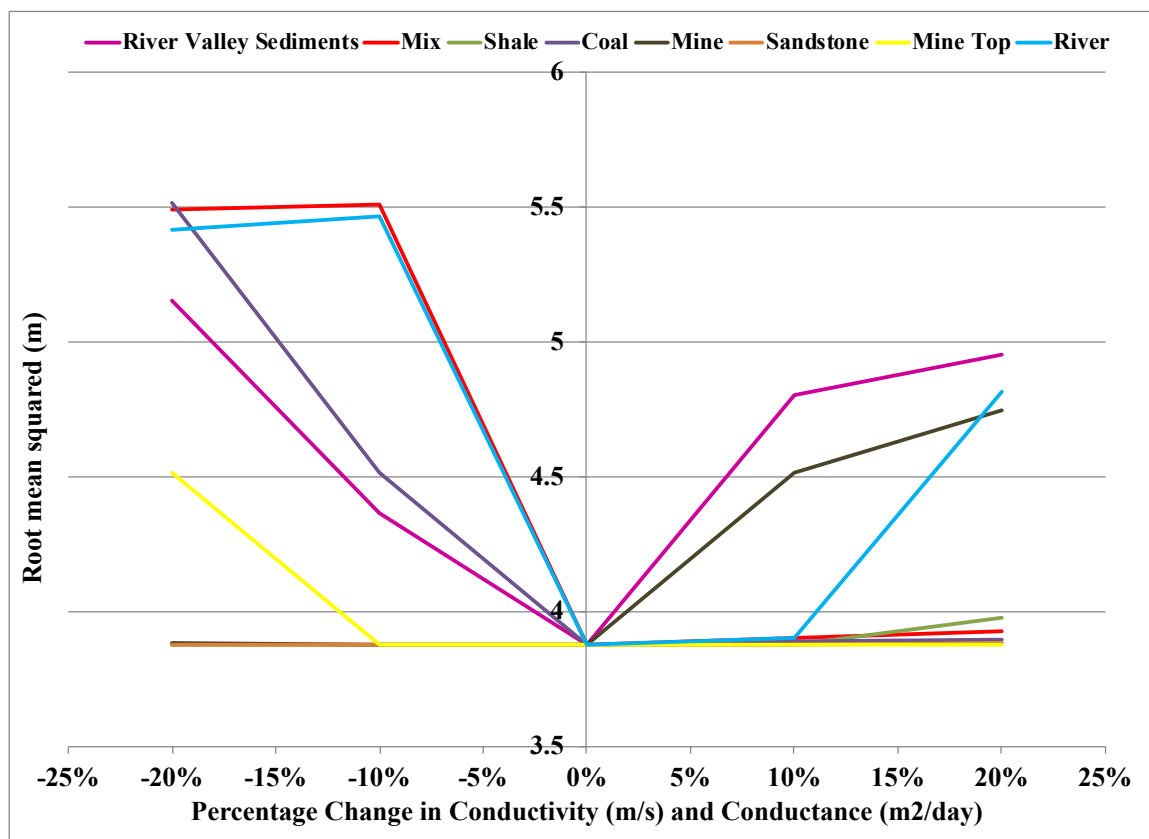
### ***Sensitivity Analysis***

A sensitivity analysis was performed on the calibrated model by inputting parameters of porosity and hydraulic conductivity of the different lithologies and river conductance. The percentage change in the river conductance, hydraulic conductivity and porosity was calculated and plotted on the x- axis with the associated root mean squared error on the y-axis as a graph to examine the sensitivity.

The results display that the conductivities that most affect the model is the river valley sediments, the mine and the river conductance (Figure 32). Therefore, the model is more sensitive to the changes in hydraulic conductivities of the mine and river valley sediments and the changes in river conductance. The sensitivity analysis for porosity resulted in no change in the root mean squared. The model is not sensitive to change in porosity of any of the lithologies.

**Figure 32**

*Sensitivity analysis for hydraulic conductivity and river conductance.*



### ***Zone Budget***

The last step of the groundwater modeling was to perform a zone budget. For this model, two sub-regions were used. Zone 1 is the area surrounding the mine represented by white cells, and Zone 2 is the area of the mine represented by blue cells (Figure 32). The resulting values for the Zone 1 water inflow of 9674.6 m<sup>3</sup>/day and total water outflow of 9674.30 m<sup>3</sup>/day. For Zone 2 a total water inflow of 484.57 m<sup>3</sup>/day and total water outflow of 484.67 m<sup>3</sup>/day. The value of Zone 2 was used later to calculate the total

heat that can be exchanged within the mine. The final product of the simulation's calibration for the layer of the mine is seen in Figure 33. The direction of the flow of water is represented by the arrows which are flowing from the mine to the river. The maximum velocity value was  $1.8\text{E-}05$  m/s with a vector of 30 and a scale of 8 in the mine layer (Figure 34). This value is close to the estimated a water velocity Richardson et al. (2016) calculated for AS-029 which was  $2.3\text{E-}06 - 1.0\text{E-}06$  m/s. Two cross sections of the direction of the flow of water are represented in Figure 35 and 36. The olive areas represent areas of unsaturation and the white areas represent areas of saturation. In the East-West transect the water is flowing to the East towards the river boundaries of the Hocking River (Figure 35). In the North-South transect there is no specific pattern of the flow direction of water, the arrows indicate circulation of groundwater (Figure 36).

**Figure 33**

*Zone budget of AS-029. Blue cells are the cells selected within the mine to calculate the zone budget.*

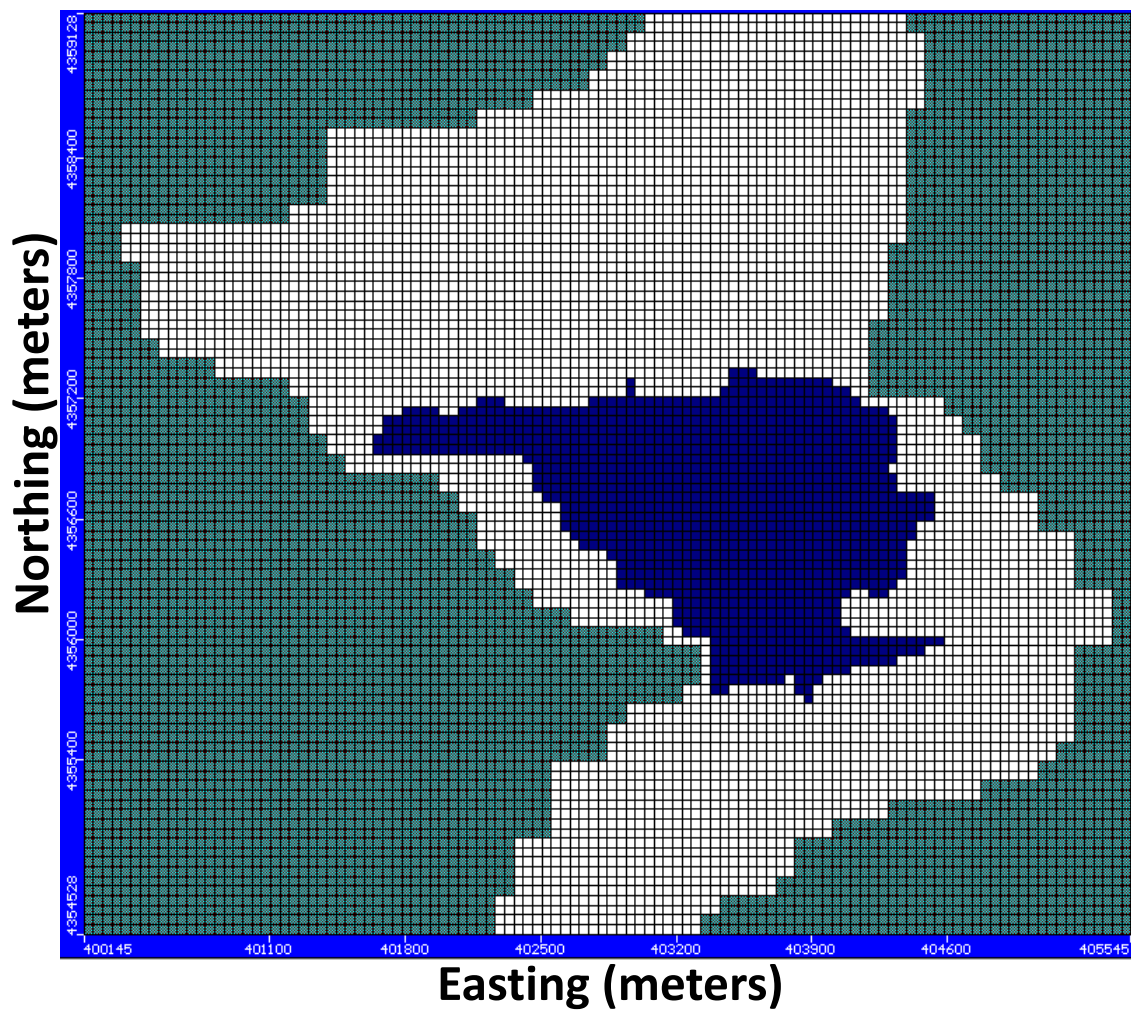


**Figure 34**

*Direction of the flow of water. Blue area is the zone budget 2 of the mine, the circles represent head monitoring and pumping wells. The maroon arrows represent the inward, blue arrows are outward and green arrows represent in plane. The two purple lines represent the cross sections in Figure 34, 35.*

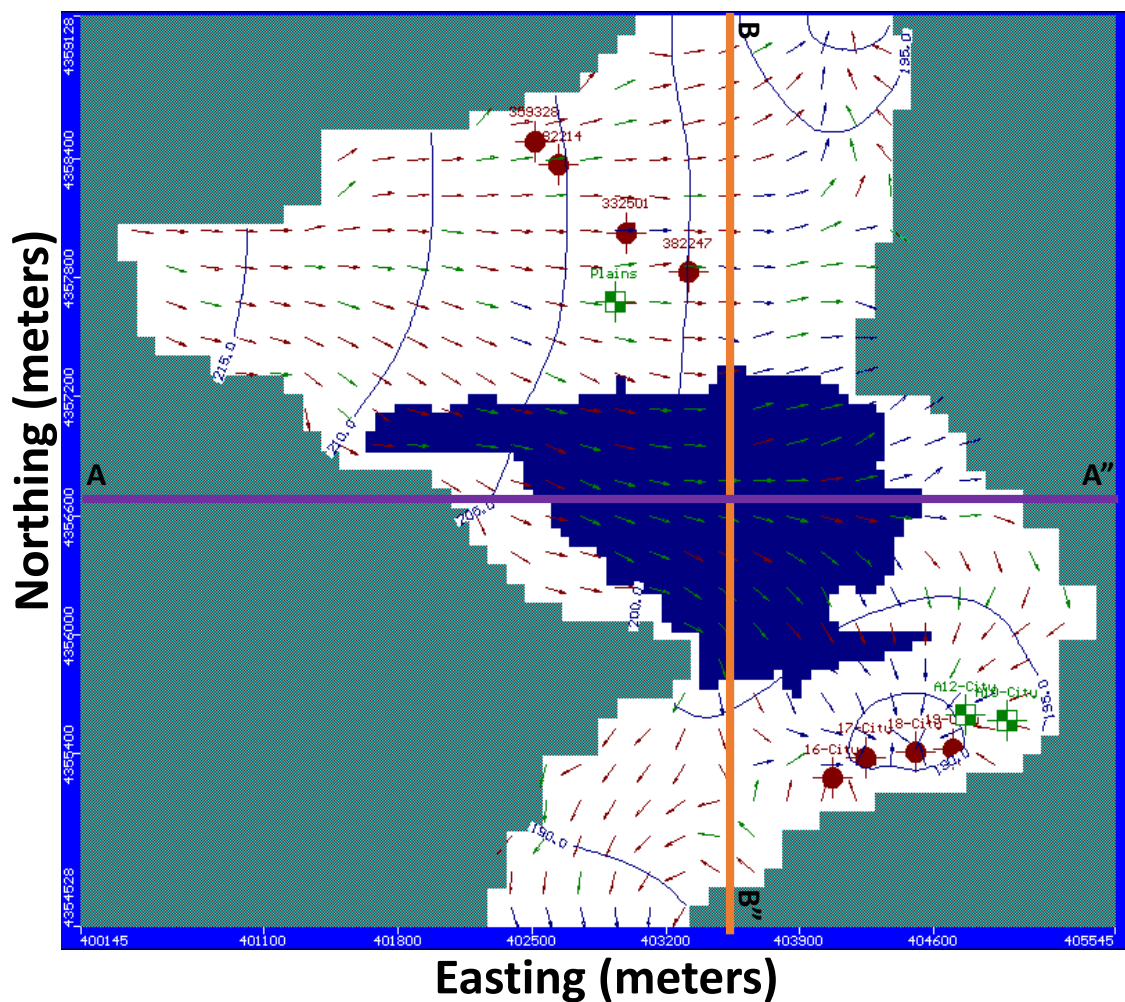


**Figure 35**

*East-West transect of the direction of the flow of water. Blue area is the zone budget 2 of the mine, the olive areas represent areas of unsaturation and the white areas represent areas of saturation. The maroon arrows represent the inward flow, blue arrows are outward flow and green arrows represent in plane.*

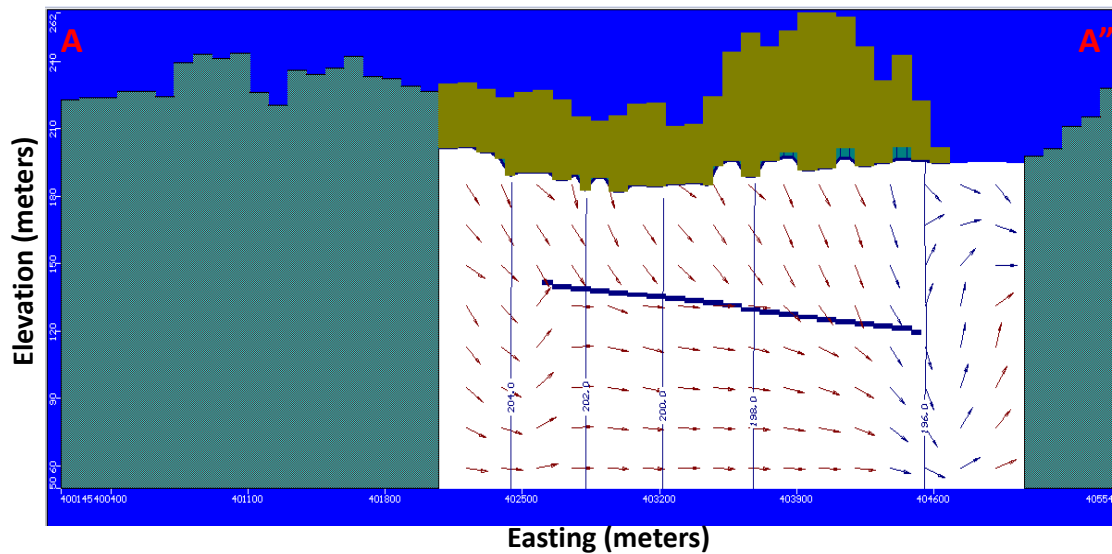
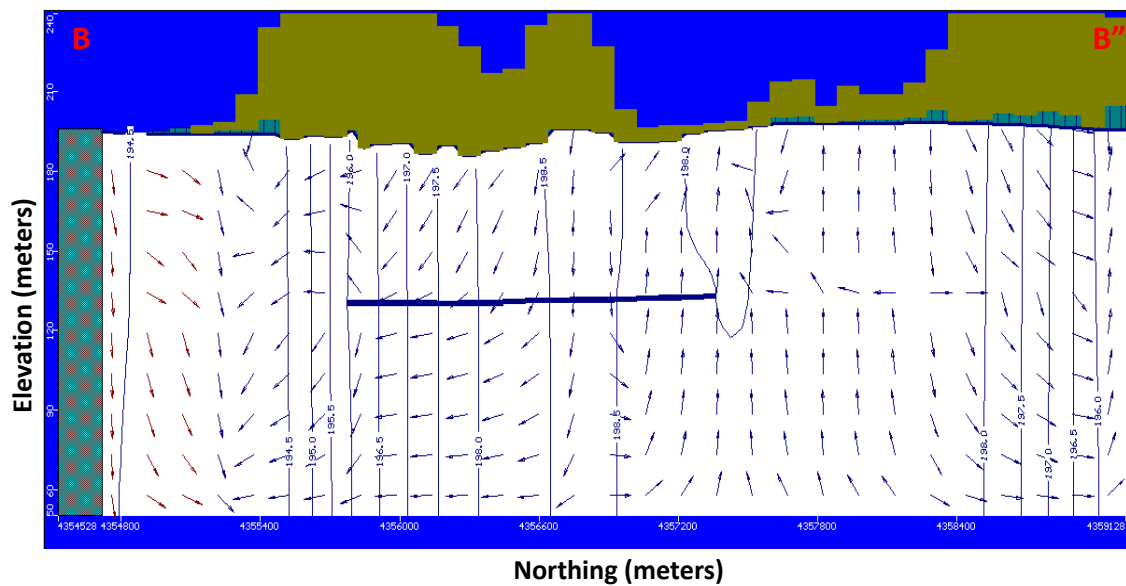


**Figure 36**

North-West transect of the direction of the flow of water. Blue area is the zone budget 2 of the mine, the olive areas represent areas of unsaturation and the white areas represent areas of saturation. The maroon arrows represent the inward flow, blue arrows are outward flow and green arrows represent in plane.



### Thermal Modeling

The overburden thickness was calculated with the values of the surface elevation and coal elevation. Following Richardson's (2014) methods, the overburden thickness was plotted against the temperature of the mine water recorded from the monitoring wells (Figure 34). The graph confirms that the overburden thickness and mine water temperature are directly proportional of each other. However, the equation produced in this graph was not used to calculate the temperature gradient in the mine because it represents only the behavior of temperature at shallower depths up to 22m depth. The mine has a depth of 99 m, considerably deeper. Instead, the empirical equation from

Richardson (2014) was used since it probably represents better the behavior of temperature with depth for the stratigraphy of mine AS-029. The following empirical equation from Richardson (2014) was used to find the temperature of the overburden thickness:

$$y = 0.0222x + 11.257$$

x – overburden thickness (meters)

The resulting values of the temperature of the overburden thickness and the coordinates of the values were used to construct a thermal model (Figure 37). The results display that most of the northern part of the mine has lower temperature than the southern are of the mine and shallower depths (Figure 38). The average temperature of the mine water is 13.5 °C, similar to the value Richardson (2014) calculated of 13.2 °C.

**Figure 37**

*Graph produced with the overburden thickness of the mine and the temperature of the mine water recorded from the monitoring wells. The dots represent the three monitoring wells coupled with the standard error.*

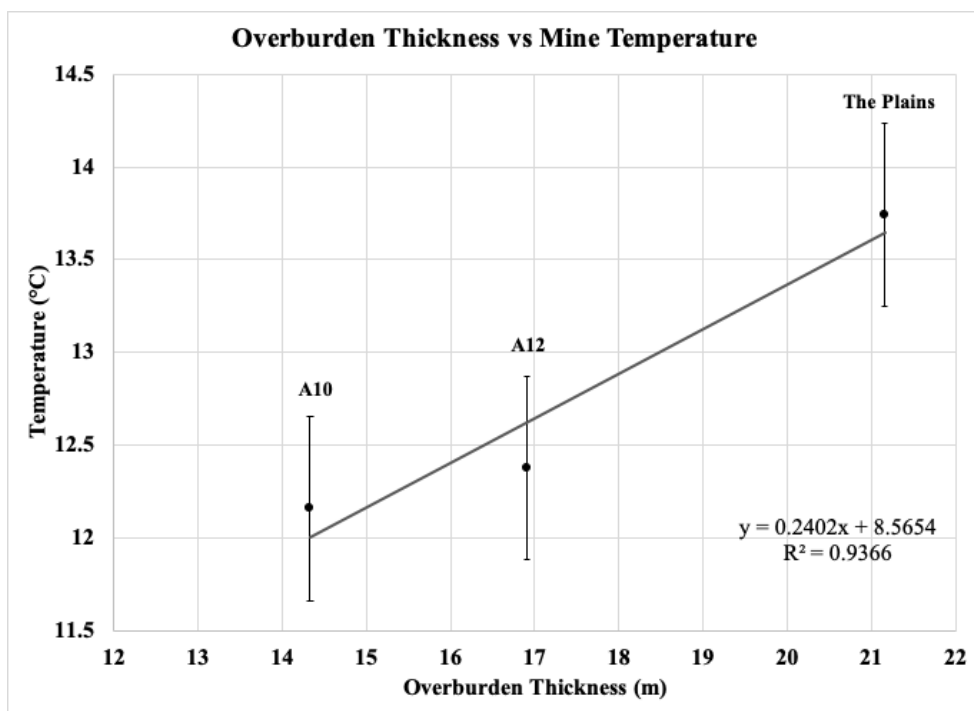
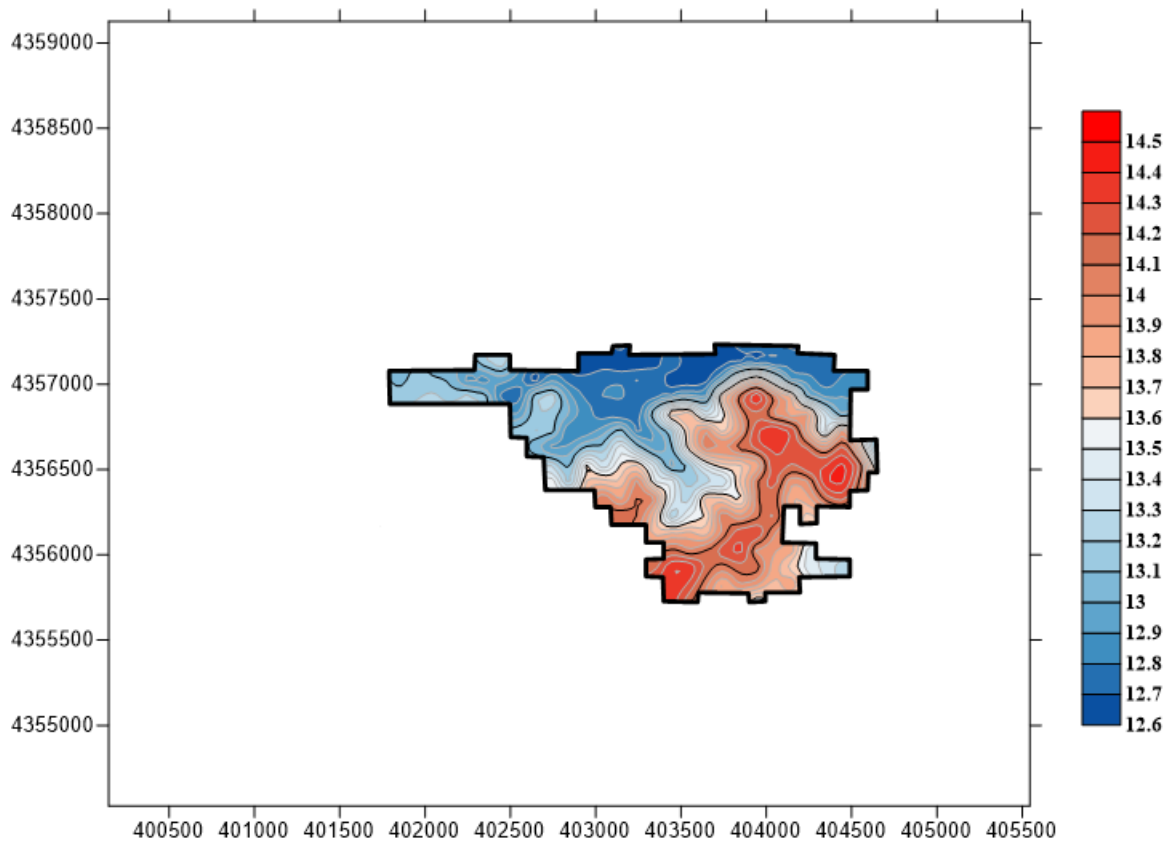


**Figure 38**

*Representation of the temperature of the mine.*



### **Total Heat Exchange Within the Mine**

The total heat available to exchange from the mine was calculated with the formula below. The Zone 2 water budget, specific heat of water, the amount of water circulating in the mine each second ( $q_m$ ) and the change in Temperature were inputted into this formula (Table 8).

$$\text{Total heat exchange per unit time} = F_m * \Delta T * C$$

$F_m$  – Zone 2 water inflow or outflow (kg/s)

$C$  – specific heat capacity of water (4,186 J/kg°C)

$\Delta T$  – temperature change in the mine (°C)

A  $\Delta T=10^\circ\text{C}$  was used to obtain the heat exchanged.

**Table 8**

*Values used to calculate the amount of heat.*

<b>Zone 2 (m<sup>3</sup>/day)</b>	<b>H<sub>2</sub>O Specific Heat (J/kg°C)</b>	<b>Q<sub>m</sub> (kg/s)</b>	<b><math>\Delta</math>Temperature (°C)</b>	<b>Total Mine Heat Exchange (MW)</b>
484.89	4186	5.61	10	0.23

The resulting heat was equal to 0.23MW. Therefore, by adding 10 degrees Celsius of temperature the total heat exchange would be 0.23MW. According to the results from Richardson et al (2016), the total heat extractable from the mine was  $1.09\text{E}+10$  kJ/y which is equal to 0.34 MW. Our results display a total mine heat exchange of 0.23 MW, somewhat different but close to the results from Richardson et al. (2016).

According to the Facilities and Management office at Ohio University, the campus would need a chiller of 2,500 tons per hour. This value was first converted into tons per second and then multiplied by the latent heat of ice in order to convert it into MW. The percentage in which the mine's heat exchange could cover Ohio University's heating/cooling system was calculated by dividing the total chiller heat by the total mine heat exchange resulting in a 2.43%. Therefore, the mine would cover only 2.43% of Ohio University's heating/cooling system. However, even when this value is low, it indicates

that it is possible to use the mine as a heat exchanger only for a small number of buildings or for the High School in The Plains. Mine AS-029 can be used to receive heat, it cannot be used to give heat because the water temperature of groundwater in this area is too low 12.6-14.5 °C. The northern area of the mine has the lowest temperatures, in this area the thermal injection would be best suitable, considering also the thinner overburden and shallower heat exchange wells.

**Table 9**

*Values used to calculate the percentage.*

<b>Total Mine Heat Exchange (MW)</b>	<b>Chiller (tons per 24 hrs.)</b>	<b>Total Chiller Heat (MW)</b>	<b>Percentage coverage for campus (%)</b>
0.23	2,500	9.66	2.43

The results from Riley et al. (2018) and Richardson et al (2014) were used to calculate certain parameters (Table 10). The fraction of the volume of the water of the mine was calculated with the results from Richardson et al (2016) by dividing the effective volume ( $2.6E+06 \text{ m}^3$ ) by the volume ( $4.3E+06 \text{ m}^3$ ) resulting in 0.6. The percentage of the volume of the mine that exchanges water every day was calculated by dividing the Zone 2 water inflow or outflow by the volume of the coal seam multiplied by the fraction of the volume of the mine water. The resulting value indicates that only 0.03% of the volume of the mine exchanges water every day and it takes 2,900 days to substitute 100% the water within the mine.

**Table 10**

*Variables used to calculate the volume of the mine that exchanges water every day and how many days it takes to substitute all of the water within the mine. The area of the mine, water in the mine and volume were extracted from the results of Riley et al. (2018). The fraction of the volume of the mine water was obtained from the results of Richardson et al (2016).*

<b>Area of the mine (ft<sup>2</sup>)</b>	<b>Water in the mine (gallons)</b>	<b>Coal seam volume (ft<sup>3</sup>)</b>	<b>Zone 2 (ft<sup>3</sup>/day)</b>	<b>Fraction of the volume of the mine water</b>	<b>Volume of the mine that exchanges water every day (%)</b>	<b>Days needed to substitute all of the water within the mine</b>
9,245,837	443,800,267	59,327,462	12274.99	0.6	0.03	2,900

## Conclusions

Even though all of the monitoring wells were placed in distant locations, the transient data analysis shows that only in well A10 it is observed an abnormal conductivity probably due to interaction of the groundwater with a salt intrusion and its shallower depth. This well also displayed very different results in the groundwater model, its calculated and observed head displayed a large difference. This may be the reason why during the calibrations the Normalized RMS could not be lowered to the desired 10% and the mean error was still high. For future references, it is best to check that all of the wells do not have a disturbance near such as the old salt brine well near well A10. The Plains well displayed the most constant temperature between the 3 monitoring wells, this well is the deepest of the 3 monitoring wells with a depth of 21.03 m. The hydraulic head of the three wells responded with different lag times to precipitation events, with The Plains well showing the faster response and the City of Athens wells showing a delayed response. This is probably due to water infiltrating in the higher elevation of The Plains and traveling towards the river valley where the City of Athens wells are located. The City of Athens wells receive vertical infiltration but also lateral infiltration produced by the groundwater flow regime observed in this area.

The groundwater model was based on average geology units extracted from a geologic map. Ideally, a fluid transport model would be performed if there is access inside of mine which is not the case for AS-029. Drilling multiple consistent boreholes within the mine and surrounding the mine would help understand the accurate geology of the area and to perform a better fluid transport model. Nonetheless, the results of this

model have displayed important information for the future installation of GSHP technology. The results of the sensitivity analysis showed that the model is more sensitive to the changes in hydraulic conductivities of the mine and river valley sediments. The river conductance also is responsible for the sensitivity of the model. The model might be more sensitive to the river valley sediments since two of the three wells are located in the river valley of the Hocking River and the high hydraulic conductivity of these sediments is important for the overall groundwater flow regime.

The rate of heat transferred vertically through the mine was not calculated in this study since it was not possible to know the exact stratigraphy of the overburden. The empirical equation from Richardson (2014) was used to get the temperature of the mine without considering the vertical heat exchange. The thermal modeling results show that most of the northern part of the mine has cooler temperatures. Thus, heat should be injected in these areas. Also, the thinner overburden would make the drilling less expensive. According to our calculations, volume of water that circulates through the mine is not easily exchanged since only 0.03% is exchanged every day and it takes 2,900 days to substitute 100% of the water within the mine. Additionally, the mine would cover only 2.43% of Ohio University's heating/cooling system if an increase in temperature of 10 °C is allowed.

The overburden thickness displayed the similar pattern as the one presented by Richardson (2014), the more overburden thickness the higher the temperatures. This is why the southern part of the mine has higher temperatures because its overburden is thicker in that area.

**Implications**

The temperature within AS-029 has important implication for the use of low temperature geothermal energy for heating or cooling purposes in Athens, Ohio. Consequently, this development would benefit Athens or The Plains by lowering heating and cooling costs, and it benefits the environment by reducing greenhouse gases. This work will also be significant for scientists interested in studying AUMs that do not have any wells drilled or open shafts, for the purpose of GSHP installation. Typically, wells are drilled into the mine to get hydrological information, however, this study shows that by using the wells surrounding the mine it is possible to model the area and study the mine's characteristics for potential heat exchange/extraction.

**Future Work**

The results of this work confirm that the mine AS-029 can be used to inject heat for GSHP installation. These results will be accessible for developers, planners and designers to install GSHPs in Athens and other localities with flooded abandoned underground coal mines.

## References

- Anderson, M.P., & Woessner, W.W., 1992, Applied Groundwater Modeling Simulation of flow and advective transport, academic press. San Diego, California.
- Banks, D., Athresh, A., Al-Habaibeh, A., & Burnside, N., 2017, Water from abandoned mines as a heat source: practical experiences of open- and closed-loop strategies, United Kingdom: Sustainable Water Resources Management, doi: 10.1007/s40899-017-0094-7.
- Barbier, Enrico. 2002. Geothermal energy technology and current status: an overview. Renewable and Sustainable Energy Reviews 6. pp 3-65.
- Bownocker J.A., and Dean E.D., 1929, Analyses of the coals of Ohio, Geological Survey of Ohio, p 370.
- Busby, J., Lewis, M., Reeves, H., & Lawley, R., 2009, Initial geological considerations before installing ground source heat pump systems: Quarterly Journal of Engineering Geology and Hydrogeology, v. 42, p. 295–306, doi: 10.1144/1470-9236/08-092.
- Crowell, D.L., 2008, Educational Leaflet No. 8 Revised edition. Ohio Division of Geological Survey, [https://ngmdb.usgs.gov/Prodesc/proddesc\\_12838.htm](https://ngmdb.usgs.gov/Prodesc/proddesc_12838.htm)
- Crowell, D.L., DeLong, R.M., Banks, C.E., Hoeffler, P.D., Gordon, C.P., McDonald, J.M., Wells, J.G., Powers, & D.M., Slucher, E.R., 2011. Known abandoned underground mines of Ohio. Ohio Department of Natural Resources, Division of Geological Survey.Database.
- Curtis, R., Lund, J., Sanner, B., Rybach, L., & Hellström, G., 2005. Ground Source Heat

Pumps - Geothermal Energy for Anyone, Anywhere: Current Worldwide

Activity: World Geothermal Congress,

[https://www.academia.edu/7518400/Ground\\_Source\\_Heat\\_Pumps\\_-](https://www.academia.edu/7518400/Ground_Source_Heat_Pumps_-_Geothermal_Energy_for_Anyone_Anywhere_Current_Worldwide_Activity)

[\\_Geothermal\\_Energy\\_for\\_Anyone\\_Anywhere\\_Current\\_Worldwide\\_Activity](https://www.academia.edu/7518400/Ground_Source_Heat_Pumps_-_Geothermal_Energy_for_Anyone_Anywhere_Current_Worldwide_Activity)

(accessed January 2020).

Domenico, P.A., & F.W. Schwartz, 1990. Physical and Chemical Hydrogeology, John Wiley & Sons, New York, 824 p.

Fetter, C., 2001, Applied hydrogeology: Fourth Edition. Upper Saddle River, New Jersey: Prentice-Hall, Inc. pp. 40-47, 81-89, 307.

Freeze, R.A., & Cherry, J.A., 1979, Groundwater. Prentice-Hall, Inc., Englewood Cliffs, New Jersey, p.190.

Gass, T.E., & Lehr, J.H., 1977. Ground water energy and the ground water heat pump. Water Well Journal. pp 42-47.

Glassley, W.E., 2010, Geothermal Energy: Renewable Energy and the Environment: CRC Press, 621 p.

Hammer, O., Harper, D.A.T., & Ryan, P.D., 2001, PAST: Paleontological Statistics Software Package for Education and Data Analysis: , p. 9.

Healy, P.F., & Ugursal, V.I., 1997. Performance and economic feasibility of ground source heat pumps in cold climate. International Journal of Energy Research. Volume 21. pp 857-870.

Helsel, D.R., 1983, Mine drainage and rock type influences on eastern Ohio stream water quality. JAWRA Journal of the American Water Resources Association, 19: 881-

888. doi:10.1111/j.1752-1688.1983.tb05936.x

Harbaugh, A.W., 2005, MODFLOW-2005, the U.S. Geological Survey modular ground-water model -- the Ground-Water Flow Process: U.S. Geological Survey Techniques and Methods 6-A16.

Legere, L., 2014, Finding value in mine water. Pittsburgh Post-Gazette. Retrieved from [www.post-gazette.com/powersource/policypowersource/2014/09/23/Finding-value-in-mine-water/stories/20140916001](http://www.post-gazette.com/powersource/policypowersource/2014/09/23/Finding-value-in-mine-water/stories/20140916001)

Hariharan, V., & Shankar, U., 2017, A review of visual MODFLOW applications in groundwater modelling: IOP Conference Series: Materials Science and Engineering, v. 263, p. 032025, doi:10.1088/1757-899X/263/3/032025.

Khadri, S.F.R., & Pande, C., 2016, Ground water flow modeling for calibrating steady state using MODFLOW software: a case study of Mahesh River basin, India: Modeling Earth Systems and Environment, v. 2, p. 39, doi:10.1007/s40808-015-0049-7.

Lambert, D.C., McDonough, K.M., & Dzombak, D.A., 2004, Long-term changes in quality of discharge water from abandoned underground coal mines in Uniontown Syncline, Fayette County, PA, USA: Water Research, v. 38, p. 277–288, doi: 10.1016/j.watres.2003.09.017.

Lund, J., Sanner, B., Rybach, L., Curtis, R., Hellstrom, G., 2004. Geothermal (ground source) heat pumps a world overview. Geo-Heat Center Bulletin. pp 1-10.

Majithia, M., Kohli, I., 1997. Main Types of Geological Maps: Purpose, Use and

Preparation. India: Oxford & IBH Pub.

McDonald, M.G., & Harbaugh, A.W., 1998, A modular three-dimensional finite difference ground-water flow model, U.S.G.S. Techniques of Water-Resources Investigations, Book 6 chapter A1, 586 p.

Mines of Ohio, Accessed January 2019, Ohio Department of Natural Resources, < <https://gis.ohiodnr.gov/MapView/?config=OhioMines> >

Mustafa Omer, A., 2008, Ground-source heat pumps systems and applications: Renewable and Sustainable Energy Reviews, v. 12, p. 344–371, doi:10.1016/j.rser.2006.10.003.

Ohio Water Wells, Accessed January 2019, Ohio Natural Resources Department, < <https://gis2.ohiodnr.gov/MapView/?config=WaterWells#>>

Ohio Watershed Data. Accessed March 2019. Voinovich School of Public Affairs. Ohio University. < [www.watersheddata.com](http://www.watersheddata.com) >

Richardson, J., 2014, Thermal and hydrological study of flooded abandoned coal mines in Ohio as potential heat exchangers [Master's thesis]: Ohio University, 601 p.

Richardson, J., Lopez, D., Leftwich, T., Angle, M., Wolfe, M., & Fugitt, F., 2016, The characterization of flooded abandoned mines in Ohio as a low-temperature geothermal resource, in Dowling, C.B., Neumann, K., and Florea, L.J., eds., Geothermal Energy: An Important Resource: Geological Society of America Special Paper 519, p. 19–41, doi:10.1130/2016.2519(02).

Riley, M., Mullins, E., Lorek, A., Shearer, R., Bauer, D., 2018. Consideration of

abandoned underground coal mine as- 029 as a ground source heat pump heat exchanger. Ohio University, 21 p.

Rollin, K E. 2002. Assessment of BGS data for ground source heat pump installations in the UK. Internal Report IR/02/196, British Geological Survey.

Sanner, Burkhard., Karystas, Constantine., Mendrios, Dimitrios., Rybach, Ladislaus., 2003. Current status of ground source heat pumps and underground thermal energy storage in Europe. *Geothermics* Volume 32. pp 579-588.

Singer, P.C., and Stumm, W., 1970, Acidic Mine Drainage: The Rate-Determining Step: *Science*, v. 167, p. 1121–1123.

Skounsen, J., Rose, A., Geidel, G., Foreman, J., Evans, R., and Hellier, W., 1998, A handbook of technologies for avoidance and remediation of acid mine drainage. Acid Drainage Technology Initiative, National Mine Land Reclamation Ctr, WVY, Morgantown, WV. 131.

Slucher, E.R., Swinford E.M., Larsen, G.E., Schumacher, G.A., Shrake, D.L., Rice, C.L., Caudill, M.R., and Rea R.G., 2006, Bedrock geologic map of Ohio, United States Geological Survey, 1:500,000.

Stout, Wilber. 1947. Generalized Section of Rocks of Ohio, Geol. Surv. Ohio, 4th ser., Information Circular, No. 4. (Originally published 1943, Bull. 44, charts opposite p. 108).

Sturgeon, M.T., 1958, Geologic map of Athens County, Ohio, Ohio Department of Natural Resources, 1:600,000.

Sturgeon, M. T., and Merrill, W. M., 1949, An additional fossiliferous member in the

Allegheny Formation (Pennsylvanian) of Ohio: *Ohio Journal of Science*, v.49, p. 1-11.

Stylianou, I.I., Florides, G., Tassou, S., Tsiolakis, E., and Christodoulides, P., 2017, Methodology for estimating the ground heat absorption rate of Ground Heat Exchangers: *Energy*, v. 127, p. 258–270, doi: 10.1016/j.energy.2017.03.070.

Twumasi, F., 2018, Applying MODFLOW and artificial neural networks to model the formation of mine pools in underground coal mines [Master's thesis]: Ohio University, p. 204.

United States Geological Survey (USGS) 03159500 Hocking River at Athens OH, Accessed February 2020, USGS, < [https://waterdata.usgs.gov/usa/nwis/uv?site\\_no=03159500](https://waterdata.usgs.gov/usa/nwis/uv?site_no=03159500) >.

Verhoeven, R., Willems, E., Harcouët-Menou, V., Boever, E. D., Hiddes, L., Veld, P. O., & Demollin, E. (2014). Minewater 2.0 project in Heerlen the Netherlands: Transformation of a geothermal mine water pilot project into a full scale hybrid sustainable energy infrastructure for heating and cooling. *Energy Procedia*, 46, 58–67. doi:10.1016/j.egypro.2014.01.158.

Watzlaf, G.R., Achman, T.E., 2007. Flooded underground coal mines: a significant source of inexpensive geothermal energy. *Reclamation Matters*. Volume 1. pp 4-7.

Weller, J. Marvin. 1931. The Conception of Cyclical Sedimentation during the Pennsylvanian Period, 111. *State Geol. Surv., Bull.* 60, pp. 163-177.

**Appendix A: Transient Data Analysis Graphs**

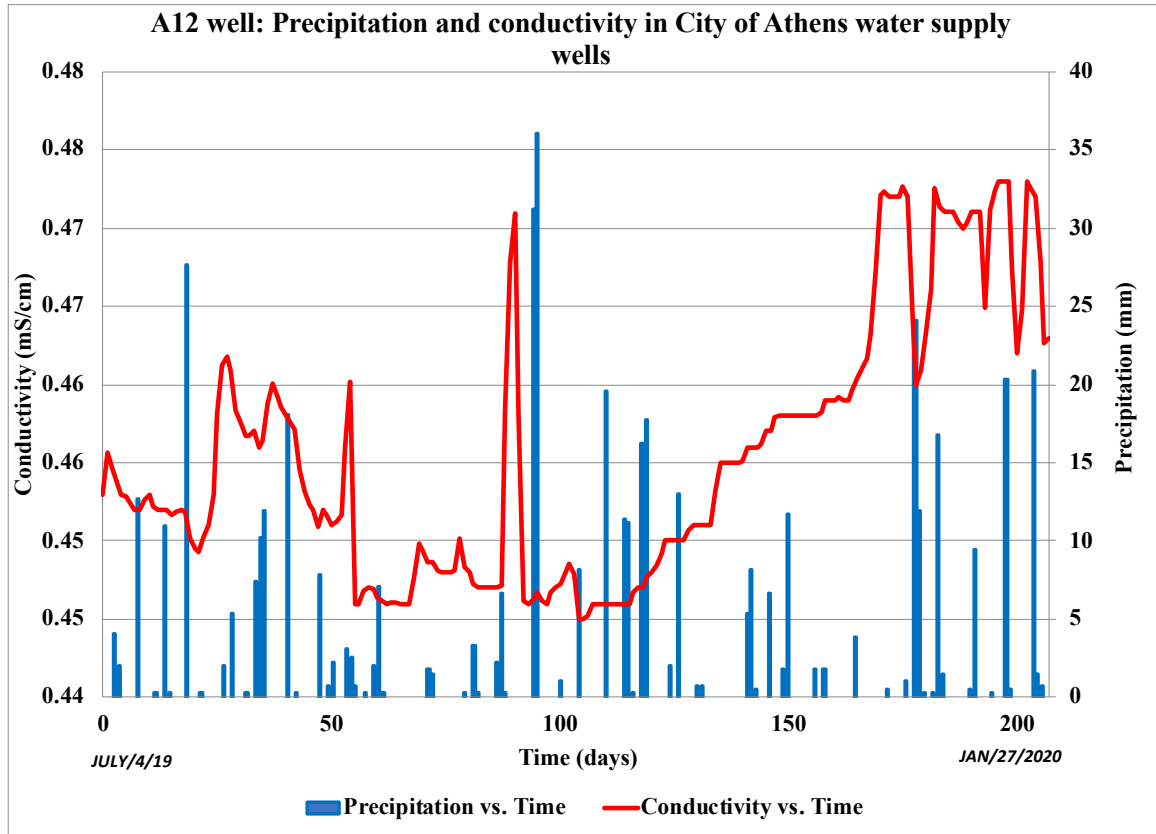


Figure A 1 Daily precipitation from the Scalia Lab and the hydraulic conductivity recorded from the A12 well.

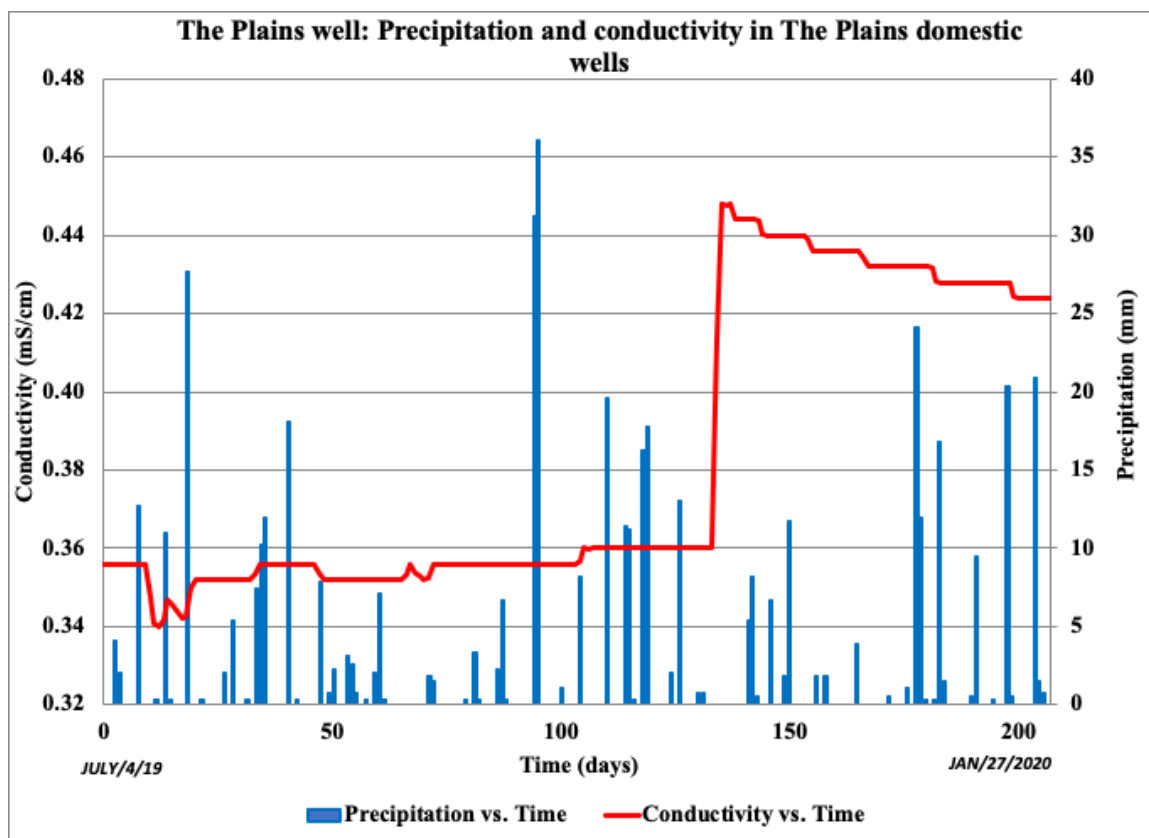


Figure A 2 Daily precipitation from the Scalia Lab and the hydraulic conductivity recorded from The Plains well.

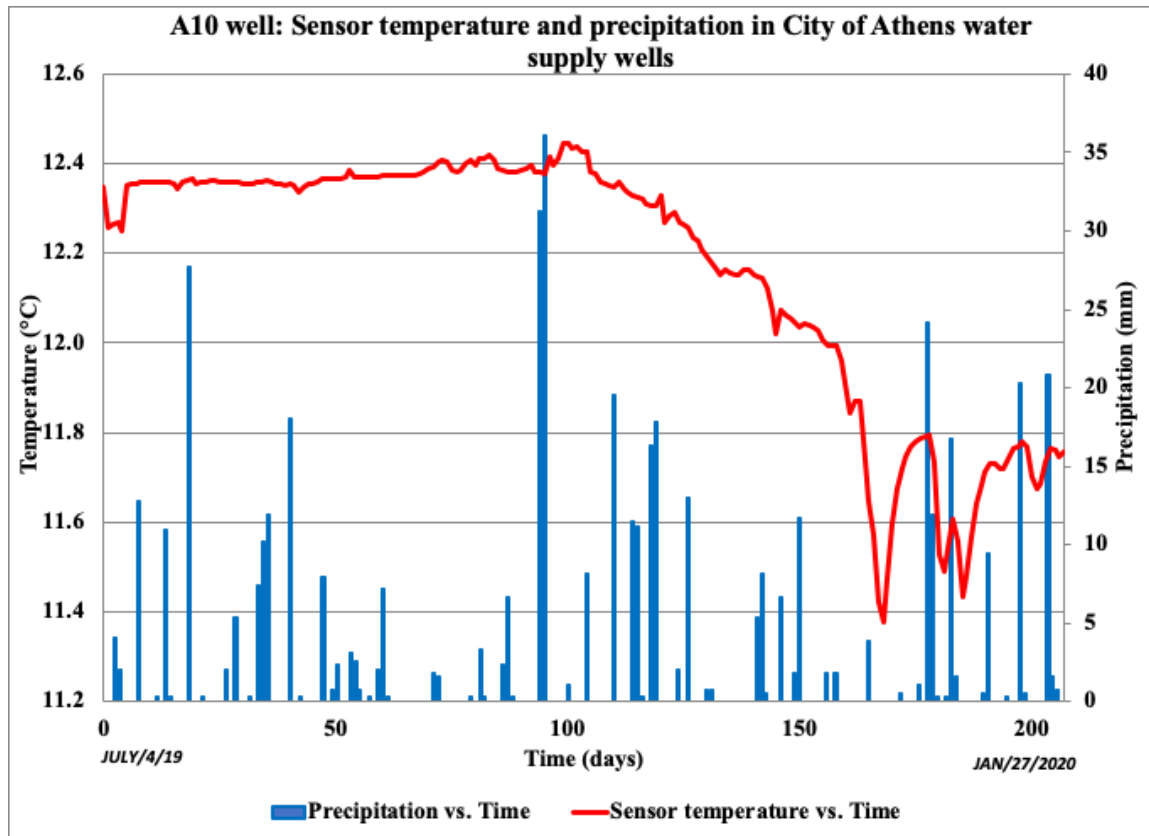


Figure A 3 Daily precipitation from the Scalia Lab and the hourly temperature recorded from the A10 well.

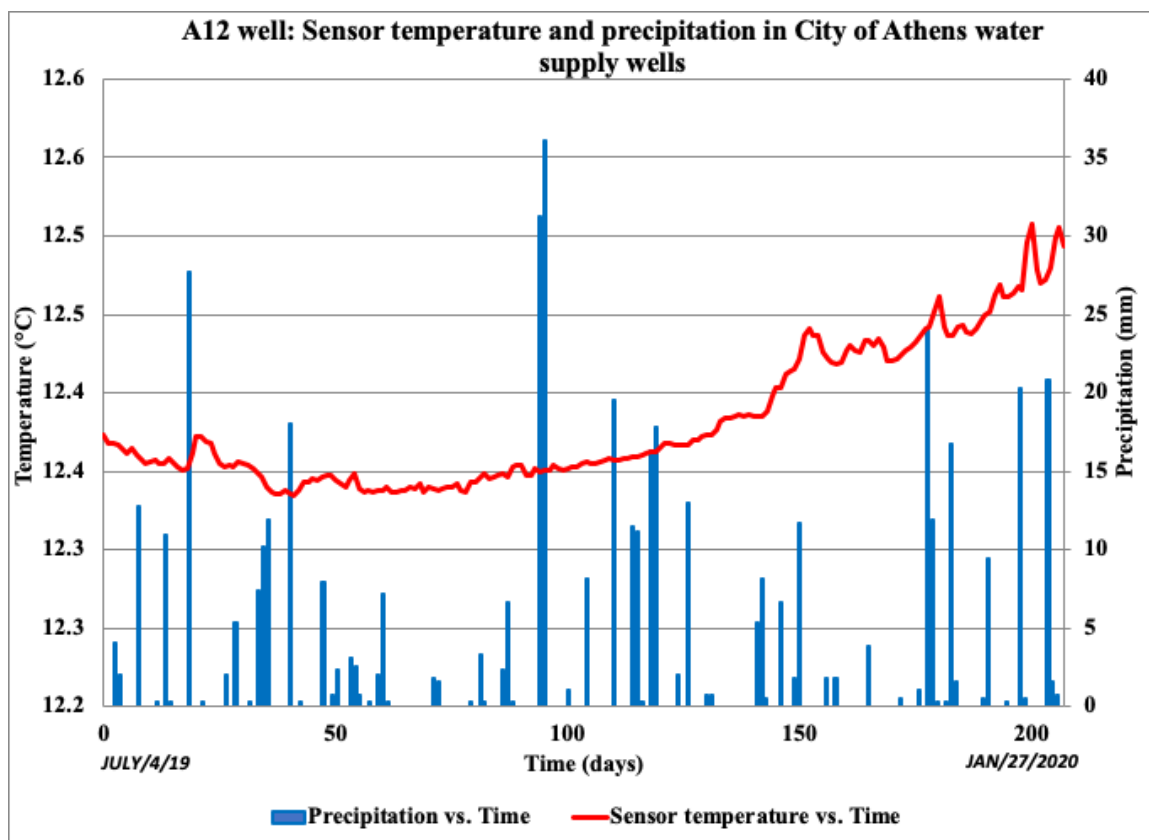


Figure A 4 Daily precipitation from the Scalia Lab and the hourly temperature recorded from the A12 well.

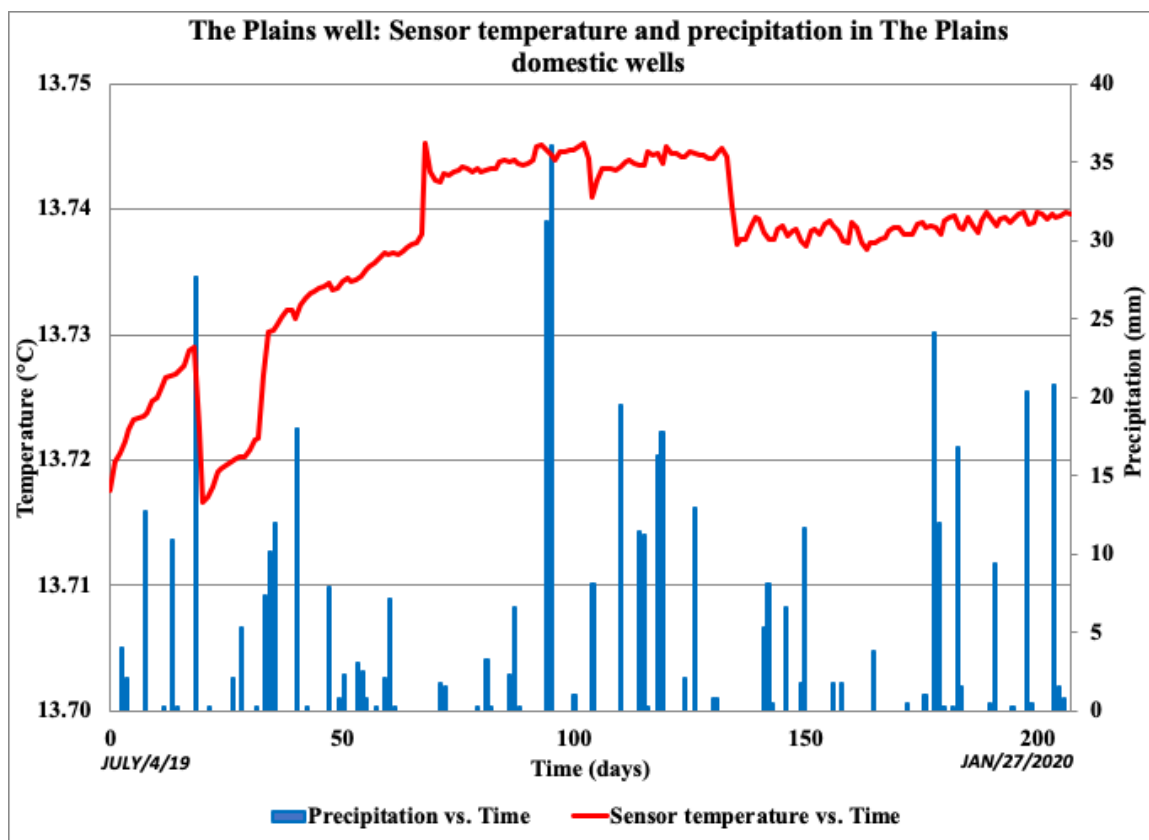


Figure A 5 Daily precipitation from the Scalia Lab and the hourly temperature recorded from The Plains well.

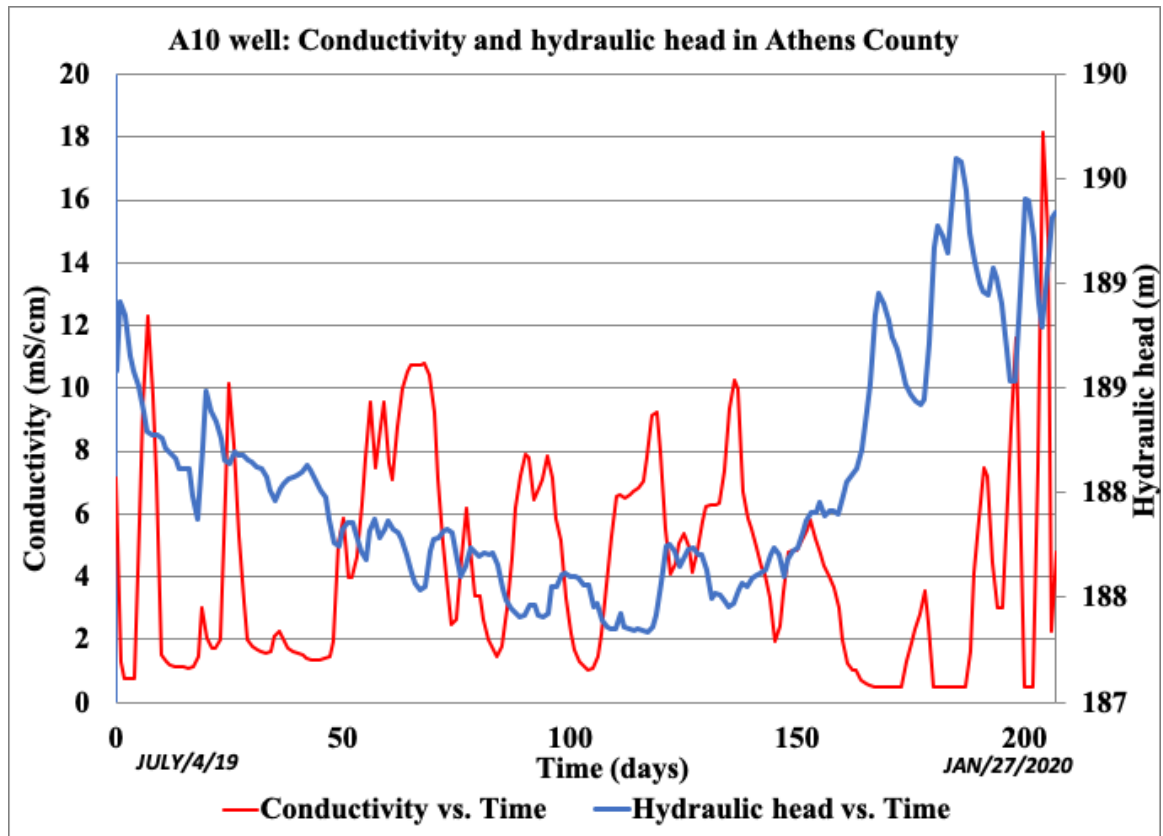


Figure A 6 Hydraulic head and conductivity values recorded from the sensor installed in the A10 well. Red lines represent the conductivity and blue line represents hydraulic head.

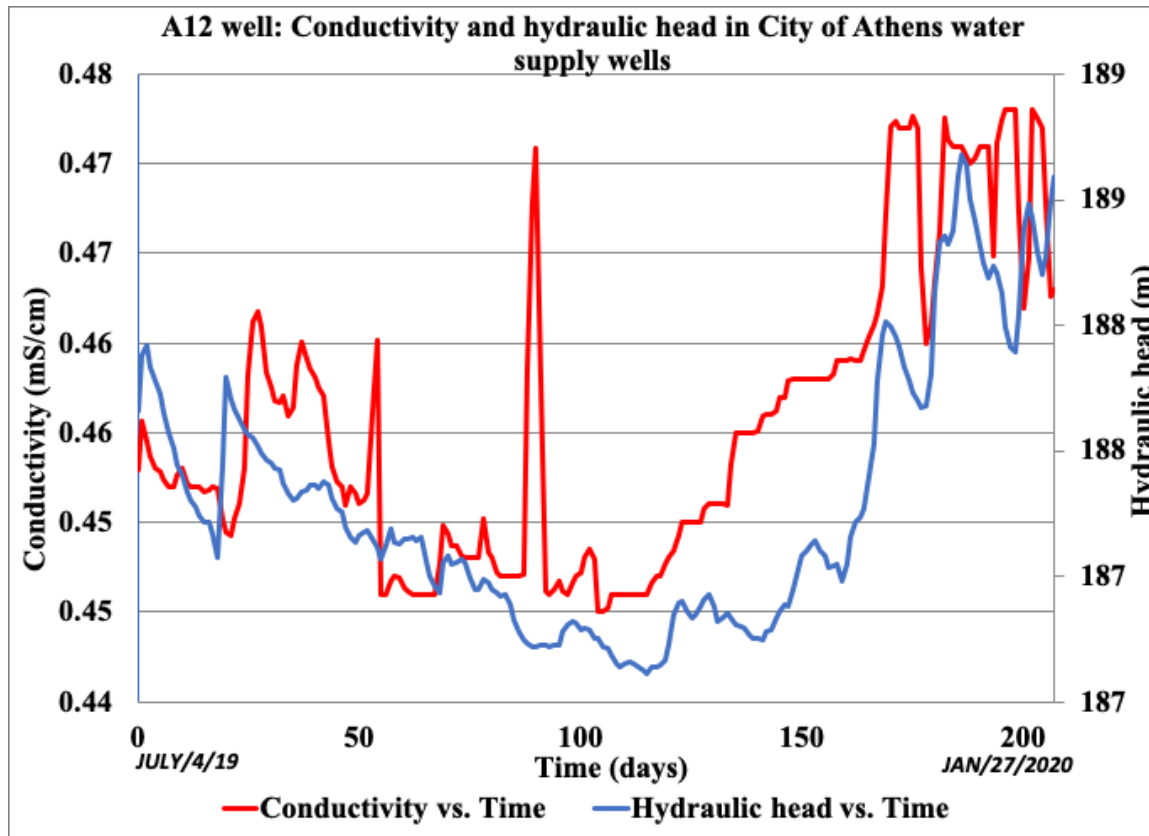


Figure A 7 Hydraulic head and conductivity values recorded from the sensor installed in the A12 well. Red lines represent the conductivity and blue line represents hydraulic head.

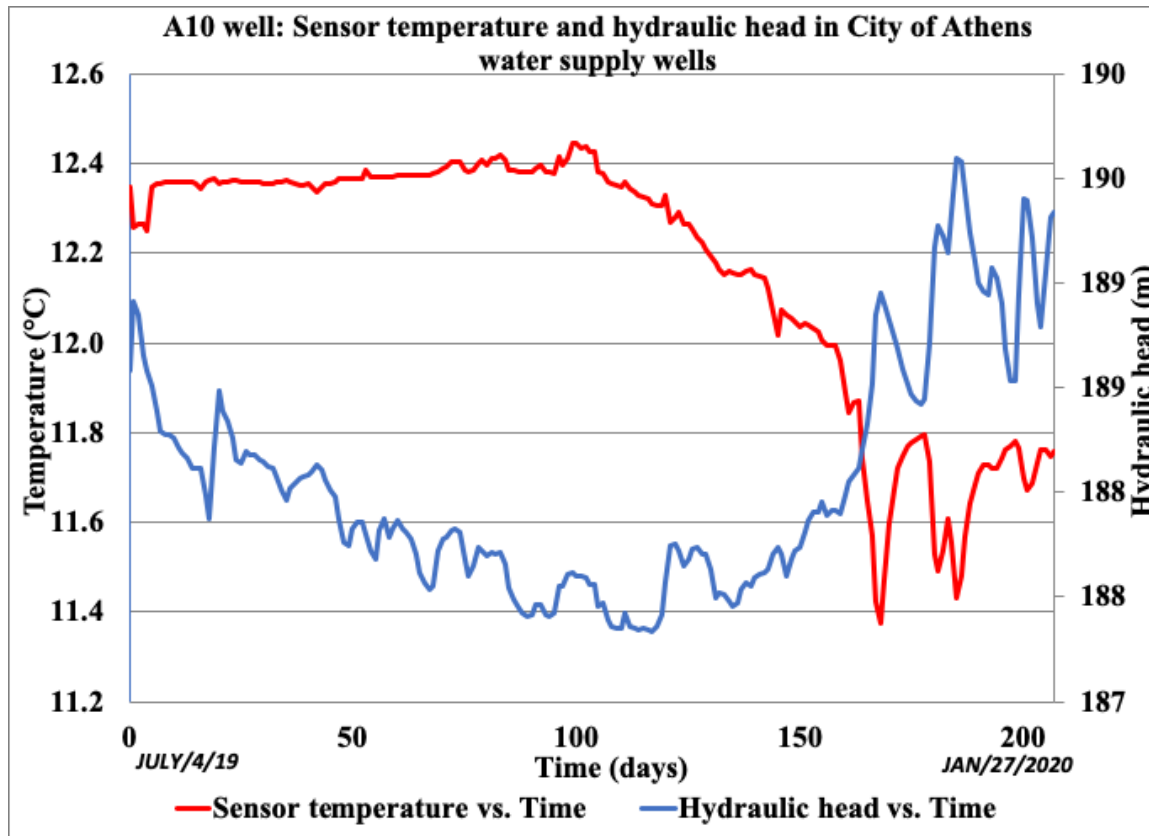


Figure A 8 Hydraulic head and temperature values recorded from the sensor installed in the A10 well. Red lines represent the sensor temperature and blue line represents hydraulic head.

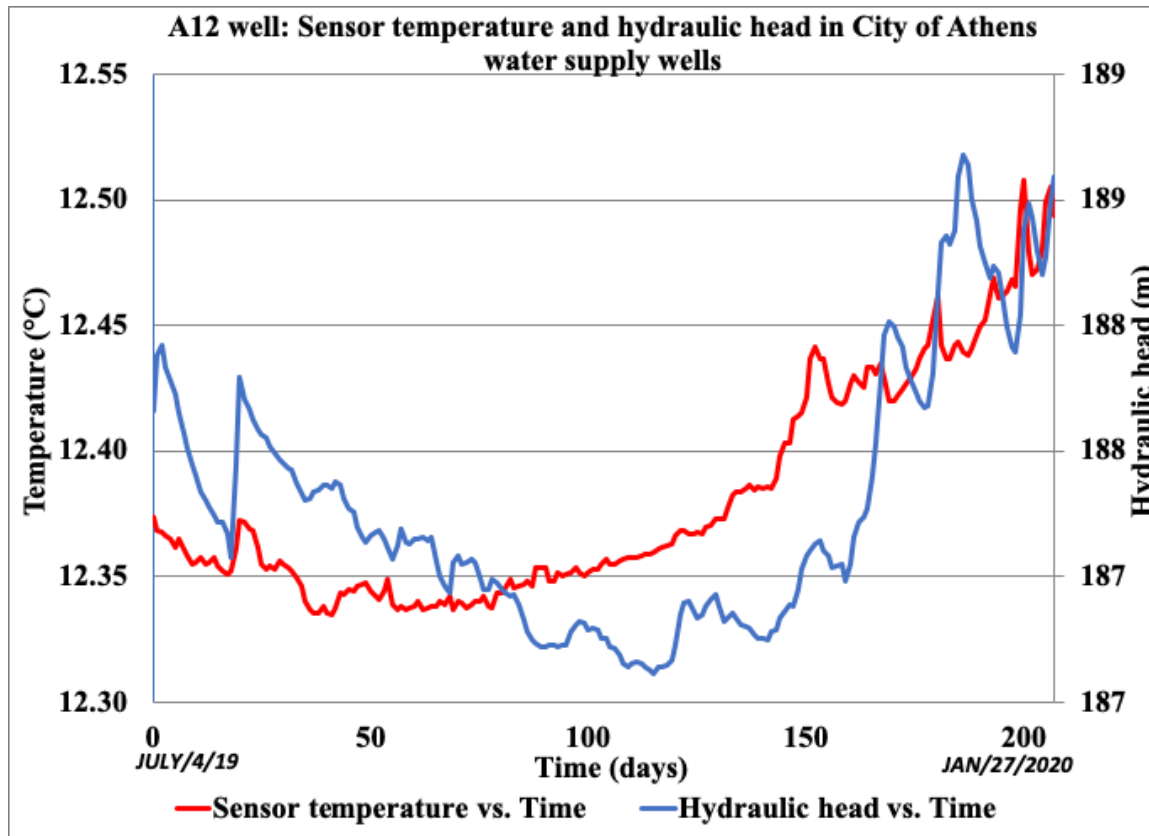


Figure A 9 Hydraulic head and temperature values recorded from the sensor installed in the A12 well. Red lines represent the sensor temperature and blue line represents hydraulic head.

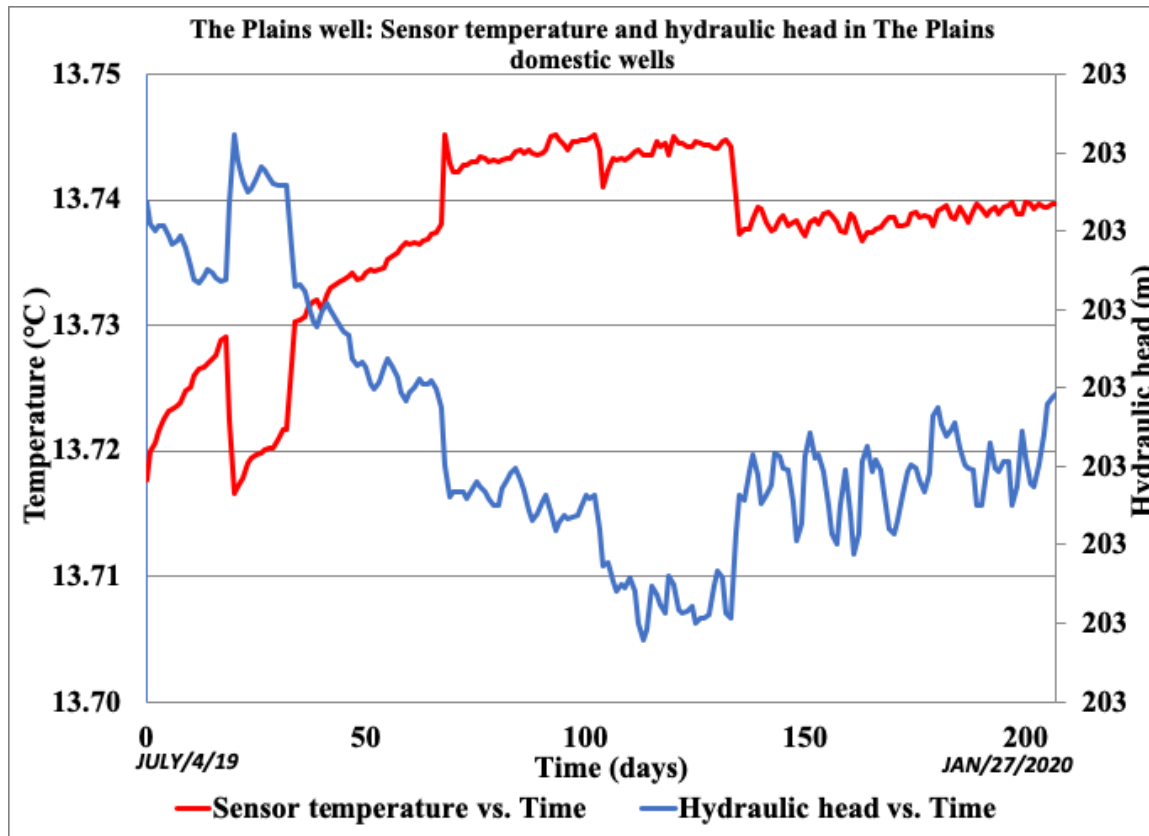


Figure A 10 Hydraulic head and temperature values recorded from the sensor installed in The Plains well. Red lines represent the sensor temperature and blue line represents hydraulic head.

## Appendix B: Cross correlation graphs

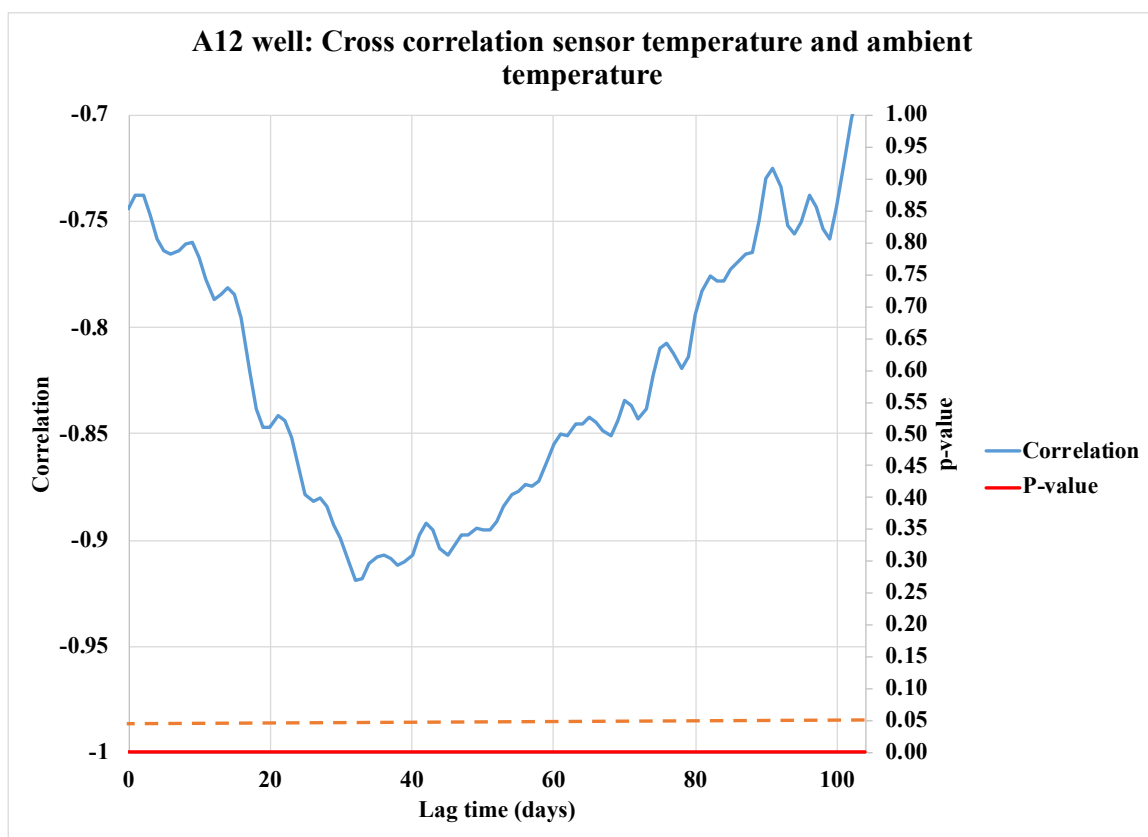


Figure B 1 Cross correlation of the daily temperature recorded from the A12 monitoring well and the ambient daily temperature from the Scalia Lab. The orange dashed line represents the alpha for the p-value.

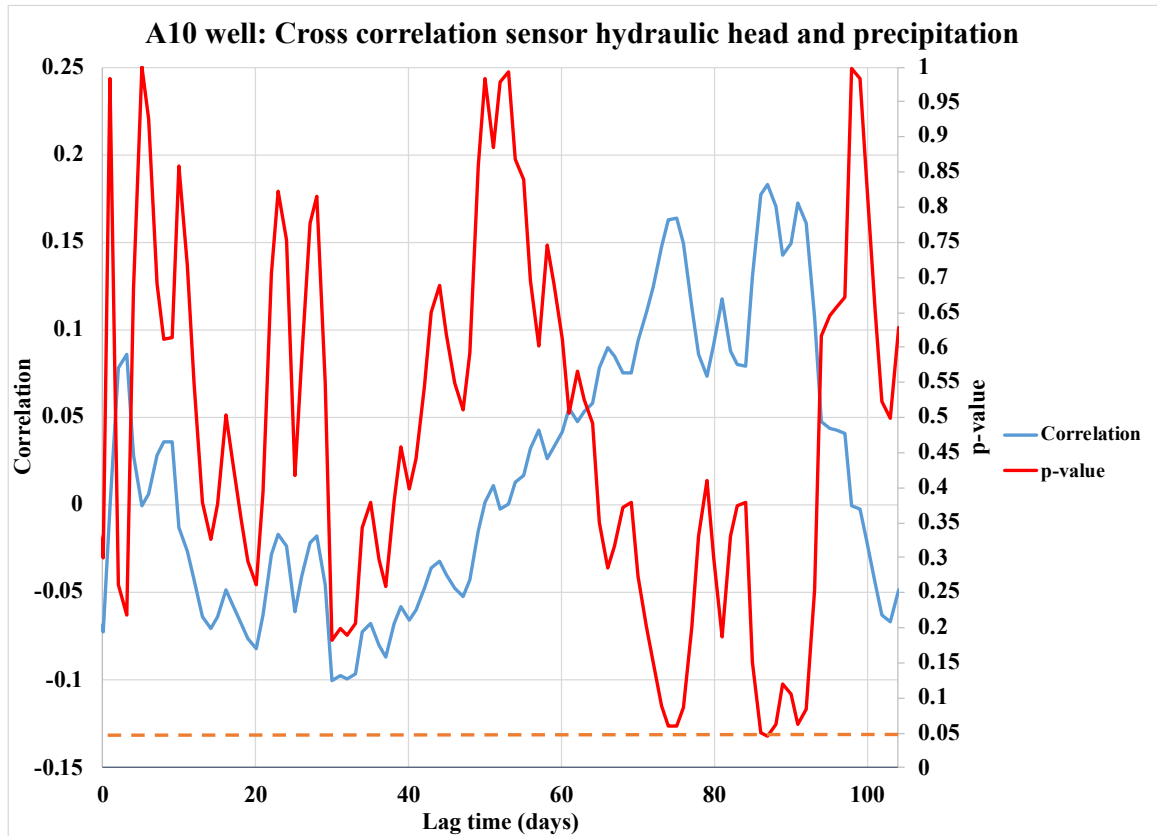


Figure B 2 Cross correlation of the daily hydraulic head recorded from the A10 monitoring well and the daily precipitation from the Scalia Lab. The orange dashed line represents the alpha for the p-value.

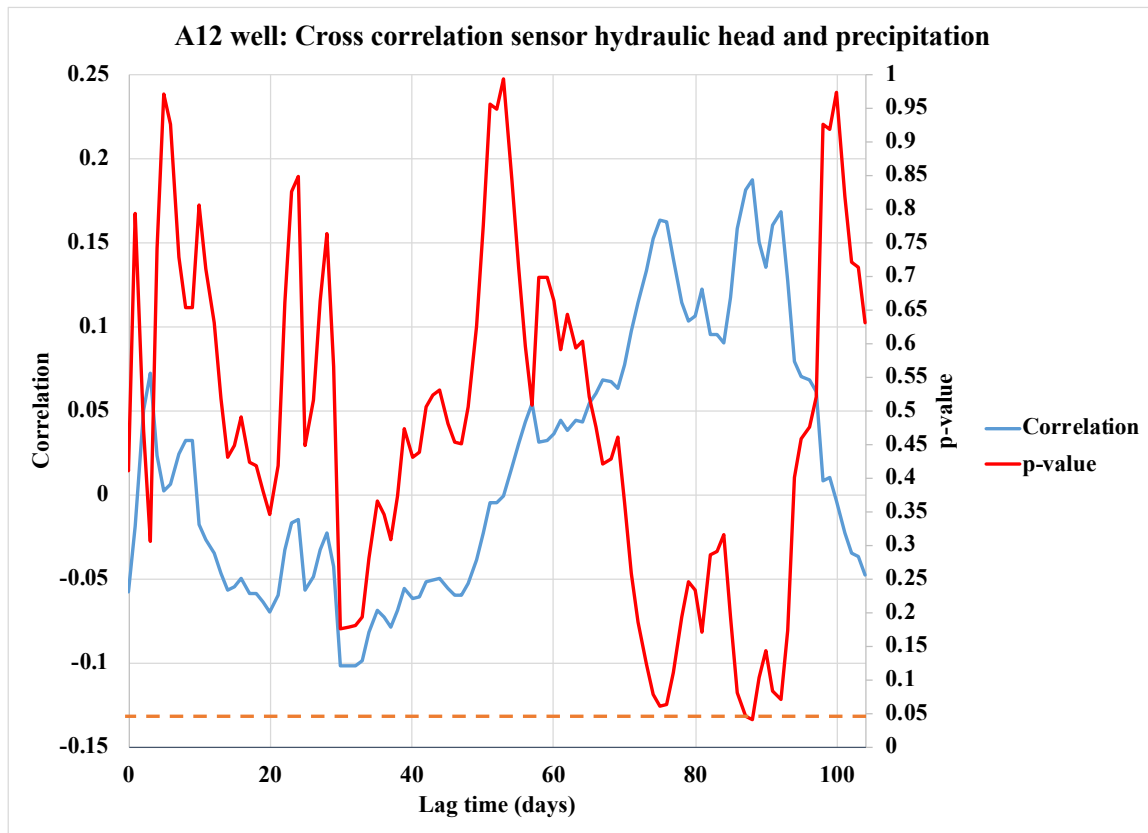


Figure B 3 Cross correlation of the daily hydraulic head recorded from the A12 monitoring well and the daily precipitation from the Scalia Lab. The orange dashed line represents the alpha for the p-value.

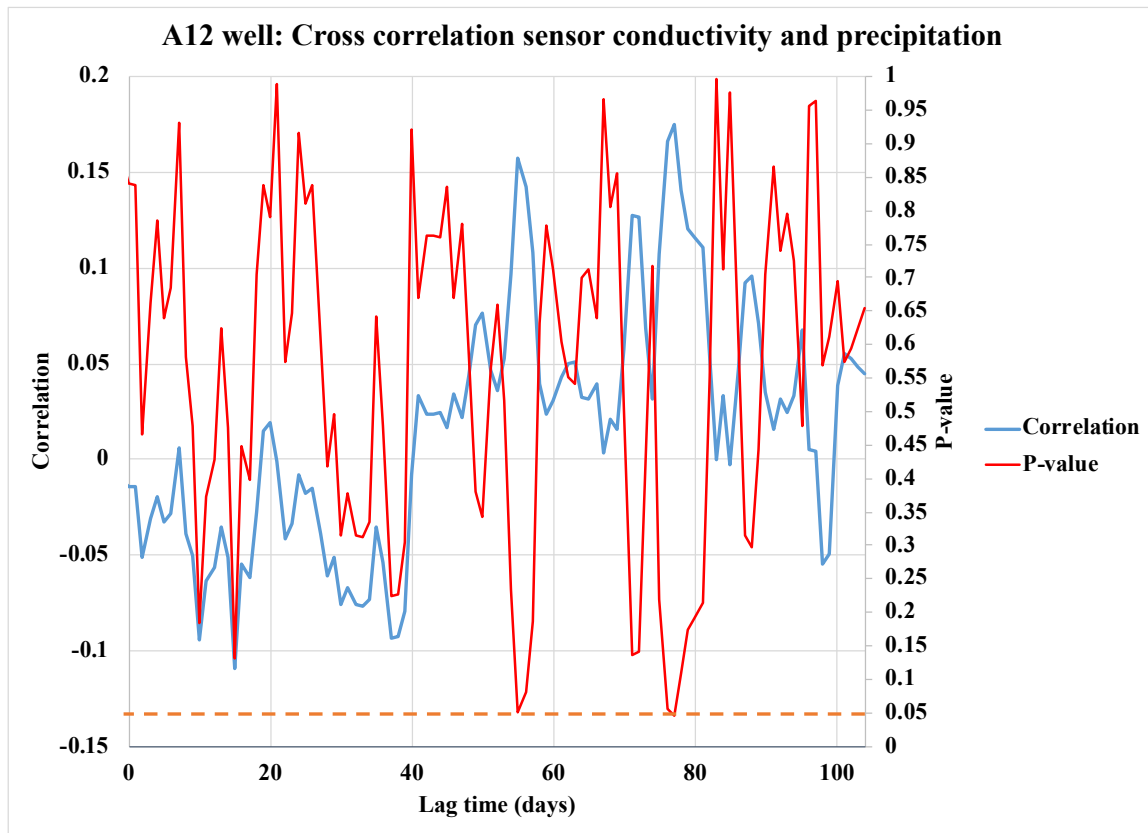


Figure B 4 Cross correlation of the daily hydraulic conductivity recorded from the A12 monitoring well and the daily precipitation from the Scalia Lab. The orange dashed line represents the alpha for the p-value.

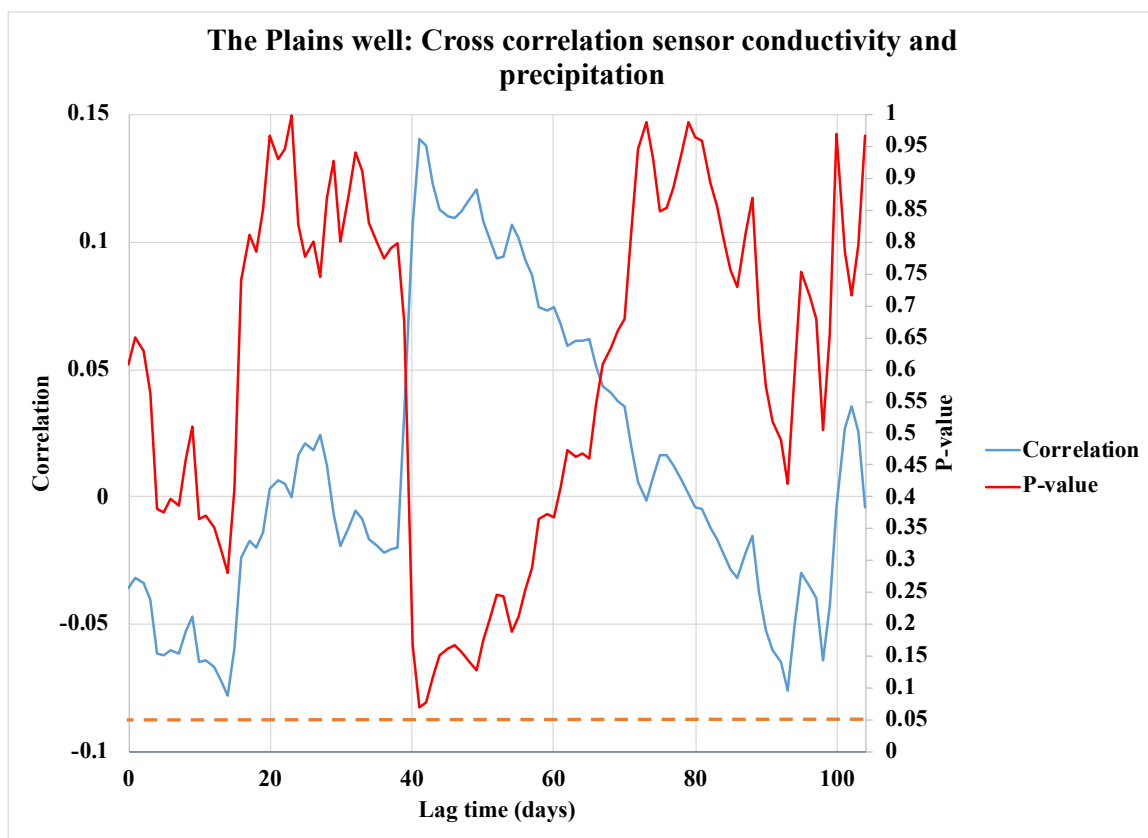


Figure B 5 Cross correlation of the daily hydraulic conductivity recorded from The Plains monitoring well and the daily precipitation from the Scalia Lab. The orange dashed line represents the alpha for the p-value.

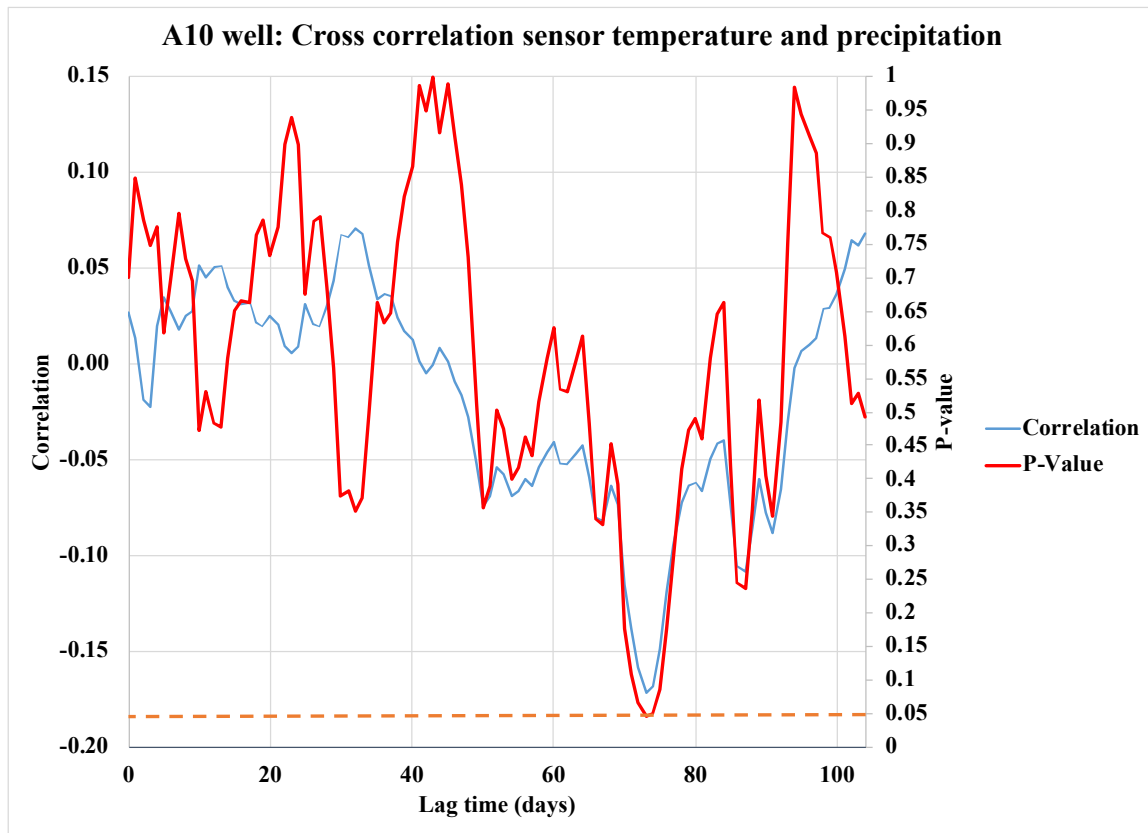


Figure B 6 Cross correlation of the daily temperature recorded from the A10 monitoring well and the daily precipitation from the Scalia Lab. The orange dashed line represents the alpha for the p-value.

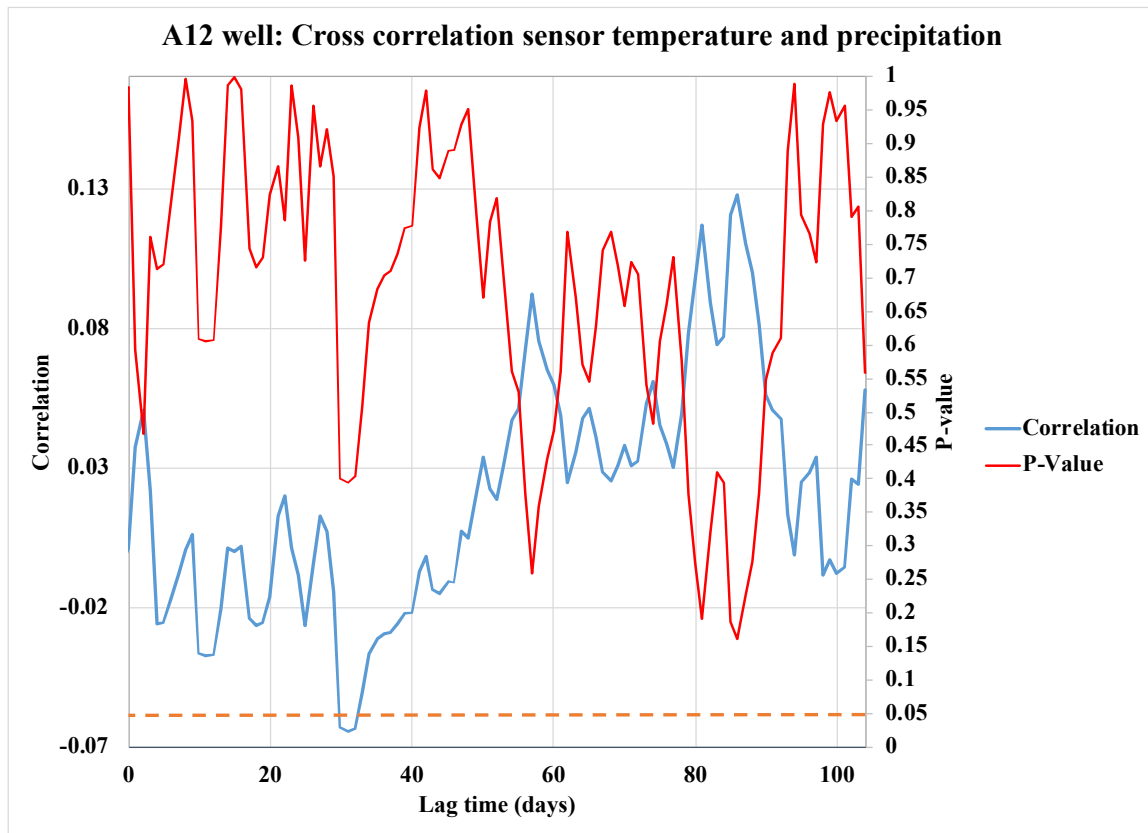


Figure B 7 Cross correlation of the daily temperature recorded from the A12 monitoring well and the daily precipitation from the Scalia Lab. The orange dashed line represents the alpha for the p-value.

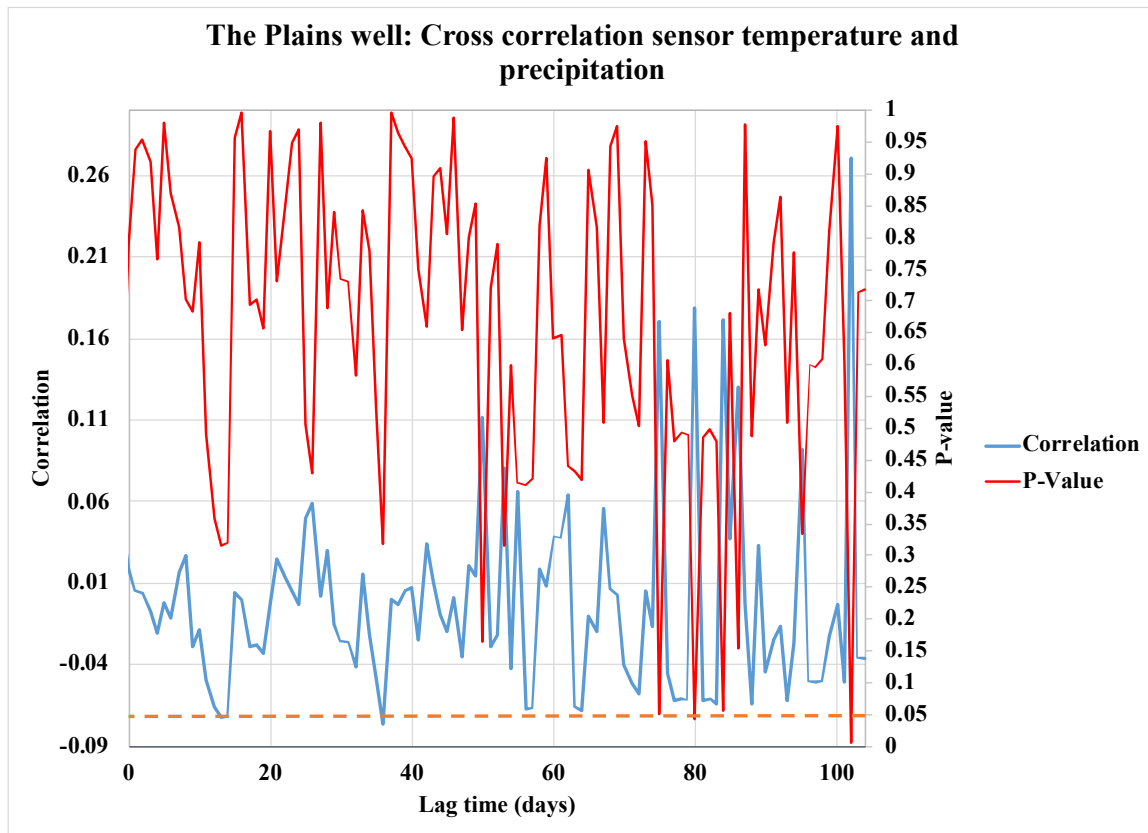


Figure B 8 Cross correlation of the daily temperature recorded from The Plains monitoring well and the daily precipitation from the Scalia Lab. The orange dashed line represents the alpha for the p-value.

### Appendix C: Tables

Table C 1 Water wells from the Ohio Department of Natural Resources water well map viewer. Some of the wells had incomplete data and did not include values, those are represented as NaN.

<b>Water Well Number</b>	<b>Long.</b>	<b>Lat.</b>	<b>Owner</b>	<b>Water level (ft)</b>	<b>Total Depth (ft)</b>	<b>Test Rate (gpm)</b>	<b>Static Water Level (ft)</b>	<b>Aquifer Type</b>	<b>Elevation (ft)</b>
391059	-82.10161	39.343705	City	NaN	47	480	4	Shale	642
391060	-82.10076	39.344706	City	NaN	48	398	6	Clay & Shale	641
391062	-82.10036	39.347562	City	NaN	38	354	7	Clay & Shale	640
391061	-82.10045	39.345887	City	Nan	42	480	8	Clay & Shale	642
391058	-82.10313	39.343007	City	NaN	59	526	9	Shale	640
391063	-82.10035	39.341354	City	NaN	46	420	9	Shale & Sandstone	638
391055	-82.10765	39.341354	City	NaN	62	529	11	Shale	635
9905052	-82.12118	39.336738	City	30	55	NaN	12	Sandstone	640
391057	-82.10452	39.342166	City	NaN	62	528	13	Shale	634
547512	-82.12499	39.33411	City	NaN	55	500	14	Shale	646
9905051	-82.12230	39.336066	City	NaN	61	NaN	16	Sand & Gravel	641
391054	-82.11302	39.339243	City	NaN	56	504	19	Boulders	640
382214	-82.13025	39.369322	Paulette Chalfant	46	46	36	20	Gravel	715
9905050	-82.12399	39.335124	City	NaN	61	NaN	21	Shale	664
400212	-82.12845	39.366633	Tomoko Rentals	38	120	1	21	Shale	710

368837	-82.13341	39.370312	Athens County Board of Developmental Disabilities	39	43	7	22	Sand & Gravel	717
411918	-82.13543	39.372124	Vale Connie and Erwin Timothy	40	40	15	23	Sand & Gravel	715
411944	-82.13096	39.368996	Dix William R III and Karin Stacy Hall	42	42	40	24	Sand & Gravel	714
359312	-82.13464	39.36636	Tomoko Rentals	70	45	10	26	Sand & Gravel	720
359328	-82.13172	39.370399	Jack Riley and Debra K	45	45	20	26	Sand & Gravel	715
411925	-82.12228	39.364528	Fred Phillips and Evelyn	43	43	30	26	Sand & Gravel	714
179967	-82.11982	39.333813	City	NaN	51	282	28	Rock	640
306773	-82.12604	39.363009	Courtney Gilbert B Trustee	42	42	5	28	Gravel	716
382247	-82.12228	39.364527	Fred Phillips and Evelyn	44	44	15	30	Sand & Gravel	
359325	-82.132376	39.367416	Susan Weaver (1), (2) Scott Thew and D Deirdre	43	105	24	50	Shale	715

306794	- 82.126669	39.363153	Zachary W Holl and Regis M Decker	108	108	30	53	Gravel	716
306797	- 82.135294	39.369483	NaN	70	70	8	55	Sand & Gravel	719
429712	- 82.142552	39.368697	Tomoko Mobile Park	108	108	22	62	Gravel	734
544768	- 82.139778	39.368195	NaN	108	107	36	62	Sand & Gravel	725
332501	- 82.126049	39.366272	Leah E Lyon	104	104	10	64	Gravel	714
359314	- 82.137031	39.369209	Emily Selway and Ronald Selway	85	85	25	65	Sand & Gravel	728
394867	-82.13609	39.368282	Joseph McGrew and Kayla McGrew	100	100	36	68	Sand & Gravel	726
400239	- 82.139583	39.368666	NaN	94	94	24	68	Gravel	727
374472	- 82.140785	39.369975	Christopher Roberts and Terry Roberts	105	105	12	75	Sand & Gravel	728
237040	- 82.131731	39.369602	The Plains Methodist Church	204	214	1	158	Shale	715
9990660	- 82.116232	39.334643	City	NaN	40	2	NaN	Bedrock	646

1013098	-82.1326	39.36927	Athens Metropolitan Housing Authority	NaN	30	NaN	NaN	Sand	715
985616	-82.13241	39.36922	Lannie Poling	NaN	24	NaN	NaN	NaN	715
400145	-82.129988	39.366338	Paul D. Kerr		48	NaN	NaN	Gravel	715
985617	-82.13462	39.369259	Quicky Lube	NaN	120	1	21	NaN	710
269868	-82.164947	39.344656	Dowler Junior		50	NaN	9	shale	662
322492	-82.157916	39.338857	Sharpe Mac	43	43	NaN	12	Gravel	655
131842	-82.139359	39.337916	Edwin Secoy	NaN	40			Sandstone	649
391054	-82.113022	39.339429	City	NaN	56	504	19	Boulders	640
391055	-82.10765	39.341354	City	NaN	62	529	11	Shale	635
57344	-82.096615	39.351217	Davis Monte	NaN	80		25	Shale	675
140419	-82.091759	39.358716	Patton W	NaN	60			Shale	972
9905051	-82.139359	39.337916	Edwin Secoy	NaN	40	NaN	nan	sandstone	649
411925	-82.126047	39.363009	Loren Cade	NaN	42	5	28	Gravel	716

Table C 2 Coordinates and water table elevation values from the wells used to construct the potentiometric map for water table.

<b>X (UTM)</b>	<b>Y (UTM)</b>	<b>Water Table (m)</b>
403375.5	4354745.2	186
402638.9	4358371.1	204
402790.5	4358070.8	205
402368.3	4358484.4	207
402196.6	4358687.7	206
402577.2	4358335.7	205
402257.0	4358047.1	198
402513.9	4358492.2	204
403318.8	4357830.5	205
402992.6	4357666.0	205
403318.9	4357830.4	204
402453.5	4358161.9	205
402939.2	4357682.6	185
402205.0	4358394.4	198
401578.6	4358315.1	191
401816.9	4358256.4	188
402996.9	4358028.1	186
402055.0	4358365.9	196
402134.7	4358262.0	191
401834.4	4358308.4	193
401732.7	4358455.0	190
402512.1	4358403.8	156
405173.9	4355738.6	191
404939.3	4355421.8	190
404818.8	4355329.9	190
404673.8	4355276.5	190
404547.9	4355243.1	190
404982.0	4355564.2	191
404759.7	4355595.6	191
404356.0	4359079.8	184
404278.3	4358035.9	183
404193.8	4357177.8	183
404550.9	4357143.9	183
405204.7	4356484.0	180
405374.2	4356014.8	178
405223.6	435508.2	181
404425.1	4355134.9	182
403326.7	4354660.0	185

Cont.

403301.3	4354574.8	185
403958.0	4355048.0	182
404355.1	4358331.5	183
404261.8	4357837.1	182
404178.8	4357380.7	182
404562.6	4357052.2	183
404804.6	4356779.0	180
404949.8	4356647.7	182
405136.6	4356481.7	180
405337.1	4356208.5	181
405330.2	4356011.4	178
405243.7	4355814.4	180
405181.5	4355534.3	181
404901.4	4355344.1	180
404521.1	4355243.9	180
403352.4	4354680.3	185
404571.8	4355210.8	189
404279.2	4355112.6	192
403986.5	4355020.2	191
403767.0	454848.8	192
403588.0	4354729.4	192

Table C 3 Values used to produce the overburden thickness temperature graph.

<b>Middle coal elevation (m)</b>	<b>Overburden Thickness (m)</b>	<b>Temperature overburden (°C)</b>
140.3230881	139.41	14.35186
130.2747192	129.36	14.12879
101.6862814	100.77	13.49412
141.5760315	140.66	14.37967
137.1752166	136.26	14.28198
125.9629537	125.05	14.03306
114.6972343	113.78	13.78297
124.7923938	123.88	14.00708
121.6460833	120.73	13.93723
113.252649	112.34	13.7509
120.7980026	119.88	13.9184
131.6953532	130.78	14.16032
142.1812431	141.27	14.39311
142.3898971	141.47	14.39774
132.5890998	131.67	14.18017
126.2481831	125.33	14.0394
131.7936201	130.88	14.16251
131.4934623	130.58	14.15584
117.4524354	116.54	13.84413
108.7802749	107.87	13.65161
99.52608406	98.61	13.44617
96.44908123	95.53	13.37786
90.26550908	89.35	13.24058
129.8231394	128.91	14.11876
124.1916198	123.28	13.99374
129.0796793	128.16	14.10226
136.4406129	135.53	14.26567
139.6802058	138.77	14.33759
123.0175571	122.10	13.96768
120.5222369	119.61	13.91228
118.6764477	117.76	13.8713
100.5000475	99.59	13.46779
113.2081478	112.29	13.74991
116.4197366	115.50	13.82121

117.7054604	116.79	13.84975
112.3650457	111.45	13.73119
125.4326148	124.52	14.02129
136.8197774	135.90	14.27409
138.4983417	137.58	14.31135
124.5259619	123.61	14.00116
132.5116876	131.60	14.17845
128.6788349	127.76	14.09336
113.9428953	113.03	13.76622
88.00821338	87.09	13.19047
102.0498086	101.13	13.50219
106.5586382	105.64	13.60229
129.2941563	128.38	14.10702
120.4998815	119.58	13.91178
127.2117757	126.30	14.06079
134.422541	133.51	14.22087
108.8793473	107.96	13.65381
129.0205429	128.11	14.10094
118.1479363	117.23	13.85957
129.8679966	128.95	14.11976
126.3682272	125.45	14.04206
99.68081455	98.77	13.4496
90.90371987	89.99	13.25475
115.0942981	114.18	13.79178
112.8166933	111.90	13.74122
103.4276887	102.51	13.53278
128.211582	127.30	14.08298
131.6105909	130.70	14.15844
115.4182726	114.50	13.79897
118.4609726	117.55	13.86652
130.1477514	129.23	14.12597
134.8389962	133.92	14.23011
111.7167436	110.80	13.7168
113.1765035	112.26	13.74921
111.2042958	110.29	13.70542
126.4452023	125.53	14.04377
101.0666404	100.15	13.48037
101.0735291	100.16	13.48052
85.14031858	84.23	13.1268

90.64358477	89.73	13.24897
92.42832075	91.51	13.2886
111.931382	111.02	13.72156
128.859627	127.94	14.09737
136.0403105	135.13	14.25678
120.4306596	119.52	13.91025
124.0154762	123.10	13.98983
141.2776372	140.36	14.37305
143.2376452	142.32	14.41656
105.5609083	104.65	13.58014
85.46886938	84.55	13.1341
111.5825843	110.67	13.71382
113.1156886	112.20	13.74786
111.1375929	110.22	13.70394
126.381848	125.47	14.04236
101.0067185	100.09	13.47904
101.0166954	100.10	13.47926
84.03593948	83.12	13.10228
90.57818411	89.66	13.24752
92.35362764	91.44	13.28694
111.8470616	110.93	13.71969
128.7703301	127.86	14.09539
135.9539716	135.04	14.25487
120.3531853	119.44	13.90853
123.9526894	123.04	13.98844
141.2354723	140.32	14.37211
142.2936377	141.38	14.39561
128.168759	127.25	14.08203
92.31670708	91.40	13.28612
81.72142324	80.81	13.0509
107.6385275	106.72	13.62626
92.29914424	91.38	13.28573
106.7674207	105.85	13.60692
110.6006392	109.69	13.69202
96.38022249	95.47	13.37633
76.88522185	75.97	12.94354
85.42836917	84.51	13.1332
102.2378378	101.32	13.50637
110.2752293	109.36	13.6848

110.2377329	109.32	13.68396
115.7432318	114.83	13.80619
137.7550945	136.84	14.29485
133.0571318	132.14	14.19056
138.7051246	137.79	14.31594
137.2023854	136.29	14.28258
143.309277	142.39	14.41815
133.6257691	132.71	14.20318
99.99672651	99.08	13.45661
79.75697849	78.84	13.00729
73.042705	72.13	12.85824
76.10942373	75.19	12.92632
85.52452908	84.61	13.13533
85.19715449	84.28	13.12806
101.2034101	100.29	13.4834
86.38864885	85.47	13.15452
75.46422212	74.55	12.91199
83.23522795	82.32	13.08451
109.5563599	108.64	13.66884
127.5238485	126.61	14.06772
124.9252232	124.01	14.01003
131.7537241	130.84	14.16162
135.3982458	134.48	14.24253
139.4501018	138.54	14.33248
135.3281279	134.41	14.24097
133.3181312	132.40	14.19635
122.2503743	121.34	13.95065
135.3332638	134.42	14.24109
114.4287629	113.51	13.77701
80.67772627	79.76	13.02773
86.37875854	85.46	13.1543
88.97015801	88.06	13.21182
85.95069597	85.04	13.14479
70.19210247	69.28	12.79495
72.04060352	71.13	12.83599
77.24986233	76.33	12.95163
86.17537686	85.26	13.14978
68.74951863	67.83	12.76293
76.34291655	75.43	12.9315

86.59182329	85.68	13.15903
110.4340292	109.52	13.68832
124.8316618	123.92	14.00795
108.4540796	107.54	13.64437
120.699424	119.78	13.91621
137.1343712	136.22	14.28107
143.0596019	142.14	14.41261
137.6034433	136.69	14.29148
117.3380025	116.42	13.84159
93.97822058	93.06	13.323
123.3520611	122.44	13.9751
74.43567114	73.52	12.88916
86.62701843	85.71	13.15981
85.92214263	85.01	13.14416
79.56979036	78.65	13.00314
72.4608947	71.55	12.84532
67.6050134	66.69	12.73752
66.59858462	65.68	12.71518
67.97165337	67.06	12.74566
89.54527568	88.63	13.22459
113.8112815	112.90	13.7633
116.0787881	115.16	13.81364
93.12018203	92.21	13.30396
103.5487485	102.63	13.53547
124.7130831	123.80	14.00532
132.1957682	131.28	14.17143
122.4265424	121.51	13.95456
116.5614562	115.65	13.82435
121.6108799	120.70	13.93645
95.9212875	95.01	13.36614
77.60866418	76.69	12.9596
88.92578293	88.01	13.21084
85.54910718	84.63	13.13588
87.73280786	86.82	13.18436
89.80036072	88.89	13.23026
86.26616558	85.35	13.1518
90.04399568	89.13	13.23566
87.23761321	86.32	13.17336
69.19306265	68.28	12.77277

67.25978748	66.34	12.72985
87.76763813	86.85	13.18513
91.73926201	90.82	13.2733
76.46189146	75.55	12.93414
69.3578708	68.44	12.77643
70.66620776	69.75	12.80548
71.87975601	70.96	12.83242
65.50700771	64.59	12.69094
67.70982954	66.79	12.73985
71.82539099	70.91	12.83121
76.85597844	75.94	12.94289
74.25383989	73.34	12.88512
115.5838621	114.67	13.80265
130.8572094	129.94	14.14172
142.6030175	141.69	14.40247
128.2844305	127.37	14.0846
117.3592509	116.44	13.84206
80.27843958	79.36	13.01887
73.97319753	73.06	12.87889
75.21019678	74.30	12.90635
82.12604958	81.21	13.05989
85.80259209	84.89	13.1415
84.23652769	83.32	13.10674
83.21854958	82.30	13.08414
73.23909348	72.32	12.86259
71.80951802	70.89	12.83086
77.3900658	76.48	12.95475
72.81748259	71.90	12.85324
62.64000046	61.73	12.6273
73.96608711	73.05	12.87873
67.23544875	66.32	12.72931
67.25910435	66.34	12.72984
69.43206765	68.52	12.77808
69.59650664	68.68	12.78173
70.95325703	70.04	12.81185
70.79376272	69.88	12.80831
62.89053577	61.98	12.63286
63.36358884	62.45	12.64336
63.85003096	62.94	12.65416

77.55459756	76.64	12.9584
102.5562915	101.64	13.51344
116.0031272	115.09	13.81196
96.17817163	95.26	13.37184
73.43157822	72.52	12.86687
72.78058276	71.87	12.85242
68.38312012	67.47	12.75479
71.06042888	70.15	12.81423
72.90997388	71.99	12.85529
87.00417917	86.09	13.16818
92.79825308	91.88	13.29681
62.58377021	61.67	12.62605
64.28869487	63.37	12.6639
61.86772666	60.95	12.61015
62.21865503	61.30	12.61794
63.47366199	62.56	12.6458
70.38464241	69.47	12.79923
63.21161514	62.30	12.63998
63.52685916	62.61	12.64698
63.92340122	63.01	12.65579
65.86262039	64.95	12.69884
66.86095388	65.95	12.721
66.13647339	65.22	12.70492
69.47800579	68.56	12.7791
67.43043179	66.52	12.73364
69.99906089	69.08	12.79067
67.94501479	67.03	12.74507
63.40260203	62.49	12.64422
67.82024465	66.91	12.7423
67.36038643	66.45	12.73209
68.12288853	67.21	12.74902
65.4160082	64.50	12.68892



**OHIO**  
UNIVERSITY

Thesis and Dissertation Services